DEFLUORIDATION OF DRINKING WATER USING BIOCHAR BASED TREATMENT TECHNOLOGY

By
Fazli Aziz
Reg. No. 8-FBAS/PHDES/F13

Supervisor
Dr. Islamud Din
Assistant Professor
DES, IIUI

Co-supervisor
Professor. Dr. Sardar Khan
DES, University of Peshawar

DEPARTMENT OF ENVIRONMENTAL SCIENCE (DES)
FACULTY OF BASIC AND APPLIED SCIENCES (FBAS)
INTERNATIONAL ISLAMIC UNIVERSITY ISLAMABAD (IIUI)

September 2020

I Environmental management

II Biochar

III Water - purification

IV Drinking water - purification

DEFLUORIDATION OF DRINKING WATER USING BIOCHAR BASED TREATMENT TECHNOLOGY

A thesis submitted to the Department of Environmental Science, Faculty of Basic and Applied Sciences, International Islamic University, *in partial fulfillment of the requirement for the award of degree of Doctor of Philosophy* in Environmental Science.

Fazli Aziz
Reg. No. 8-FBAS/PHDES/F13

Supervisor
Dr. Islamud Din
Assistant Professor
DES, IIUI

Co-supervisor
Professor. Dr. Sardar Khan
DES, University of Peshawar

DEPARTMENT OF ENVIRONMENTAL SCIENCE
FACULTY OF BASIC AND APPLIED SCIENCES
INTERNATIONAL ISLAMIC UNIVERSITY ISLAMABAD

2020

بِسْمِ اللّٰهِ الرَّحْمٰنِ الرَّحِيْمِ

Dedicated

To

My Beloved Parents, Brothers, Sisters, Daughter and Wife for their never-ending Love, Prayers, Care and Support, without which I would not be able to Complete this Work.

DECLARATION

I, Fazli Aziz, PhD scholar in the Department of Environmental Science, registration No 8-FBAS/PHDES/F13, hereby declare that the thesis titled "Defluoridation of Drinking Water Using Biochar Based Treatment Technology" is my own original research work and has not been submitted as research work or thesis in any form in any other university or institute in Pakistan or abroad for the award of any degree. However, one paper from this research has been published in journal of Fluoride and the other is accepted in Polish Journal of Environmental Studies.

11/02/2021

Dated:

Deponent

Fazli Aziz

FORWARDING SHEET BY RESEARCH SUPERVISOR

The thesis entitled "Defluoridation of Drinking Water Using Biochar Based Treatment Technology" submitted by Fazli Aziz in partial fulfillment of PhD degree in Environmental Science has been completed under my guidance and supervision. I am satisfied with the quality of student's research work and allow him to submit this thesis for further process of graduation with PhD Degree from Department of Environmental Science, as per IIU rules & regulations.

Date:

Dr. Islamud Din
Assistant Professor
Department of Environmental Science
International Islamic University, Islamabad

INTERNATIONAL ISLAMIC UNIVERSITY ISLAMABAD
Faculty of Basic and Applied Sciences
Department of Environmental Science

Dated: 04-02-2021

FINAL APPROVAL

It is to certify that we have read the thesis submitted by **Mr. Fazli Aziz Reg# 08/FBAS/PHDES/F-13**. Thesis is of sufficient standard to warrant its acceptance by the International Islamic University, Islamabad for PhD Degree in Environmental Science.

COMMITTEE

Supervisor
Dr. Islam Ud Din
Assistant Professor
Department of Environmental Science

Co- Supervisor
Professor. Dr. Sardar Khan
Vice Chancellor,
Kohat University of Science and Technology

Internal Examiner
Professor. Dr. Muhammad Irfan Khan
Department of Environmental Science

External Examiner
Dr. Shaheen Begum
Associate Professor
Department of Environmental Science,
Fatima Jinnah Women University, Rawalpindi

External Examiner
Dr. Muhammad Arshad
Associate Professor
Institute of Environmental Science and Engineering,
NUST, Islamabad

Chairman,DES
Dr. Muhammad Ibrar Shinwari
Associate Professor

Dean,FBAS
Professor. Dr. Muhammad Irfan Khan
Faculty of Basic and Applied Sciences

ABSTRACT

The groundwater quality at the world level is affected by both geochemical structures and the underlying strata of the rocks. Fluoride (F^-) is an important component, needed for the normal growth of teeth and bones, which is mostly found in rocks (minerals), soil, food, air, groundwater, and in the human body. High F^- contamination in groundwater is a global issue, which causes severe health complications in living organisms, particularly in the residents of the rural communities of developing nations. Both natural as well as human activities are causing F^- contamination in groundwater. The study aimed to assess the F^- level in the drinking water of district Malakand, its threats to human health, and F^- removal from water by using different materials including plant leaves, commercial granular activated carbon, biochar, and clay particles. The collected water samples (n = 30) were analyzed for different cations and anions. The F^- concentration in drinking water samples was measured by F^- meter and was found substantially high in most of the samples than the WHO (World-Health-Organization) permissible limit i.e. 1.5 mg/L. The cationic and anionic concentrations were found in the sequence of: sodium (Na) > calcium (Ca) > magnesium (Mg) > potassium (K), and sulfates (SO_4) > bicarbonates (HCO_3) >chloride (Cl) > F^-, respectively. Among the anions, sulfates (SO_4) were found as a dominant specie in all water samples while among cations, sodium (Na) was found in excess in all water samples except in Batoo locality, where Ca exceeds Na. As given by the Gibbs diagram, contact of water with rock was the primary cause for the ions distribution in the water of the investigated area. Piper tri-linear plot depicts that the mixed (Ca-Mg-Cl) and Ca-Cl_2 were the main water forms found in the study area. Health risk assessment i.e. Community fluorosis index (CFI) was assessed via Dean's classification. The results obtained from water analysis and CFI values showed that the water was not suitable for drinking purposes. Therefore, further research study was conducted to find out a suitable, environment friendly, and an inexpensive adsorbent using adsorption method for F^- removal. For this purpose, various materials (Biochar, Dodonaea leaf powder (DLP), granular activated carbon (GAC), and clay) were tested under batch adsorption method by optimizing different parameters like contact-time, dosage of adsorbent, pH, and initial F^- concentrations. The highest de-fluoridation of 90% was achieved with biochar BC750 followed by BC250 (85%), BC500 (80%), BC1000 (75%), DLP (45%), GAC (40%) and clay (5%) in an acidic medium at pH 2. The results revealed that percent F^- adsorption increases with increase in dose amount and contact time, while F^- removal decreased by increasing F^- and pH level of the

medium. Biochar characterization was made through Scanning Electron Microscopy (SEM), Energy Dispersive X-ray Spectroscopy (EDS), Fourier Transform Infrared Spectroscopy (FTIR), Electrical Conductivity (EC), yield, pH, moisture content, Point of Zero Charge (pHpzc), and bulk density. The optimum contact time for BC250, BC500, BC750, BC1000, GAC, DLP, and clay were 95 minutes, 145 minutes, 125 minutes, 145 minutes, 15 minutes, 145 minutes, and 75 minutes, respectively. The adsorption data of F^- were applied to adsorption isotherm models (Langmuir and Freundlich) and adsorption kinetics (Pseudo First-Order and Pseudo Second-Order). The R^2 values obtained for BC500, BC750, BC1000, and GAC data showed its best fitting to both Langmuir as well as Freundlich-models. Similarly, DLP adsorption data were best following the Langmuir isotherm than the Freundlich isotherm model. The entire adsorbents strongly followed the Pseudo Second-Order as compared to Pseudo First-Order-Kinetic model, because the values of qe (calculated) as well as qe (experimental) obtained from the Pseudo Second-Order were resembling very closely with each other. Thus, the biochar was proved to be an effective and environmentally friendly material as compared to other commercial materials for the defluoridation of water.

ACKNOWLEDGEMENTS

I thank the Almighty Allah who is the most kind and merciful. I am thankful to ALLAH for sound wellbeing and health that were essential to accomplish this work. All respects to His Holy Prophet Hazrat Muhammad (SAW) for enlightening our conscience with the essence of faith in Allah and love for the environment of which man is an integral part.

Foremost, I say my heartiest thanks to my respected supervisor Dr. Islamud Din, Assistant Professor and co-supervisor (Professor Dr. Sardar Khan), for delivering the whole essential materials (instruments) for conducting this research study, for their sympathetic supervision, vast understanding, persistent support, inspiration, and sincere relationship in my study time. A lot of motivating conversations with them have greatly structured the current study and enhanced my confidence. I am also extremely obliged to Dr. Muhammad Ibrar Shinwari, the chairman department of environmental sciences IIU, for his encouraging and kind behavior with the students.

I like to thank Dr. Ghulam Mustafa Assistant Professor (SA-CIRB) for his outstanding support and suggestions in writing research article and its submission to the journal. I too like to thank Dr. Muhammad Mumtaz and Dr. Waqar Adil, Associate Professors at Department of Physics, IIUI for providing lab facilities for my research work.

I wish to thank Mr. Mumtaz Khan, my lab mate PhD Scholar for the assistance he provided on some important analytical techniques in the lab. I am very thankful to the whole faculty as well as to the office members of the Department of Environmental Science, International Islamic University, Islamabad, for their fruitful research discussion and suggestions that have made my work easy.

Finally, I truly grant and present my heartfelt acknowledgement to my whole relatives, particularly my brothers, sisters, wife, and daughter Arsh aziz, for supporting me spiritually as well as financially throughout my lifetime. During this study, I am highly thankful to all the mates that I met in IIUI, who delivered me exciting interdisciplinary and intercultural understandings.

Fazli Aziz

TABLE OF CONTENTS

LIST OF FIGURES

LIST OF TABLES

LIST OF ABBREVIATIONS

AC	Activated Carbon
AKC	Activated Kikar Leaves Carbon
Al-IEBA	Al-Impregnated Eucalyptus Bark Ash
ANC	Activated Neem Leaves Carbon
APHA	American Public Health Association
AR	Analytical Reagent
AWWA	American Water Works Association
BC	Biochar
BET	Brunauer–Emmett–Teller
CAC	Chemically Activated Coal
Cal	Calculated
Ce	Concentration at Equilibrium
CFI	Community Fluorosis Index
Ci	Initial Concentration
CIRBS	Centre for Interdisciplinary Research in Basic Sciences
Ct	Concentration at Time
DBBC	Dodonaea Viscosa Bark Biochar
DLP	Dodoneae Viscosa-Leaf Powder
DNA	Deoxyribonucleic Acid
EC	Electrical Conductivity
EDS	Energy Dispersive X-Ray Spectroscopy
FTIR	Fourier Transform Infrared Spectroscopy
F^-	Fluoride
GAC	Granular Activated Carbon
HQ	Hazard Quotient
IIUI	International Islamic University, Islamabad
KP	Khyber Pakhtunkhwa

M	Molarity
MER	Main Ethiopian Rift
NC	Natural Coal
PAC	Physically Activated Coal
PCA	Principal Component Analysis
pH_f	Final pH
pH_i	Initial pH
pHpzc	pH Point of Zero Charge
PPBC-La	Lanthanum-Loaded Pomelo Peel Biochar
PTEs	Potentially Toxic Elements
PZC	Point of Zero Charge
R	Rotation
Rpm	Revolutions Per Minute
SD	Standard Deviation
SEM	Scanning Electron Microscopy
TDFI	Total Daily Fluoride Intake
TDS	Total Dissolved Solids
TH	Total Hardness
TISAB	Total Ionic Strength Adjustment Buffer
UAE	United Arab Emirates
US	United States
V	Volume
W	Weight
WHO	World Health Organization
XRD	X Ray Diffraction
Y	Yield

CHAPTER 1

INTRODUCTION

1.1. INTRODUCTION

Groundwater quality at global scale is affected by both geochemical structures and underlying strata of the rocks (Radfarda et al., 2019; Saby et al., 2016). An estimation has made that the groundwater fulfills the agricultural, industrial and domestic requirements of about one third of the world population (Rashid et al., 2018). Supply of clean and safe drinking water as well as groundwater contamination are global issues (Guo et al., 2017).

Fluoride (F^-) occurrence in drinking water is a global problem, which is responsible for dangerous health issues in living organisms, specifically in the residents of the rural communities of the developing nations (Adimalla et al., 2019; Alarcón-Herrera et al., 2020; Kimambo et al., 2019). F^- is an important component needed for normal growth of teeth and bones (Daiwile et al., 2019; Dutta et al., 2017), which mostly happens in rocks (minerals), soil, food, air, groundwater and in the human body (Fallahzadeh et al., 2018; Patel et al., 2016; Xiao et al., 2015; Yousefi et al., 2018). Both natural and human activities are causing F^- contamination into ground water (Thivya et al., 2017).

Physicochemical factors like temperature, TDS, pH, bicarbonates, and acidity of the host rock and wells depth can disturb F^- occurrence in groundwater (Mandinic et al., 2010; Rashid et al., 2018), and is generally found in higher concentrations in the rocks containing minerals for instance, fluorspar, fluorite, fluoroapatites, cryolite, topaz, amphiboles, mica, biotite, hornblende, fluorite, muscovite, fluorspar, villianmite, and tourmaline. Besides these minerals, sedimentary and igneous rocks as well as some weathering silicates are also causing F^- contamination (Doherty et al., 2014; Mondal et al., 2016).

Formations and weathering of calcium and magnesium containing mineral rocks and their leaching into groundwater also leads to F^- contamination (Thivya et al., 2017). In addition to these natural causes, the water bodies contamination with F^- also occurs due to industrial effluent, agricultural runoffs, mining etc, and thus causing health issues in human beings (Ranjan & Ranjan, 2015). The chief route of F^- exposure for people is drinking of F^- containing water (Narsimha &

Sudarshan, 2017). The health risk caused by consumption of high F^- containing water is found in 200 million peoples of about 20 countries in the world (Thivya et al., 2017).

As an important calcium-seeking element, higher concentrations of F^- can cause dental and bones fluorosis especially in teenagers (Sezgin et al., 2018; Yuan et al., 2020). Its ingestion above the WHO permissible level for a maximum period can cause dental problems (fluorosis), while a level above 3.5 mg/l build skeletal defects (fluorosis) (Antonijevic et al., 2016; Suthar, 2011; Zhang et al., 2017). Similarly, F^- concentrations above 10.0 mg/ L in drinking-water causes many additional illnesses, including increase blood pressure, neurological issues, and cancer in people (Neisi et al., 2018; Zhang et al., 2016). Initially bone fluorosis is recognized by rigidity and aching in the joints and then leads to problems in muscles movement, ligaments muscle calcification, high osteosclerosis, difficulties in movement of joints, crippling deformities in bone, and other main joints (Zohoori & Duckworth, 2017).

Epidemiologic evidence has shown a strong positive relation between exposure to a high F^- level and dental fluorosis (Lima-Arsati et al., 2018). Dental fluorosis has gained importance globally since the last few decades (Martinez-Mier, 2018). Increased subsurface opacity as well as porosity of teeth, dark brown stained tooth patches are the prominent symptoms of fluorosis (dental) (Zohoori & Duckworth, 2017). Earlier research works found that exposure to high level of F^- causes genetic changes in susceptible humans and can be linked with the risk of fluorosis (Pramanik & Saha, 2017).

F^- in drinking water also affect the IQ level in children (Razdan et al., 2017). Recent studies showed that large number of individuals (about 20 lacs) from 25 states comprising Iran, India, China, Sri Lanka, Pakistan and Thailand have shown the signs fluorosis (dental and skeletal) (Rasool et al., 2018). Excessive F^- amount in groundwater and occurrence of fluorosis have been testified in nearly each African state (Malago et al., 2017). Approximately 50 million population in the northern China is consuming maximum F^- containing ground-water and approximately 60% people are suffering from fluorosis (dental) and nearly ten percent individuals are suffering from other type of fluorosis (skeletal) (He et al., 2013). In several countries e.g. Kenya, Tunisia and Ethiopia (Guissouma et al., 2017; Olaka et al., 2016), India (Vikas et al., 2013) China (Currell et al., 2011), Brazil (de Souza et al., 2013), and Pakistan (Rafique et al., 2015; Rashid et al., 2018) fluorosis (both dental and skeletal) is reported.

Therefore, it is extremely desirable to eliminate excessive F^- from water to avert fluorosis in the residents of those areas having high levels of F^- in their groundwater which they are mostly using for drinking purposes. The different methods used for F^- adsorption from water are ion exchange method, chemical precipitation, electro dialysis method and adsorption process (Yadav et al., 2018), but the adsorption method is mostly used for F^- removal because it is easy to operate, it requires less energy and it is inexpensive as compared to other methods.

Different adsorbents including *Eucalyptus* bark ash (Ghosh & Mondal, 2019), cattle bones char (Shahid et al., 2019), thermally activated sepiolite (Lee et al., 2020), biomass (Annadurai et al., 2019) and *Ziziphus* (Jujube) leaf (Mahvi et al., 2018) have been applied for adsorption of F^- from water (Mohan et al., 2017; Yadav et al., 2018). Currently, researcher's interest has been shifted towards biomass-based materials for the sorption of F^- from water, as they are cheap, economical and abundantly available materials (Yadav et al., 2013). Therefore an environment friendly material i.e. biochar was prepared and its capacity for F^- removal was compared with *Dodonaea* plant leaves powder, activated carbon and clay particles for excessive F^- removal from water.

A black solid, high carbon containing by-product prepared by pyrolysis of low-cost materials (biomass) under anaerobic environment is known as biochar (IBI, 2012; Song et al., 2018a). Large surface area and maximum porosity make the biochar an efficient adsorbent for contaminants removal from water (Sun et al., 2018). Other uses of biochar are soil amendment, controlling of waste and climate change mitigation (Ruan et al., 2019).

Biochar can be prepared from a variety of biomasses e.g. crop remainings, forest residues, domestic residues , animals' dung and other products (Luo et al., 2019). Therefore, the bark of a common and abundantly available plant named *Dodonaea Viscosa* was used for biochar preparation to exclude high F^- from water. *Dodonaea Viscosa* is the plant of Sapindaceae family and is abundantly found in the study area and its common name is *Dodonaea,* while locally its Pashto name is *Ghorhaskay*. Its flowering season is from February to March and the leaves, wood, bark and seeds of the plant are used for different purposes. It is found in different regions of Khyber-Pakhtunkhwa (KP), e.g. Hazara, Swat, Dir, Gilgit, Kurram. In Punjab, Baluchistan and Kashmir, it can be found in various localities (Qureshi et al., 2008).

The available literature about the biochar production from plants barks was reviewed thoroughly and it was concluded that removal of F^- with biochar prepared from the bark of *Dodonaea viscosa* plant has not been studied up till now. Thus the study suggested an inexpensive and efficient biochar adsorbent for F^- adsorption from the water.

1.2. PROBLEM STATEMENT

The main problem in the study area was fluorosis, because Ingestion of excessive F^- in drinking water cause fluorosis, affecting both teeth and bones. The removal of this excessive F^- from drinking water is difficult and costly. The preferred choice is to have a safe drinking water supply with safe F^- levels. In case, this option is limited, defluoridation may be the only solution. The different methods used for F^- removal includes; ion exchange method, chemical precipitation method, coagulation etc, but these methods are expensive and difficult to perform. Therefore some cheap and easily applicable methods with locally available materials are necessary to develop for F^- removal from drinking water and adsorption method is the best choice, because it is an easy, low cost and environmentally friendly method.

1.3. Hypothesis

The fluorosis in the study area is caused by high levels of F^- in groundwater and the maximum F^- can be removed using biochar as an adsorbent.

1.4. Significance of the study

The materials used as adsorbents in this study for de-fluoridation of water are of low cost, environmentally friendly and locally available. They are capable in removing F^- from contaminated water as compared to commercial filtration plants, adsorbents, and conventional processes. The study will aware the local community about the health risks associated with the excessive F^- level in drinking water by publicizing the study results. Through de-fluoridation of water by using low cost materials, the people will get economic benefits in a sense that they will spend less money on health issues related to high F^- concentrations.

1.5. AIM AND OBJECTIVES OF THE STUDY

The aim of the study was to reduce and abate the problem of fluorosis by lowering the higher level of F^- in the groundwater of the area. For that purpose the following objectives were framed.

1. To assess F^- in drinking water of district Malakand and its associated health risk (Fluorosis).
2. To prepare biochar from the local plant *Dodonaea viscosa* biomass (barks) and to characterize it.
3. To assess the efficacy of different biochar's for F^- removal.
4. To compare the biochar performance of F^- removal with different materials such as commercial activated carbon, local clay particles, and plant leaves powder.

CHAPTER 2

REVIEW OF LITERATURE

2.1. FLUORIDE (F^-) IN WATER AND ITS HEALTH RISKS

The F^- level and its health risk was investigated in 10 districts of Tianjin (China). The study revealed that F^- concentrations were higher in the zones having maximum depth of the wells and that the risk was mainly caused by the ingestion route. The study was also helpful in providing information for health authorities for making health policies (Zhang et al., 2020). Similarly, the source, release and mobility as well as factors controlling F^- abundance in water were studied. The mean F^- level in the area was 1.7 mg/L and granitic rocks weathering, and ion-exchange mechanisms were the main causes of F^- in groundwater. Their work found that children were more vulnerable than adults (Mukherjee & Singh, 2020).

A pioneer study was conducted on several aspects of F^- metabolism in children and their parent, living at lower altitude and higher altitude regions in Nepal. They found that the F^- level was higher at lower altitude than at higher altitude and concluded that higher altitude living were responsible for decreased urinary F^- excretion, and increased F^- retaining in children for a given F^- dose (Sah et al., 2020). Another study found that 10% children were at risk for dental decay, tooth fluorosis (1.3%) and bone fluorosis (0.06%). The results showed that hazard quotient (HQ) was above 1, which represented non-carcinogenic health threats due to F^-. They suggested that this research will benefit the government departments to formulate strong strategies to reduce children exposure to F^- (Yuan et al., 2020).

A study was performed a study to evaluate the F^- quantity and permissible level in groundwater from Sukulu Hills, a phosphate mining region in Tororo District, Uganda, where the main water source for drinking is ground-water. The results find that all water sources were contained average F^- concentrations. Their results indicted a risk to the local community dependent on this water and were exposed to risks of high F^- ingestion (Egor & Birungi, 2020).

The F^- level and fluorosis incidence in pastoral regions of Iran was determined. The study found out that dental cavity risk was found absent in both regions, but both dental and skeletal

fluorosis risks were very important in some areas of the investigated regions. Similarly, they also told that Children were highly affected by fluorosis (Aslani et al., 2019).

Rashid *et al.* (2018) investigated the F^- concentration and physicochemical features of water in a region, near to River Swat, specifically the fate and occurrence of F^- and the hydro-geochemistry. Most water samples were beyond the safe limit of the WHO. It was concluded through Dean's classification that the groundwater having high concentration of F^-, was unsuitable for drinking.

Yousefi *et al.* (2018) investigated the levels and health risks of F^- in Iran. The study stated that 57% of samples were containing high F than the WHO limit for drinking water. Health risk assessment showed that most of the rural inhabitants were woe from fluorosis because of consumption of the F^- contaminated water. Therefore, it was suggested to take actions for reducing F^- and controlling of fluorosis. The F^- level in both urine of children and in groundwater of Haryana state was evaluated. The results showed that comparatively high ingestion of maximum food and drinking of more water by the boys might be the main cause for dental fluorosis among boys as compared to girl's cases. Hydro-geochemical studies of the water exposed that water-rock interactions were mainly controlling the groundwater quality (Haritash et al., 2018). Dental fluorosis was common in school children and girls were more susceptible than boys. It was found that water fluoridation above 1.2 ppm was the main reason of dental fluorosis in school children (Kotha, 2017).

A questionnaire based research work was conducted to calculate the fluorosis (dental) incidence among youngsters going to school and to know the elements connected with dental fluorosis in Kolar taluka, India. The results concluded that adolescents (64.3%) were suffering with fluorosis (dental) and above 50% were suffering either with moderate or severe fluorosis according to the Dean's formula. Installation of defluoridation units or organizing training workshops for public about defluoridation techniques in the region should be encouraged (Verma et al., 2017).

The study mainly focused on to know the level of F^- in water and the hydrogeological situations in Mexico as well as to determine the link between under nutrition and dental enamel fluorosis in teenagers living in areas having various F^- levels in water. The study found that sub

populations with chronic undernutrition were highly exposed to enamel fluorosis (Irigoyen-Camacho et al., 2016).

The F^- concentrations in various brands bottled water available in Abu Dhabi markets was determined, to know, whether F^- improves health or causes health issues and reported that one brand possesses high F^- concentrations, which was beyond the recommended limits, which may pose health issues (Abouleish, 2016). The geochemistry and F^- concentration of geothermal springs in Namibia was investigated, which stated that geothermal springs of Namibia were complying drinking water limits and conclude that the water could be used only for thermal spas etc. Treatment would be required to reduce dissolved fluorine levels for drinking purposes (Sracek et al., 2015).

Wu *et al.* (2014) used statistical analysis (both multivariate and correlation) to show hydro-geochemical factors controlling key ion chemistry of waters in a mine area, located in Sichuan, China. According to results, water features in the site were fit before the project launching. Multiple factors were involved in the changing chemistry of the waters in the area and ion exchange and natural mineral weathering were the important factors.

A research work on water quality evaluation and major ion chemistry of water bodies of Burdwan District, India, was performed. Hydro chemical indices proved its inland origin having minimum salinity risk and the reactions (Base-Exchange) were greatly active than the cation-anion-exchange processes. Gibbs diagram represented that weathering of the rocks and water quality was associated to the area lithology. Quality of the water was found to be fit for livestock and irrigation purposes (Samanta et al., 2013). The association between high F^- ingestion and hypertension in peoples living in F^- prevalent regions was calculated. The work showed the linkages between high F^- consumption and high blood pressure in elders, which confirmed that exposure to enhanced F^- dosages could boost the levels of plasma in peoples residing in F^- prevalent localities (Sun et al., 2013).

The F^- assessment in branded (bottled) water and its occurrence in F^- prevailing and non-endemic parts was reported. The findings showed that bottled waters (Algerian) can be considered as an appropriate cause of nutritional F^-. Major changes were noticed in F^- amounts of analyzed bottled waters. The information were helpful for general peoples as well as for dentists (Bengharez et al., 2012).

Rango *et al.* (2010) did their research on the geochemistry and evaluation of water characteristics of natural waters of the Main Ethiopian Rift (MER), especially on the origin and distribution of arsenic and F^-. They reported that beside high F^- issue in the area, some other geochemical irregularities have also to be included in water quality problems and further study has to be done to identify their potential health effects over the residents of MER and more segments of the East African Rift.

Mandinic *et al.* (2010) investigated the F^- level in drinking water and hair of school children (12-years old) from various Serbian towns. Correlation study showed statistically significant positive linkages between F^- in wells water and in hair, for all areas. Dental study of school children showed teeth fluorosis only in Vranjska Banja region. The study indicated that F^- level in hair sample is greatly linked with F^- in water as well as with dental fluorosis, indicating that hair might be considered as biomarker of high informative potential in assessing chronic contact to F^- and to individual children at fluorosis risk regardless of teeth development phase.

Viswanathan *et al.* (2009) studied mapping of F^- prevalent regions and evaluation of its exposure. They tried to assess the contact with F^- through drinking water from different age group peoples and to interpret the F^- prevalent area through their mapping. From the study it was known that Nilakottai block had high F^- prevalence. Their study also finds that, the people in Nilakottai block were warned to use drinking water by having F^- level below 1 mg/l. The study recommended the provision of drinking water containing minimum F^- to the affected regions.

Kumar *et al.* (2009) studied groundwater chemistry and hydro-geochemistry of the Manimuktha River basin, India. Water samples (n=26) from bore wells were evaluated for geochemical changes and characteristics of groundwater. They reported that the characteristics of groundwater were mainly changed because of human and natural activities.

Malinowska *et al.* (2008) studied the F^- evaluation and its ingestion by peoples from tea and herbal uses on a daily basis. They reported through this study the routine ingestion of F^- gained from herbal drinks and tea for adults and children. They also found that higher ingestion of F^- through taking black tea, particularly in regions having great level of F^- drinking water, accelerate teeth fluorosis risk in youngsters during dental growth. The chronic contact with maximum level of F^- can result in skeletal fluorosis.

The exposure and risk evaluation for trace metals and F^- in black tea was estimated. Fifty individuals were selected arbitrarily for provision of samples from the tea that they drink, and a questionnaire was provided to collect data about them and their daily tea ingestion. According to their study neither F^- nor aluminum concentration in black tea were responsible for diseases (fluorosis and Alzheimer's) (Sofuoglu & Kavcar, 2008).

Budipramana *et al.* (2002) performed a study to know the occurrence and effects of dental caries and dental fluorosis in a fluorosis prevalent zone, with F^- in drinking water. They stated that caries occurrence in the sub-district was 62% and 68% for permanent and primary teeth, respectively. Fluorosis frequency was 96% with average community fluorosis index (CFI) of 1.71.

2.2. DEFLUORIDATION USING PLANT LEAVES (ADSORBENT)

George and Tembhurkar (2019) used an adsorbent prepared from the *Nucifera linn* root for F^- removal. The results stated that the adsorption data of F^- onto prepared adsorbent best suited to the isotherm model of Langmuir. The kinetic study indicated that the mechanism was chemisorption and was supporting the second order model strongly.

Annadurai *et al.* (2019) investigated column and batch methods for F^- adsorption from water by applying dead, live and different pretreated *Aspergillus niger* biomass. Their findings revealed that high adsorption of F^- was occurred in 30 to 80 min with the fungal dead biomass when matched to live and different pretreated biomass. The data were following pseudo second order. In column mode, 89% of F^- adsorption was noticed. The results recommended that fungal dead biomass could be an appropriate adsorbent for F^- adsorption from aqueous media.

Tirkey *et al.* (2018) used Jamun (*Syzygium cumini*) leaf ash for F^- adsorption from liquid media. The adsorbent was characterized by EDS, FT-IR, and XRD analysis. Maximum adsorption was achieved within 60 minutes from solution of F^- (6 mg/L) 6.5 g/ L (dosage) and pH 6.5. Freundlich model, Pseudo second order and intra-particle model were in good compliance to the data. The findings revealed that this work will be helpful in scheming novel low-cost and calcium based adsorbent from the bio wastes treating F^- contaminated water.

Khound and Bharali (2018) applied Indian sandal wood leaf powder for F^- removal from water solution. Their study proved that the data were in good agreement to Temkin, Langmuir, and Freundlich isotherms. The observations revealed that Sandal wood leaf powder can be successfully used for F^- adsorption from aqueous media.

Mahvi *et al.* (2018) used ziziphus leaf as adsorbent for F^- removal. The investigations proved that the Langmuir model was highly fitted than the Frendlich isotherm. The study followed first-order kinetic model strongly. The work specified that the proposed adsorbent can be applied successfully for F^- adsorption.

Naghizadeh *et al.* (2017) used Nano-chitosan for F^- adsorption from water. They investigated to assess the efficiency of Nano-Chitosan for F^- uptake from the aqueous media. The results find out that high adsorption was taking place at pH=3. Pseudo second order kinetic model was applied successfully. The research concluded that Nano Chitosan can be successfully applied for F^- adsorption from liquid media.

Awasthi *et al.* (2016) stated that natural adsorbents can be proved a potential and economical alternative for F^- adsorption. They mentioned that there are several methods for Fadsorption from water but some of those methods are costly and difficult to afford by poor persons. Therefore a low-cost process, e.g. Adsorption is needed. The researchers investigated efficiency of few medicinal plants for F^- treatment.

Bharali and Bhattacharyya (2015) utilized neem leaves for F^- adsorption. Contact time, dosage quantity, and temperature were examined. They stated that the removal process followed Freundlich, Langmuir as well as Temkin models. They reported that this adsorbent can be applied effectively for F^- removal.

Mwakabona *et al.* (2014) compared the F^- adsorbing ability of sisal leaf biomass with other plant materials, having same functional groups but various solubility and stereochemistry of the active compounds. They stated that solubility of the active molecules have an important function in F^- removal by using plant biomasses, and therefore it was concluded that getting proper information's about the solubility and stereochemistry of these compounds was crucial for explaining the defluoridation efficiencies of plant biomasses.

Tomar *et al.* (2014) explained F^- removal from water using Lemon leaf powder under batch mode of experiments. The results indicated that both models (Langmuir and Freundlich) best followed in the study but most suitable was Freundlich model. This work reported that Lemon leaf could successfully remove F^- from water.

Shyam and Kalwania (2014) used Aloe Vera and Calcium Chloride for F^- removal from water. The effect of contact time, dose amount, pH and F^- level was studied. The adsorption isotherms (Langmuir and Freundlich) were modeled onto the data.

Ramanjaneyulu *et al.* (2013) applied Shell of Tamarind and the powder of Pipal leaves for F^- adsorption from Drinking Water. Different parameters were examined and optimized for F^- removal. Tamarind fruit shell showed maximum removal efficiency at pH 2, initial F^- amount (3 mg/L), contact time (90 min), adsorbent amount (2g/100ml). The Pipal leaf powder indicated 79% of highest removal rate at pH 2, dose of 2.0 g/L. They reported that the study followed both models (Langmuir and Freundlich).

Harikumar *et al.* (2012) used an herbal plant commonly known as Vetiver for F^- adsorption from water under batch method. Vetiver root activated with phosphoric acid revealed best removal efficiency than the fresh powdered root. The results found that F^- adsorption was higher by maximum dose and long time at a given initial adsorbate level. Freundlich and Langmuir models were drawn and kinetic constants were calculated in their study.

Piyush *et al.* (2012) investigated the de-fluoridation of water by using Tinospora Cordifolia under batch method and the isothermal models (Langmuir and Freundlich) were found suitable. They reported that the proposed adsorbent could be a best and inexpensive adsorbent for F^- reduction in water.

Maheshwari (2006) studied F^- in drinking water and its adsorption. They described a detailed information's about the existing F^- removal methods and benefits and short comings of each method. The study described that method selection should be site specific according to local requirement's and actual situations as each method has some drawbacks and no single technique can work for the aim in varied situations.

The influence of F^- concentration in the water on the F^- release from tea was investigated to check the ability of tea leaves to absorb F^- from water. Depending upon the F^- level of the water,

dried tea leaves were able also to absorb F^-. Thus, if a cup of tea is prepared of water having high F^- level, the F^- concentration of the infusion may actually be lesser than the original F^- amount of the water (Malde et al., 2006).

2.3. DEFLUORIDATION USING BIOCHAR (ADSORBENT)

Shahid *et al.* (2019) prepared biochar from cattle bones and it was used for F^- adsorption from water. The adsorbent was synthesized at various temperatures (350-700°C) and XRD, SEM, FTIR techniques were used for their characterization. The results revealed that about 10.56 mg of F^- was removed by 1 g of bone char. Both Freundlich and Langmuir models were plotted for the results and concluded that bone char could remove maximum F^- from contaminated water.

Ghosh and Mondal (2019) conducted a research work on F^- removal by using Al-impregnated *Eucalyptus* bark ash (Al-IEBA). The data followed three isotherm models and Freundlich model was more suitable than Langumir and other models. Similarly, the study of kinetics found that the Pseudo First-order model was fitted well than intra-particle-diffusion and Pseudo-Second-order models. The work concluded that removal of F^- with Al-IEBA could be achieved successfully.

Wang *et al.* (2018) used pomelo peel biochar (PPBC-La) loaded with lanthanum, for F^- adsorption and observed that the data were obeying Pseudo second-order kinetic and Freundlich model.

Roy *et al.* (2018) investigated tea waste biochar, which is chemically reduced and was applied for removal of F^- from wastewater. Various parameters were evaluated, and the data were fitted to isotherms, kinetics and thermodynamics. They stated that the equilibrium data was best suited to the Pseudo Second order kinetics model and Langmuir model. The prepared adsorbent achieved 98.31% F^- removal at optimum conditions.

Kanouo *et al.* (2018) discussed the quality of Biochar prepared from Corncob and Eucalyptus bark using a locally assembled Kiln. The adsorbents were characterized for physical properties and revealed that the kiln could be a suitable alternate for biochar production from locally available materials.

Roy and Das (2017) evaluated the F^- removal efficiency of activated biochar from wastewater. The adsorbent was characterized completely. Langmuir model was well suited to the

data. Study of thermodynamic displayed that F^- removal via activated biochar was endothermic. It was determined that activated biochar was inexpensive and environmentally friendly.

Papari *et al.* (2017) investigated F^- ion adsorption from liquid media, sea and groundwater using powdered and granular biochar of *Conocarpus Erectus* and was characterized through BET, FTIR and SEM. They stated that high F^- removal was occurred at 6 pH, for both adsorbents. The adsorption data was suitable to the adsorption model (Langmuir). Data also obeyed Second-order kinetics model.

Halder *et al.* (2016) investigated F^- adsorption onto a biochar activated by steam. The obtained from the shell of *Cocos Nucifera* and was analyzed through SEM, FTIR and XRD techniques. The study found that this adsorbent could be an important sorbent for the F^- remediation.

Fellet *et al.* (2014) studied the effect of various amended biochar on elements adsorption by metal accumulator plant species, which were cultivated on dumps of mine. The study focused on to know the effects of various biochar's produced from numerous biomasses. Biochar has great efficiency for phytoremediation but its effects are greatly dependent on parent material, which were vital for selecting biochar.

Mohan *et al.* (2014) studied F^- adsorption from ground water by two types of biochar (magnetic and nonmagnetic), prepared from corn Stover. Both the biochar were used for F^- uptake to substitute the existing commercial expensive adsorbents. F^- adsorption was high at pH 2.0. Pseudo-first order kinetics fitted well to the data. Both biochar's were efficient in removing F^- from contaminated water.

A research study was conducted on F^- uptake from water using activated carbon of sugarcane, wheat straw, and sawdust. The data was best suited to Freundlich adsorption model and Pseudo First and Second Order kinetics (Yadav *et al.*, 2013).

Mohan *et al.* (2012) reported the F^- removal from water using biochar at various pH, temperatures, and dose. High F^- removal was noticed at pH (2). Different adsorption models were applied.

Yao *et al.* (2011) utilized biochar for phosphate removal from water. Lab scale tests were made to evaluate phosphate sorption efficiency of the two types of biochar's, three Fe-modified

biochar/AC adsorbents and an activated carbon. The study disclosed that sugar beet tailings (anaerobically digested) can be used as source products for biochar preparation to reclaim phosphate.

2.4. DEFLUORIDATION USING ACTIVATED CARBON (ADSORBENT)

Choong *et al.* (2020) did their study on F^- removal by using functionalized carbon with magnesium silicate versus powdered activated carbon prepared from palm shell for water treatment. Their findings concluded that palm shell carbon (activated) could be an efficient sorbent for groundwater treatment containing high level of F^-, while functionalized carbon with magnesium silicate would be an alternate adsorbent for F^- reduction. Finally it was declared that both adsorbents can be successfully applied for adsorption of F^- from liquid media.

Kumari *et al.* (2020) used facile technique for preparation of a suitable adsorbent from alumina by nitric acid activation. F^- adsortion from water was studied on batch scale and indicated that Freundlich and Pseudo Second Order kinetic model were best fitted. The prepared adsorbent could also have the regeneration and reusability ability, which made it an important adsorbent for practical application in the field of wastewater treatment.

Mahvi *et al.* (2019) studied F^- removal from water using eucalyptus bark activated carbon (EBAC). Various parameters were studied. The study recommended that the F^- adsorption onto the EBAC was endothermic in nature.

Mukherjee *et al.* (2018) reported highest F^- removal of 89% by Aegle marmelos (bael shell/wood apple (BAC), whereas Parthenium hysterophorus (PHAC) removed 78% F^-. The Langmuir isotherm model was found well fitted and Pseudo-Second order kinetic was strictly obeyed. They reported that by comparing the adsorption capabilities of both the materials, the BAC was found an efficient adsorbent than PHAC for F^- reduction from aqueous media.

Singh *et al.* (2017) did research on adsorption of F^- from water by Bael shell activated carbon (ACBS) under batch operations. The kinetics, thermodynamic and equilibrium phenomenon was explained. The kinetics were well followed by Second-order kinetic model. The adsorption isotherm data followed Redlich–Peterson, Langmuir, Temkin and Freundlich isotherm well. F^- from real water samples was lessened to the acceptable level by using the proposed adsorbent.

Sajjad *et al.* (2017) conducted their research on the uptake of elements (potentially toxic) from industrial wastewater by applying activated carbon. Langmuir isotherm model showed best fitting to the data. The findings indicated the successful uptake of numerous potentially toxic elements from wastewaters by activated carbon (AC).

Regassa *et al.* (2016) used natural and activated Coal for F^- removal from water. High removal was occurred at pH (2) for activated coal and for natural coal (NC) at pH 4. The results were following Langmuir and Freundlich models. The study found that these materials could be successfully applied for F^- removal from groundwater.

Poudyal and Babel (2015) studied the efficiency of domestic sewage sludge and activated carbon (granular) for F^- sorption. The influence of different factors was investigated under batch mode at room temperature. Though maximum adsorption was noticed in acidic range, but study was performed at neutral pH from drinking water perspective. The sludge removal data well followed the Freundlich model.

Getachew *et al.* (2015) performed de-fluoridation study of water using banana peel and coffee husk activated carbon. The study presented that sufficient removal was noticed at pH value of 2 for both the adsorbents. By comparison it was noticed that coffee husk was more suitable than banana peel for removal of F^-. Langmuir model was well obeyed by the adsorption data. Likewise, pseudo second-order kinetics was best matched.

Suneetha *et al.* (2015) also applied active carbon obtained from the Vitex negundo plant barks for F^- adsorption from water. Different parameters were investigated under batch process in this study. They concluded that carbon (activated with nitric acid) was proved a suitable adsorbent for F^- removal from waters. Isotherm and kinetic model of Langmuir and Pseudo-second order was obeyed by the adsorption data, respectively.

Kumar *et al.* (2008) efficiently removed F^- by thermally activated carbon prepared from the neem and kikar leaves. Optimum pH was 6 for both materials in the study. The study found that adsorption process strictly followed the Freundlich model. Field water samples were also studied for F^- adsorption.

Daifullah *et al.* (2007) used rice straw activated carbon (modified with $KMnO_4$) for F^- removal from water. Pseudo Second order adsorption kinetics, Langmuir, Freundlich and

Dubinin–Radushkevich were practiced on the data. According to thermodynamic study, the nature of adsorption process was chemical.

Tripathy *et al.* (2006) worked on F^- adsorption using alum-impregnated activated alumina. About 99% F^- removal was achieved at pH 6.5. The desorption study concluded that regeneration of adsorbent is simple by following base–acid rinsing method, but re-impregnation was recommended for second time use of adsorbent for F^- sorption.

A study of F^- adsorption by carbonaceous adsorbents was performed, which stated that the procedure of F^- uptake onto bone char was chemical and endothermic in nature. The study concluded that bone char could be successfully applied for F^- adsorption from drinking water (Abe et al., 2004).

2.5. DEFLUORIDATION USING CLAY PARTICLES (ADSORBENT)

Lee *et al.* (2020) prepared and used thermally activated sepiolite for adsorption of F^- from water. The study found that the sepiolite activated at 950^0C was efficient in F^- removal than other temperatures. Langmuir and Pseudo-second order kinetics models were obeyed strictly. Likewise, thermodynamic study discovered that F^- remediation onto thermally activated sepiolite was endothermic in nature and could be useful for F^- elimination from liquids.

Nabbou *et al.* (2019) mainly studied the use of clay, and kaolinite for F^- adsorption from Saharan groundwater Algeria. Outcomes of the work declared that F^- removal was maximum at pH ranging from 4.5 to 6. The findings stated that Freundlich and pseudo second-order kinetics models were best followed. The process was endothermic in nature and recommended that the kaolinite was a successful adsorbent for F^- removal from groundwater.

Amor *et al.* (2018) investigated natural clay minerals for F^- from water. Their work mainly focused on developing inexpensive particles for removal of F^-. Two types of clays were studied under batch method for taking out F^- from drinking water to reduce fluorosis incidence. The results find out that F^- removal with kaolinite was more than smectite. Both models of adsorption (Langmuir and Freundlich) were best followed.

Iriel *et al.* (2018) examined the effectiveness of lateritic soil for F^- adsorption from water and the F^- adsorption data was applied to the model of Dubinin-Ataskhov showing that the F^- removal on the soils elements obeyed physical process with 0.48 mg/g removal efficacy. The study reported that lateritic soils could successfully be applied for defuoridation purposes at home level.

Mobarak *et al.* (2018) applied clay particles, which were highly rich in organic matter. The clay material was modified with cationic surfactant/H_2O_2 and was used for removal of F^-, which was observed under various parameters. Langmuir adsorption model and Pseudo Second-order kinetics was sufficiently followed by the data. This work proposed a novel technique for developing a new adsorbent prepared from clay and could be effectively applied for F^- reduction from water.

Vinati *et al.* (2015) conducted a detailed review of clay minerals as well as of clay for adsorption of F^- from water. Among the various available methods, adsorption method for de-fluoridation was thought an effective and easy way to develop and perform. The study reported the current trends in scientific research and improvement on the use of clay and clay elements for F^- segregation from water.

Ma *et al.* (2011) explored the F^- adsorption from liquids using granular bentonite (acid treated) under column and batch techniques. Batch experiments showed that high removal was occurred at pH of 4.95 and contact time (40 min) by well following Pseudo Second Order-kinetics model, Freundlich models and Redlich Peterson than Langmuir model. Similarly, the Column method experiments were made at various concentrations and changing speeds of flow, which best followed the Thomas model.

Fan *et al.* (2003) did studies on kinetics of adsorption for F^- using low cost adsorbents. They mainly focused on determining the kinetics of adsorption and removal efficiency of economic adsorbents at low F^- level. Different adsorbents were used and F^- removal on hydroxyapatite was observed in strong fitting to kinetics models, while others materials followed only the Pseudo second order equation.

Çengeloğlu *et al.* (2002) noticed the red mud efficiency for F^- adsorption from water. The study declared that highest removal was achieved at 5.5 value of pH and the Langmuir model was found suitable, illustrating the chemical nature of the process.

Srimurali *et al.* (1998) explained the F^- removal from water by different cheap materials. The study found that *Nirmali* seeds and lignite were not efficient adsorbents, while kaolinite clay was little better. Charfines and bentonite were proved efficient adsorbents. Similarly, chemical pretreatment of charfines showed no fruitful results for F^- removal from water.

On the basis of the relevant literature review, the following research questions have been framed.

- No research study on the main causes of fluorosis in the area was conducted before this study.
- The excessive F^- in the groundwater of the area might be the main cause of fluorosis.
- We can prepare good quality adsorbent for F^- removal from the bark of *Dodonaea viscosa*, locally abundantly available plant.
- The excessive F^- could be removed by applying biochar as an adsorbent prepared from locally available biomass adsorbents.
- The biochar application as an adsorbent for F^- may or may not be the actual solution for preventing fluorosis in the area.

CHAPTER 3

MATERIALS AND METHODS

3.1. STUDY AREA PROFILE

The investigated region is located at longitude 71°43′22″ E and latitude 34°29′38″. The area is at a distance of 120 kilometers north of Peshawar city in the district Malakand, Khyber Pakhtunkhwa. The study area is about 550 m above from sea level and the Hazarnau, which has an elevation of about 1900 m, is the highest peak in the area. The climate is semiarid to arid with average rainfall of 600 millimeter (mL) per year. The temperature of the area is variable, but the annual maximum temperature is about 40 °C in June-July and a minimum 0 °C in December-January (Zabihullah et al., 2006).

The soil structure ranges from clay to coarse materials with a predominance of sands. The soil of the area is generally classified into four types including loamy, sandy, clay and semiarid. The 4047 hectares of the area are common property, mostly mountains under the forest cover, but according to a recent study, 25% plant species were endangered, 29% were vulnerable, 15% were rare while 24% were infrequent and the main reasons for plant species vulnerability were overgrazing and extensive anthropogenic activities (Muhammad et al., 2018). The total population of the area (Union Council Kot) was 25961 (PBS, 2018) and onions, wheat, maize, and tomato are mainly harvesting crops. The main water sources of the area are springs, bore wells, dug wells, tube wells, and stream water and the peoples of the area use this water for drinking, bathing, washing, and other household uses.

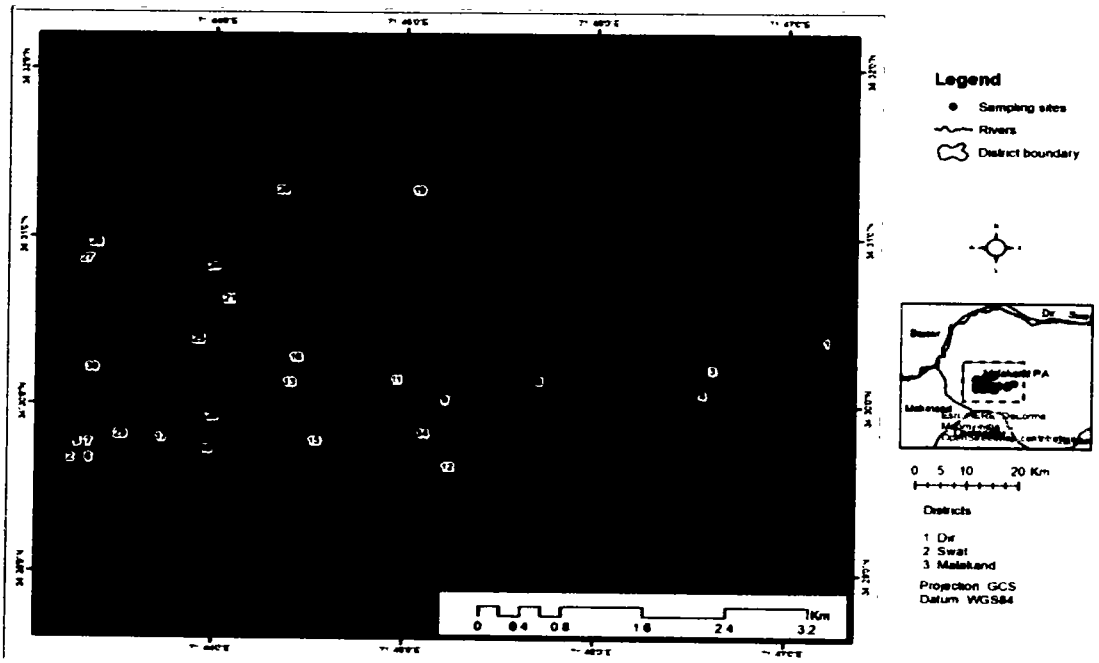

Figure 1: Map Showing Samples collection Points

3.2. GEOLOGY OF THE AREA

Epidote, Beryl, Rutile, Chromite, etc. are the significant minerals that have been discovered from the study area and its surroundings. Besides feldspar and quartz, fluorite is generally linked with beryl. Key mineral elements are feldspar, mica, garnet and quartz and the accessory minerals are graphite, magnetite, amphibole, apatite, magnetite, and muscovite etc (Hussain et al., 1984). Malakand and its adjacent regions geology mainly contains various stages rocks (granitic and metamorphic) (Khaliq et al., 2003). Calcite, fluorite and tourmaline ingredients were observed in some pegmatites (Chaudhry et al., 1976; Chaudhry et al., 1974). In Barh and Kot-Batoo zone, some main anticlines were discovered. The key synclines of local extension passes via the middle of granite (Malakand) in NE-SW side and in Barh (south side) stream with many native synclines in the region (AHMAD et al., 2003; Khaliq et al., 2003).

3.3. WATER SAMPLES COLLECTION AND TREATMENT

Water samples (n = 30), were obtained from bore wells, open dugwells, community tube-wells and hand pumps after proper purging. For major cations measurement the samples filtration was done using filter paper (0.45 μm size). Samples pH was brought <2 by adding HNO_3 (50% diluted) and were kept in clean polyethylene bottles (500 ml).

3.4. PHYSICOCHEMICAL ANALYSIS

Electrical conductivity (EC), pH and total dissolved solids (TDS) were determined on the spot by their respective electrodes. Alkalinity was measured titrimetrically and sulfate (SO_4) spectrophotometrically by following Standard Method (APHA AWWA, 1998). Chloride and F^- levels were determined by Mohr's technique and F^- meter (ExStik FL—700) respectively. Flame photometer (AFP−100) was used for K, Na and Ca analysis. Concentration of magnesium (Mg) was determined by using atomic-absorption spectrometer.

3.5. STATISTICAL CALCULATIONS

Correlation (Pearson) and principle component analysis (PCA) were done by XLSTAT, other statistical analyses were performed through Microsoft Excel (2013) and Grapher ™ (Version 13) was used to draw Gibbs and Piper plots.

3.6. CHEMICALS/REAGENTS

Ultrapure analytical grade chemicals were procured from International suppliers.

3.7. *DODONAEA VISCOSA* LEAF POWDER (DLP) PREPARATION

Dodonaea viscosa plant leaves were properly washed after collection and were fully sun dried for about 72 hours before making its powder, which were then passed via sieve to get the desired size (less than 1.5 mm). DLP (40 g) and 1 M HNO_3 (400 mL) were poured in conical flask (1000 mL), which were then heated (20 min). After filtration, dH_2O was used for powder washing

and again subjected for treating with 0.5 M NaOH (400 mL). The mixture was reheated for 20 min (1,000 ml conical flask). The powder were thoroughly rinsed again with dH_2O and were dried in a drying oven for 3 hours (110°C). After proper cooling, the powder were stored for analysis (Tomar et al., 2014).

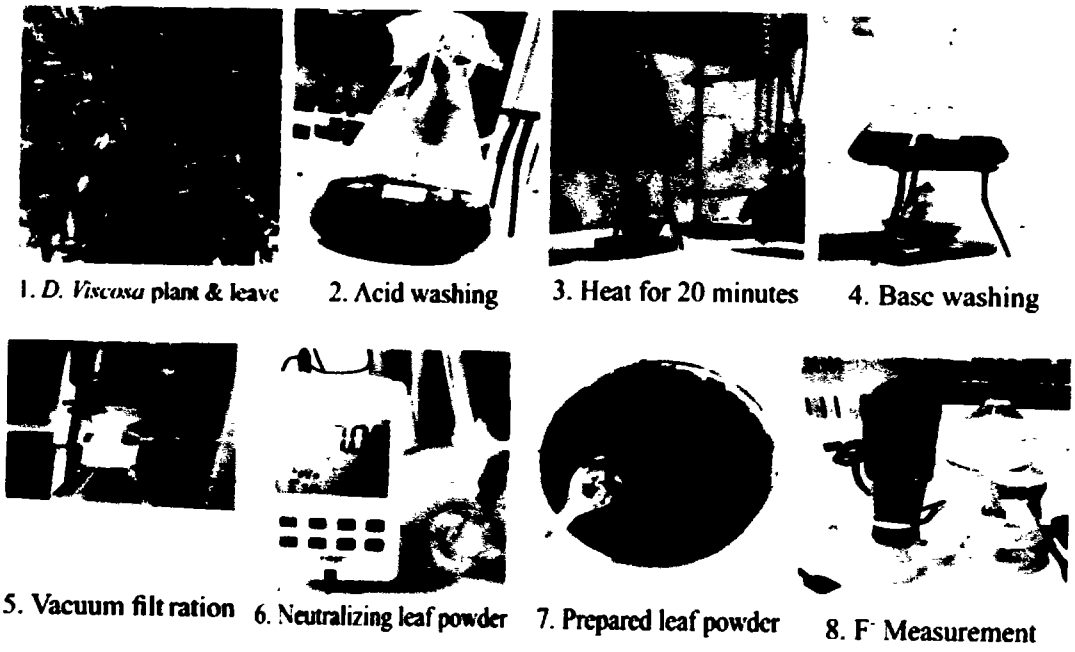

Figure 2: Stepwise DLP Preparation and its Application for F^- Removal

3.8. GRANULAR ACTIVATED CARBON (GAC)

GAC was purchased from a local supplier and was applied for F^- adsorption from water beyond any modification (chemically or physically).

3.9. CLAY PARTICLES

Clay particles were obtained from a local potter shop and were grounded manually. The clay was washed and purified by sedimentation using freshly prepared distilled water. After removing some organic matter particles and other impurities, the clay was isolated from water, which was

then subjected to drying (at 105 ^{0}C) for one day. After the drying, the clay was used for F^- removal without any physical or chemical activation (Nabbou et al., 2019).

3.10. *DODONAEA VISCOSA* BARK BIOCHAR (DBBC) PREPARATION

After the collection, the plant bark was rinsed with distilled water and was dried (at 80 °C) for 72 hours. The bark was broken into tiny pieces manually and was feed in a steel cylinder (8 inch height and 5 inch width) already purged with nitrogen gas (10 psi). After feeding, the cylinder was re-purged with nitrogen gas to make an inert atmosphere and was pyrolized in a furnace (purged with nitrogen gas) for two hours at different temperatures ranging from 250 °C to 1000 °C. In this way, four different types of biochar were prepared at 250 °C, 500 °C, 750 °C, 1000 °C. After pyrolysis, the biochar samples were allowed overnight to cool down in the furnace. After 11 hours, the biochar containing cylinder was taken out from the furnace and the biochar were transferred to a glass container for placing in a desiccator. After complete cooling, the biochar were passed through a sieve having size less than 1.5 mm and were kept in a glass container for further experimental work (Choudhary et al., 2017; Wang et al., 2018), which were labeled as BC250, BC500, BC750, and BC1000 on temperature basis.

3.11. CHARACTERIZATION OF BIOCHAR

3.11.1. Percent Yield

The percent yield (Y) of biochar was calculated according to (Du et al., 2019) as following.

$$\text{Percent Yield} = \left(\frac{W1}{W2}\right)100 \qquad \text{Euation (1)}$$

Where W_1 and W_2 are the weights of the biomass before and after pyrolysis, respectively.

3.11.2. Moisture Content

The moisture content was calculated according to (Rajapaksha et al., 2019).

3.11.3. Bulk Density

A clean 5 mL tube was weighed (W_1) and filled with biochar sample and weighed again (W_2). The difference between W_2 and W_1 is the mass of biochar in the tube. The bulk density of biochar was calculated through the following formula (Roy & Das, 2017).

$$\text{Bulk Density} = \frac{W2 - W1}{\text{Volume}} \qquad \text{Equation (2)}$$

3.11.4. pH and Electrical Conductivity

The pH and EC of DBBC were calculated by mixing biochar samples and fresh distilled water (1:5), which were stirred at 110 rpm. Afterward, giving it 30 minutes, the pH and E.C of the supernatant were determined by pH meter and EC meter, respectively (Tang et al., 2019).

3.11.5. Point of Zero Charge (PZC)

The pH_{pzc} of the biochar was measured by following the solid addition technique (Balistrieri & Murray, 1981). First prepared, a sequence of flasks (100 ml), having 0.1 M NaCl (50 mL) solution with initial pH (pHi) ranging from 2 to 11 adjusted with 1 M hydrochloric acid or 1 M sodium hydroxide solutions. Before shaking for 4 hours at 150 rpm and 25 °C on a magnetic stirrer, biochar sample (0.1 g) was administered to these flasks and the supernatant final pH (pH_f) was determined by pH meter. The change between pHinitial and pH_{final} ($\Delta pH = pHi - pH_f$) was calculated. Then, a graph was drawn between initial pH (pHi) values and the difference of (initial and final) pH values. The intersection point of the obtained curve and pHi was noted as PZC.

3.11.6. SEM/EDS

The biochar samples were examined through SEM and EDS using KYKY-EM6900 (China) SEM instrument. The biochar samples for SEM and EDS were prepared according to (Fellet et al., 2014) and the operating parameters are shown over each image in chapter 4.

3.11.7. FTIR

The biochar samples were characterized for surface organic functional groups by FTIR tecnique on an IR-Tracer-100 (Shimadzu) spectrometer between 400 and 3600 cm^{-1}. A sample of biochar for FTIR study was made according to (Mohan et al., 2012).

3.12. FLUORIDE SOLUTIONS

Fluoride stock solution (1000 mg/L) was synthesized by taking appropriate amount (2.21 g) of sodium fluoride (NaF) in 1 L of deionized water. Different F^- solutions (100 mg/L, 10 mg/L, 6 mg/L, 5 mg/L, 2 mg/L, 1mg/L) were prepared from 1000 mg/L F^- solution. F^- in the samples and solutions was measured via F^- meter (ExStik FL-700). F determination followed the adding of one TISAB (Total-Ionic-Strength Adjustment-Buffer) tablet to the 20 ml of the sample and then the F^- meter was immersed in the sample and the screen showed the F^- concentration in mg/L. TISAB was provided with the F^- meter by the company. Shaker model NB-205L made in Korea was applied for shaking of samples. Solutions pH during the experiments was measured by pH meter (HI2002). BDH buffer solutions supplied by the company with meter were used for calibration and standardization. The remaining F^- levels in the solutions were determined via F^- meter (Tomar et al., 2014).

3.13. pH ADJUSTING SOLUTIONS

- HNO_3 (0.5 M) solution was prepared in 250 ml volumetric flask from molarity calculations. 5.5 ml of nitric acid were taken and were diluted with distilled water up to the mark.
- NaOH (0.1 M) was prepared by adding 1 g of sodium hydroxide (NaOH) in 250 mL freshly prepared deionized water for pH adjustment.

3.14. ADSORPTION STUDIES

Specific amount of adsorbent was added in 100 ml conical flasks having 50 mL F^- solution and were placed for shaking in a shaker (NB-205L, Korea) for 145 min, 200 rpm and 30°C except, where contact time effect was investigated. HNO_3 (0.5 M) or NaOH (0.1 M) were used for pH

adjustment during the investigation of the influence of different factors on F^- adsorption. The solution was filtered by filter paper (Whatman) # 42 and F^- level in the filtrate was measured through the F^- meter (Tomar et al., 2014). This study particularly concentrated on the parameters effecting adsorption process e.g. dose amount, pH, initial concentration of adsorbate and contact time. Each parameter was optimized for maximum removal efficiency. During optimization of a specific parameter, the remaining parameters were kept constant and the conditions of that specific parameter were changed. Equation (3) was used for calculating percent removal of the F^- and equation (4) was used for determining F^- adsorbed q_e (mg/g) at equilibrium. Similarly equation (5) was used for calculating q_t, which is the quantity of F^- removed (mg/g) at time t.

$$\text{Percent Fluoride Removal} = \left(\frac{Ci - Ce}{Ci}\right) 100 \qquad \text{Equation (3)}$$

$$\text{Fluoride adsorbed at equilibrium qe (mg/g)} = \left(\frac{Ci - Ce}{W}\right) V \qquad \text{Equation (4)}$$

$$\text{Fluoride adsorbed at equilibrium time qt} \left(\frac{mg}{g}\right) = \left(\frac{Ci - Ct}{W}\right) V \qquad \text{Equation (5)}$$

Where, C_i and Ce (mg/L) are the initial and equilibrium time concentrations of F^-, respectively. Similarly the F^- concentrations at time (t) was represented by Ct (mg/L), W is the dry adsorbent weight in grams (g) and V denotes the volume (L).

3.14.1. Dose Effect

Different adsorbents were studied in different range of doses to select a best amount of dose for F^- removal. All experiments were conducted at pH 7 except for DLP where the pH was kept at 2 because at 7 pH its F^- adsorption efficiency was very low as compared to at pH 2. Maximum time selected for all initial experiments was 145 minutes, revolution per minute (rpm) was 200, and the temperature was kept at 30 ^{0}C. Dose range for *Dodonaea viscosa* leaf powder adsorbent was from 1 to 10 g and for biochar as well as for commercial granular activated carbon (GAC) and

clay was from 1 to 7 g. The dose amount which showed higher adsorption of F^- from the solution, was chosen as the best dose for further analysis.

3.14.2. pH Study

The effect of pH was studied from 2 to 10. During the experiments, the F^- solution was taken in 100 ml flasks having various pH (2, 4, 6, 7, 8, and 10). Adjustment of pH was performed via 0.1M NaOH and 0.5M HNO_3. After pH adjustment, the required amount of each adsorbent dose was administered in the flasks and was shaken at 200 rpm for 145 min. The remaining F^- level in the filtrate was measured through the F^- meter and pH was optimized for each adsorbent.

3.14.3. Contact Time Study

Contact time was calculated at various times from 5-145 min. The solution pH was kept 7 and optimum dose of each adsorbent was shaken at 200 rpm and at temperature of 30 °C at different intervals 5, 15, 25, 35, 45, 55, 65, 75, 85, 95, 105, 115, 125, 135 and 145. The optimum time was selected after getting equilibrium.

3.14.4. Initial Concentration Effect

The effect of initial F^- concentration ranging from 2-10 mg/L was determined, while the pH, dose, contact time and temperature were maintained at their optimum values. F^- Solutions having various initial concentrations were synthesized from freshly prepared stock solution of 100 mg/L of F^-. The samples were placed in the shaker at 200 rpm, 30 °C temperature, pH 7 and for time 145 minutes. After shaking the remaining F^- was determined through the F^- meter.

3.15. ADSORPTION ISOTHERMS MODELS

Langmuir and Freundlich are suitable models for the explanation of adsorption procedure by various adsorbing materials (Langmuir, 1916; LeVan & Vermeulen, 1981). The linear forms of

these models were plotted to the equilibrium removal data for the materials studied. The study was conducted at various F^- concentrations ranging from 2-10 mg/L (2, 3, 5, 6, 8 and 10 mg/L).

3.15.1. Langmuir Model

The model describes single layer adsorption of F^- over homogeneous surface of adsorbent and is denoted by the equation as follows (6).

$$\frac{1}{qe} = \frac{1}{Q0} + \frac{1}{bQ0Ce} \qquad \text{Equation (6)}$$

Where, $C_e = F^-$ concentration (mg/L) at equilibrium, q_e denotes the quantity of F^- adsorbed per unit mass of adsorbent (mg/g), Q_o and b are the Langmuir parameters. The constants b and Q_0 were obtained from the fitting curve slope and intercept, by plotting $1/q_e$ against $1/C_e$.

3.15.2. Freundlich Model

Generally Freundlich model is denoted by the equation (7) (Freundlich, 1906; LeVan & Vermeulen, 1981).

$$\text{Log } qe = \text{Log } Kf + \left(\frac{1}{n}\right) \text{Log } Ce \qquad \text{Equation (7)}$$

Where, 1/n and K_f are known as Freundlich parameters. The 1/n is equal to the slope and shows the surface heterogeneity. Mostly, n and K_f can be attained from the curve slope and intercept drawn between Log q_e vs. Log C_e. R^2 values show the fitness of these models to the data achieved. Higher R^2 value means better fitting of the model to the data.

3.16. KINETIC STUDIES

The kinetics studies are helpful for the equilibrium time calculation. The remaining F^- level in the filtrate was measured after known intervals of time and qt, (mg/g) was calculated from equation (8):

$$qt = \left(\frac{Ci - Ct}{W}\right)V \qquad \text{Equation (8)}$$

Where, C_i is initial concentrations (mg/l) and C_t is amount of F^- at any time t. W represent weight (g) and V means volume of solution (L). The kinetic data were applied to two commonly used kinetics linear models as described under.

3.16.1. Pseudo-First-Order

The experimental kinetic data from batch study was applied and the model was calculated according to equation (9):

$$Log(qe - qt) = Logqe - \frac{k1}{2.303}t \qquad \text{Equation (9)}$$

Where, q_e is equilibrium adsorption capacity, which must be predetermined and qt (mg/g) is the removal at time, t (min), while k_1 (min^{-1}) is rate constant. The values of the rate constant were calculated by plotting Log (qe-qt) against t.

3.16.2. Pseudo-Second-Order

The adsorption kinetics were also described by following the below formula for the model:

$$\frac{T}{qt} = \frac{1}{h} + \frac{1}{qe}t \qquad \text{Equation (10)}$$

Where the initial adsorption rate is denoted by h (mg/ (g. min)) and is equal to $k_2q_e^2$. The rate constant is 'k_2' (g/mg min) and quantity of F^- adsorbed at equilibrium is shown by q_e (mg/g). Similarly the F^- adsorbed at any time t is indicated with q_t (mg/g) value. The constants were achieved by plotting t/qt values versus t.

CHAPTER 4

RESULTS AND DISCUSSION

Results of DBBC characterization i.e. pH, E.C, pH_{pzc}, percent yield, moisture content, bulk density, FTIR, SEM and EDS, are listed in this chapter along with full details of the findings of the studied parameters (adsorbent amount, pH, contact time and initial F^- level). Similarly, the results of the F^- removal data modeling over Langmuir and Freundlich models as well as Pseudo-First-Order and Pseudo-Second-Order kinetics are explained here.

4.1. RESULTS OBTAINED FROM WATER SAMPLES ANALYSIS

The basic statistics of the assessed parameters of the ground water samples along with WHO permissible limits are listed in Table 1, which shows that pH of all water samples collected from Barh, Maina, Sunni Sakhra, Munai Sha and Batoo areas were within the WHO permissible limits. The EC values in all samples were beyond the limits except few samples, whose EC values were below the WHO limit. Similarly, TDS values of the samples were within the WHO limits except for two samples in Barh area. This change in TDS and EC levels shows that the groundwater characteristics were not uniform and governed by various factors (Nagarajan et al., 2010). Based on the TDS levels, most of the groundwater were of fresh waters (TDS less than 1,000 mg/l) (Freeze & Cherry, 1979). The dominant anions in the studied area were SO_4 and bicarbonates (HCO_3), while Cl was only dominant in Barh area. Na and Ca were abundant cations in all areas except Batoo region where Ca was the dominant cation. The values of all cations were within the WHO values. The ratio of Na and Cl in groundwater samples from Barh (0.42–4.76 mg/L), Maina (0.67–8.3 mg/L), Sunni Sakhra (0.78–4.24 mg/L) and Batoo (0.86–1.68 mg/L) areas shows geogenic origin of both minerals (halite and silicates), while in the Monai Sha area the Na/Cl ratio (1.05–3.54 mg/L) of the samples shows that source of Na is weathering of silicate minerals only (Meybeck, 1987). In all water samples, the anions sequence was SO_4 >HCO_3 >Cl >F, and while the cations order was Na>Ca>Mg>K, except Batoo area, where the cationic order was Ca>Na>Mg>K. The concentrations of all anions were within the WHO limits, except F^-.

Table 1: Statistical presentation of groundwater samples (n=30)

Samples area ⟶		Barh (n=6)		Maina (n=6)		Sunni Sakhra (n=6)		Munai Shaa (n=8)		Batoo (n= 4)	
Statistics	WHO	Range	Mean ±SD	Range	Mean ±SD	Range	Mean ±SD	Range	Mean ±SD	Range	Mean ±SD
pH	6 5–9 2	6 6–7 5	7 ± 0.3	7 2–8 5	8 ± 0.5	7 4–7 7	7±0.4	6 8–8 2	8 ± 0.4	7 1–7 7	7±0.2
E.CμS/cm	400	527–2470	1334± 96	294–1180	733±295	369–1070	789±270	222–1328	663±399	668–1063	884±207
TDS mg/L	1000	263–1235	667±398	147–590	366±147	184–535	394±135	111–664	331±199	334–532	442±103
F^- mg/L	1.50	0 2–5 3	2.5±2.1	0 5–4 8	2.5±1.6	1 8–5 5	3.5±1.2	1 2–5 5	2.4±1.4	0 7–3 1	2±1.01
Cl^- mg/L	250	11–333	131±144	4–53	28±20	11–67	33±23	11–64	28±18	18–50	34±14
SO_4 mg/L	500	280–468	372±70.7	318–411	365±38	343–450	378±42	350–387	364±15.4	357–477	408±56.4
HCO_3mg/L	–	50–255	163±77	60–195	159±50	35–265	198±85	60–360	163±95	120–225	175±50
Na mg/L	200	31 8–152	87±51	33 2–89 5	54±20.8	21 2–70 9	50.5±17	19 8–117	46.8±32	30 4–47 3	40±7.18
K mg/L	12	1 5–30 7	11±12.6	0 9–10 2	2.7±3 6	0 8–1 3	1.13±0.2	0 7–1 6	1.46±0.84	1 3–2 7	1.7±0.62
Ca mg/L	100	39 2–141	83±40.7	26 3–74 4	50±15.3	25 1–58 9	46±13 2	8 8–60 7	34±21.5	48 2–57 6	52.6±3.85
Mg mg/L	50	18 3–32 2	24.4±4.7	17 2–30 7	24.1±4.8	12 4–27 2	20.7±6.1	13 9–30 0	23±5.6	22 7–31 9	27.2±3.8

4.2. FLUORIDE LEVEL

Fluoride level was beyond the WHO limit for drinking water (Table 1). The area wise order of F^- concentration was; Sunni Sakhra > Munai Shaa > Barh > Maina > Batoo. The geological structure of Malakand and nearby regions comprises of granitic and metamorphic rocks of various stages (Khaliq et al., 2003). Several researchers investigated that host rocks in the study area were mostly rich in fluorite, which was usually associated with beryl. Therefore, the F^- bearing minerals (fluorite) in the parent rocks (both granite and gneissic) of this area were responsible for the F^- contamination (Khaliq et al., 2003) and thus were causing fluorosis in the study area.

4.3. CORRELATION

Pearson's Correlation matrix (Wu et al., 2014) was practiced for studying the interrelationship between drinking water physicochemical factors at a significance level of 0.05 (Table 2). F^- showed both positive and negative correlation with HCO_3, Na and Ca, Mg, SO_4, K, Cl, respectively. Because of the natural dissolution of F^- from the underlying strata, F^- and Na are positively correlated. Similarly, Na was found in significant positive correlation with Ca, HCO_3, Cl, and SO_4, and these ions are highly responsible for maximum total alkalinity and total hardness of water. Na, Ca and K were in strong positive correlation with HCO_3 which suggest the chemical interaction of silicates with CO_2 and water. For example, albite dissolution produces HCO_3 and Na in groundwater (Li et al., 2016).

Table 2: Pearson's correlation between different parameters of water samples (n=30)

Variables	pH	E.C	TDS	F^-	Cl	HCO_3	Na	K	Ca	Mg	SO_4
pH	**1**										
E.C	-0.241	**1**									
TDS	-0.241	**1.000**	**1**								
F^-	-0.056	-0.151	-0.152	**1**							
Cl	-0.283	**0.868**	**0.868**	-0.021	**1**						
HCO3	0.086	**0.618**	**0.618**	0.013	0.304	**1**					
Na	-0.241	**0.868**	**0.868**	0.244	**0.807**	**0.568**	**1**				
K	-0.217	**0.703**	**0.703**	-0.325	**0.650**	0.210	**0.617**	**1**			
Ca	-0.282	**0.960**	**0.960**	-0.147	**0.856**	**0.506**	**0.834**	**0.683**	**1**		
Mg	0.099	0.012	0.012	-0.061	-0.043	0.083	0.020	0.189	-0.022	**1**	
SO4	0.164	**0.590**	**0.591**	-0.297	**0.575**	0.304	0.325	0.337	**0.493**	-0.050	**1**

Bold figures are changed from 0 with a significance level alpha=0.05

4.4. GIBB'S DIAGRAM

Weathering of parent rocks and anthropogenic sources are greatly responsible for changing the groundwater chemistry of a region. Gibb's diagram (Gibbs, 1970) basically explain the three controlling mechanisms i.e. precipitation, evaporation, and water-rock interaction and was established by drawing TDS values versus the weight ratios of cations and anions (Figure 3). The

diagram represented that the maximum samples were occupied in the water-rock interaction zone. The diagram implies that the local hydrogeological conditions and weathering processes participate greatly in making of groundwater quality in this region.

$$\text{Anions ratio} = \frac{\text{Cl}}{(\text{Cl} + \text{HCO3})} \qquad \text{Equation (11)}$$

$$\text{Ratio of Cations} = \frac{\text{Na}}{(\text{Na} + \text{Ca})} \qquad \text{Equation (12)}$$

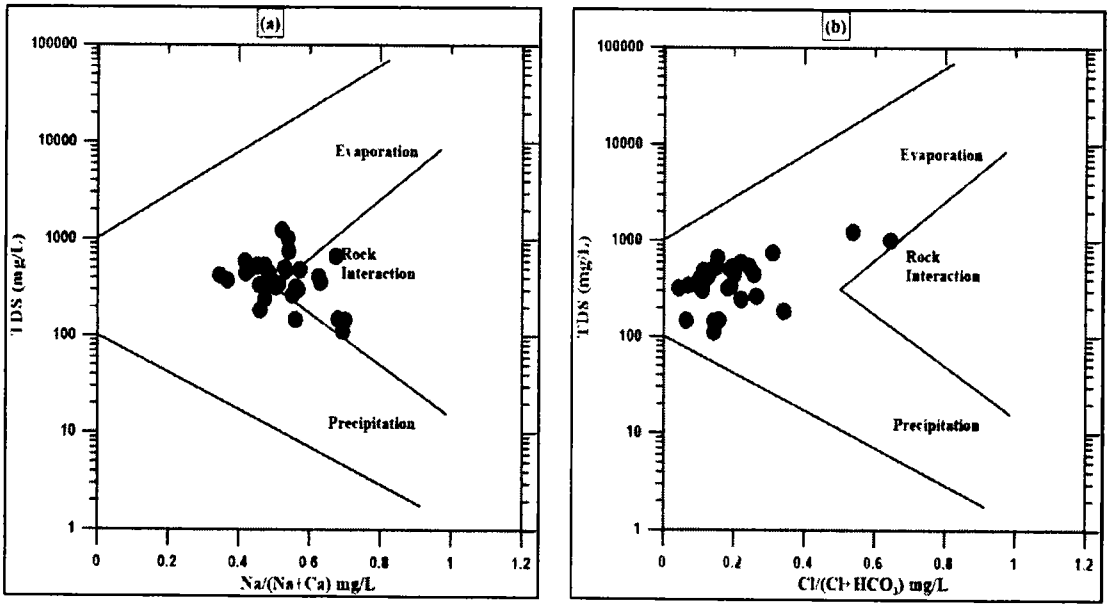

Figure 3: Gibbs Diagram (a) Na/ (Ca + Na) mg/L against TDS mg/L (Cationic); (b) Cl/ (HCO_3 + Cl mg/L versus TDS mg/L (Anionic)

4.5. PRINCIPAL COMPONENT ANALYSIS (PCA)

PCA was applied to work out the causes of groundwater contamination. PCA was calculated by Varimax rotation (Kaiser normalization) and F1, F2, and F3 were the drawn factors. Results of PCA (Table 3) revealed that HCO_3, Cl, K, Ca, Na, Mg, and SO_4 controlled the water characteristics and that the origin is mainly natural. Finding out potential sources of pollution helps in reducing the variables number with high loading. The results of 11 hydrogeochemical observations of 30 water samples showed three major eigenvalues (Table 3). The maximum contribution was of F1 in variability with an eigenvalue of 5.82 and is mostly dominated by hydrogeochemical variables like Na, TDS, EC, HCO_3, SO_4, Ca, K and Cl and their correlation coefficients were calculated

(Table 3). These parameters depict that anions and cations are mainly coming from the interaction of rock and water as well as from weathering of available minerals (Purushotham et al., 2011). F2 contributed 12.86% in variability (eigenvalue = 1.41). High loading for F^- and Na was evident. Therefore, natural processes take great part in presence of F^- in this region. The substantial contribution of F2, which is generally caused by natural activities, comprising weathering of carbonate and minerals dissolution (fluorite, feldspar, muscovite, biotite, and calcite) considerably affecting the groundwater quality. Presence of K may be due to plagioclase, orthoclase and muscovite feldspar minerals found in salt deposits containing sylvite (KCl) and granite rock. Factor F3 shows 10.81% of the over-all variance and 1.19 eigenvalue. A high loading of pH, F^- and HCO_3 was observed here (Table 3). HCO_3 comes from carbonate dissolution and biodegradation of organic matter (Ayoob & Gupta, 2006; Young et al., 2011). Three factor variables with various factor loadings suggests that the hydro-geochemistry of groundwater is not uniform. HCO_3 and Na have good positive factor loadings and shows that these ions are mainly coming from the same origin e.g. Gypsum and carbonate dissolution as well as from weathering mechanisms. Mg may be coming from the water-rocks interaction because it shows moderate positive loadings.

Table 3: The loading matrix of varimax RPCA and factor composition in groundwater

Component	(F1	F2	F3)
pH	-00.25	**-0.57**	**0.64**
E.C	**0.99**	-00.01	0.03
TDS	**0.99**	-0.01	0.03
F^-	-0.13	**0.78**	**0.47**
Cl	**0.90**	0.10	-0.11
HCO_3	**0.58**	-0.03	**0.59**
Na	**0.88**	**0.34**	0.19
K	**0.75**	-0.16	-0.34
Ca	**0.96**	0.05	-0.06
Mg	0.03	-0.27	0.12
SO_4	**0.59**	**-0.49**	0.11
Eigen value	5.8167	1.4142	1.1885
Variability (%)	52.8795	12.8565	10.8050
Cumulative %	52.8795	65.7360	76.5410

Note: Values in bold are considered significant.

4.6. PIPER DIAGRAM

Data of biochemical examination of water samples were modeled on the Piper plot (Piper, 1944) to classify water into different classes (Figure 4). The plot showed that the waters of the study area are mostly dominated by mixed Ca—Mg—Cl^- water type, which shows that the samples comes under the rock forms of mixed Ca—Mg—Cl^- type. The possible reason for this type of water may be the local geology of the area, which contains igneous rocks, in which the major units of gneisses and granites were found (Khaliq et al., 2003). Similarly, chemical processes (Reverse-Ion-Exchange) are also accountable for the formation of [mixed Ca—Mg—Cl water type. None of the samples fall under Na—Cl and Na—HCO_3 zone, which shows the absence of waters that comes from halite dissolution (saline). Groundwater also get SO_4, Ca and Mg from gypsum, calcite and dolomite weathering (Ruiz-Pico et al., 2019).

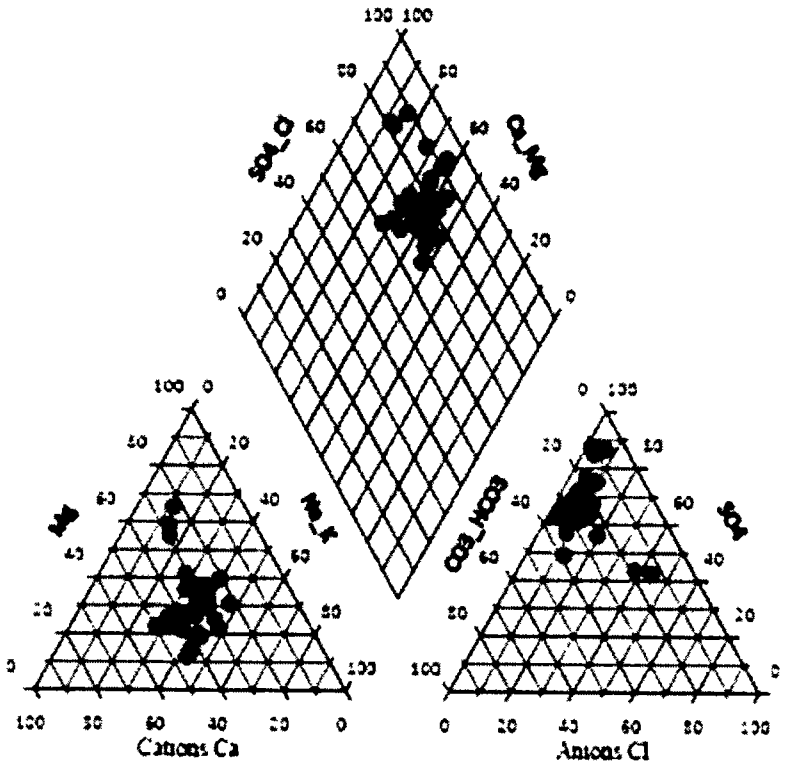

Figure 4: Piper Trilinear Diagram for Water Classification

4.7. COMMUNITY FLUOROSIS INDEX (CFI)

The observed symptoms of dental-fluorosis in the peoples were categorized into 7 groups on the basis of the Dean's equation (Dean, 1942; Dean & Elvove, 1935) and a numerical value was allotted to each group i.e. severe (4), moderately severe (3), moderate (2), mild (1.5), very mild (1), questionable (0.5), and normal (0) . Various persons were observed and classified into different groups. Then the CFI was calculated according to the following equation (13):

$$CFI = \Sigma \frac{(\text{Number of persons} \times \text{Dean's numerical weight})}{\text{Total number of persons examined}} \qquad \text{Equation (13)}$$

If CFI value is greater than 0.6 it shows the presence of health-related issues to the residents of the region.

The percent frequency of fluorosis (dental) was determined by the ratio of number of persons suffering from fluorosis to the total number of persons studied. During the study, 552 boys, 309 girl students (8 to 16 years of age), 800 men and 400 women (17 to 62 years of age) were visited. The percentage of dental fluorosis and its CFI values are recorded in Table 4. Assessment of health risk i.e., CFI was determined by using Dean's formula. The values of the CFI and percent incidence of fluorosis in all endemic areas are given in Table 4. The percent fluorosis incidence is higher in those areas, where F^- concentration is maximum (Table 1 and 4). The values of the CFI and percentage occurrence of fluorosis showed that teenagers specifically females are at high risk, because the females spend most of their time at home and all the routine activities are done at homes. They rarely come out of their home, that's why they consume much F^- containing water and are highly suffered by fluorosis (Rashid et al., 2018). Similarly, mining operations, minerals exploration and digging of new bore wells also increase water pollution in the investigated area. The maximum usage of this contaminated water increases the incidence of fluorosis in this area.

Table 4: Community fluorosis-index (CFI) and dental-fluorosis incidences in the study area

Location	Group	No. of persons inspected according to Dean's taxonomy							Total Individuals	Community fluorosis Index (CFI)	%age of fluorosis incidence
		0	0.5	1	1.5	2	3	4			
Barh	Boys	3	6	7	8	12	5	9	50	1.94	52
	Girls	2	4	7	4	5	8	5	35	1.97	51
	Male	15	10	20	18	24	18	15	120	1.78	48
	Female	3	6	7	8	5	13	8	50	2.06	52
Maina	Boys	7	4	8	10	7	11	8	55	1.89	51
	Girls	8	4	5	6	8	9	5	45	1.75	49
	Male	50	36	23	28	20	30	13	200	1.32	32
	Female	6	8	13	16	14	17	6	80	1.80	46
Sunni Sakhra	Boys	2	4	5	6	7	9	7	40	2.12	58
	Girls	0	2	3	4	5	6	5	25	2.32	64
	Male	15	16	13	12	8	14	12	90	1.61	38
	Female	2	8	5	10	4	7	4	40	1.72	38
Munai Shaa	Boys	5	4	6	10	8	9	8	50	1.96	50
	Girls	6	2	6	4	8	9	5	40	1.90	55
	Male	30	20	15	39	44	75	48	150	1.54	39
	Female	7	6	9	16	20	14	8	80	1.87	53
Batoo	Boys	10	6	4	4	8	5	3	40	1.40	48
	Girls	8	2	5	2	3	3	2	25	1.28	32
	Male	8	12	13	14	11	14	8	80	1.70	41
	Female	7	2	3	6	5	5	2	30	1.53	46
Control	Boys	0	0	0	0	0	0	0	60	0	0
	Girls	0	0	0	0	0	0	0	50	0	0
	Male	0	0	0	0	0	0	0	160	0	0
	Female	0	0	0	0	0	0	0	120	0	0

4.8. ADSORPTION STUDY USING SELECTED ADSORBENTS

4.8.1. Biochar Characterization

a) Biochar Yield, EC and Moisture Content

Results showed that the percent yield of biochar decreased with temperature increase, which is almost linked to the elimination of VOC, s (volatile organic compounds) in the pyrolysis (Table 5). The findings were concordant with the earlier works (Hu et al., 2020; Tang et al., 2019). Similarly, moisture content and EC also decreased with temperature increase.

b) Bulk Density and pH

The pH of biochar increase with the rise in pyrolysis temperature, which may be due to breakdown of phenols and organic acids at higher temperature (Hu et al., 2020; Tang et al., 2019). Similarly, bulk density increased with temperature increase.

c) SEM

SEM images of biochar before and after F^- removal are presented in Figures (5, 6, 7, and 8). The working parameters were fixed as: HV range was from 20 to 24 KV, Magnification range was from 2.59 to 2.66 KX, 10 μm, Working Distance (WD) range was from 8.8 to 16.6 mm, and DET: SE: for biochar SEM analysis. The images clearly describe that the biochar possess porous and rough surface. The surface of biochar is also composed of several voids of different sizes due to the emission of volatile matter during pyrolysis. However, the spaces on the surface of the used biochar seem to be packed and many brighter particles are visible after F^- adsorption, which can be ascribed to F^- adsorption on biochar surface. A similar morphology has been reported in the previous studies for F^- adsorption (Mohan et al., 2014; Papari et al., 2017; Wang et al., 2018; Zhou et al., 2019).

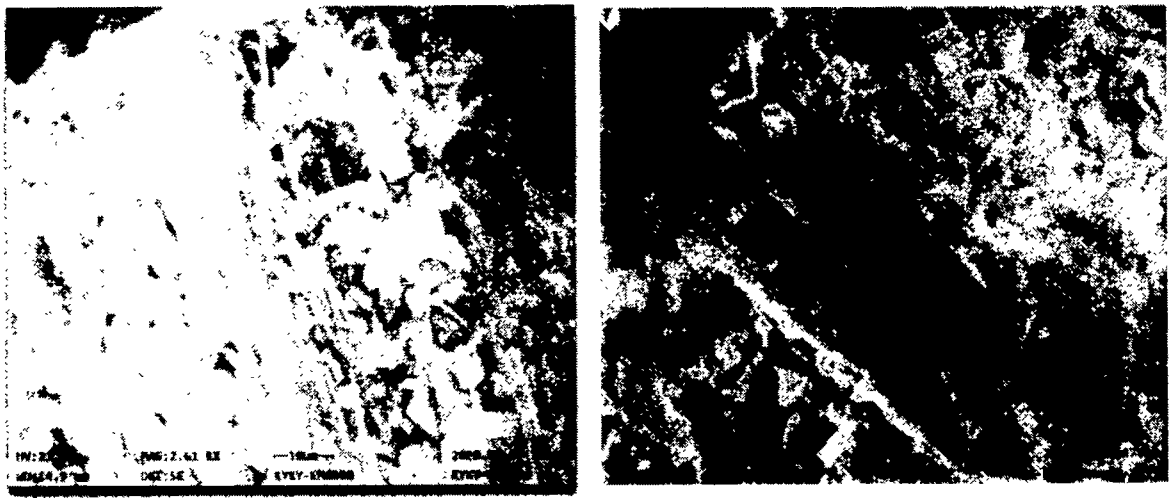

Figure 5: Before F^- Adsorption (Left), After F^- Adsorption (Right) BC250

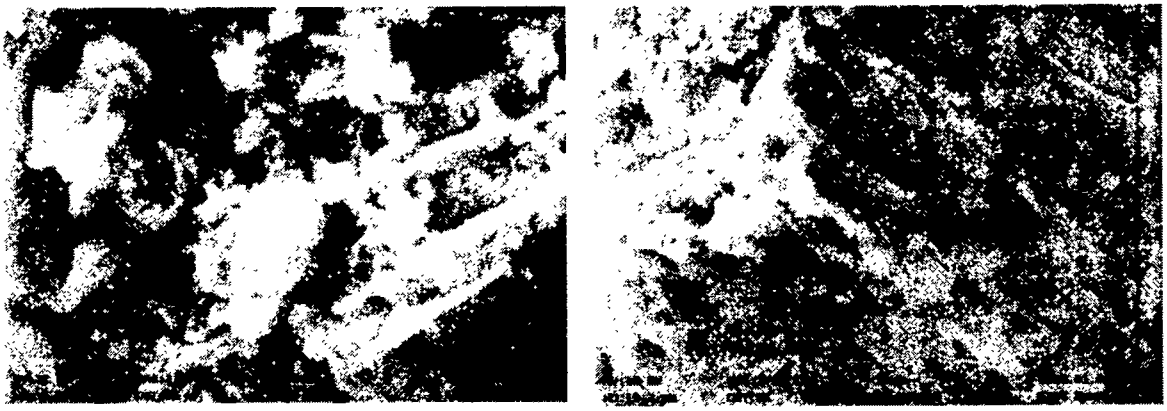

Figure 6: Before F^- Adsorption (Left), After F^- Adsorption (Right) BC500

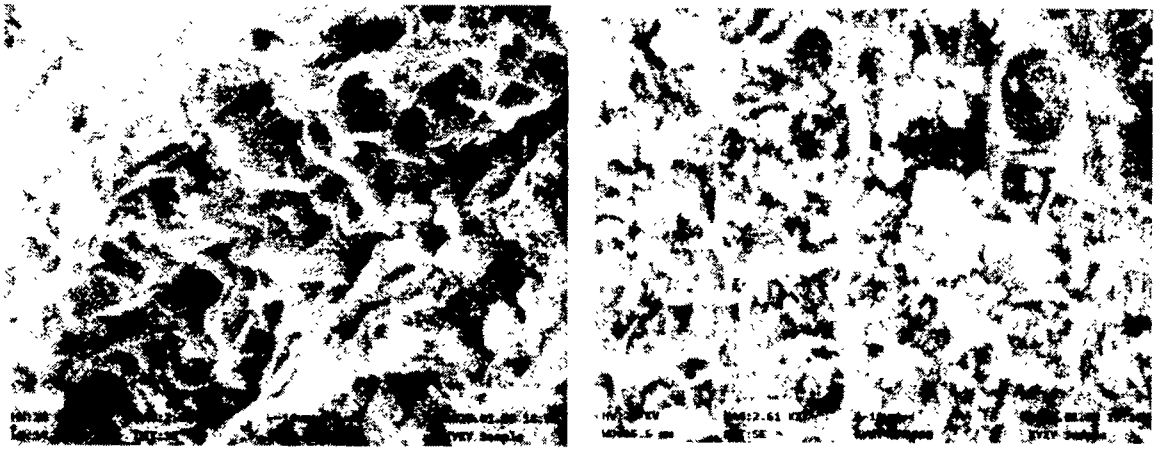

Figure 7: Before F^- Adsorption (Left), After F^- Adsorption (Right) BC750

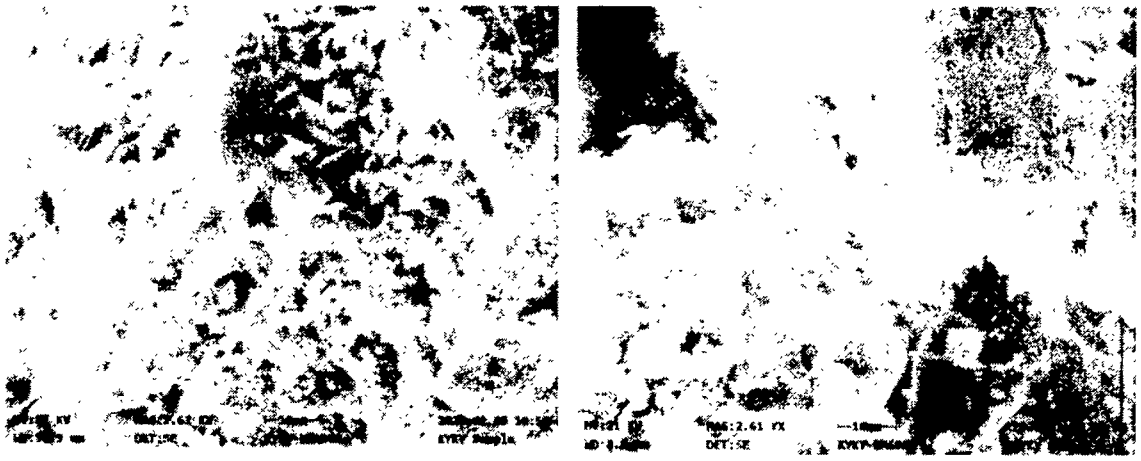

Figure 8: Before F^- Adsorption (Left), After F^- Adsorption (Right) BC1000

d) EDS

The peaks obtained in EDS spectra of BC250, BC500, BC750, BC1000 identified various elements shown in the Figures (9, 10, 11, 12, 13, 14, 15 and 16). Carbon, oxygen, calcium, sodium, magnesium and potassium are found in maximum ratio in the biochar samples. The corresponding EDS range clearly indicates the existence of F^- after adsorption. The study follows the earlier texts (Choudhary et al., 2017; Shahid et al., 2019).

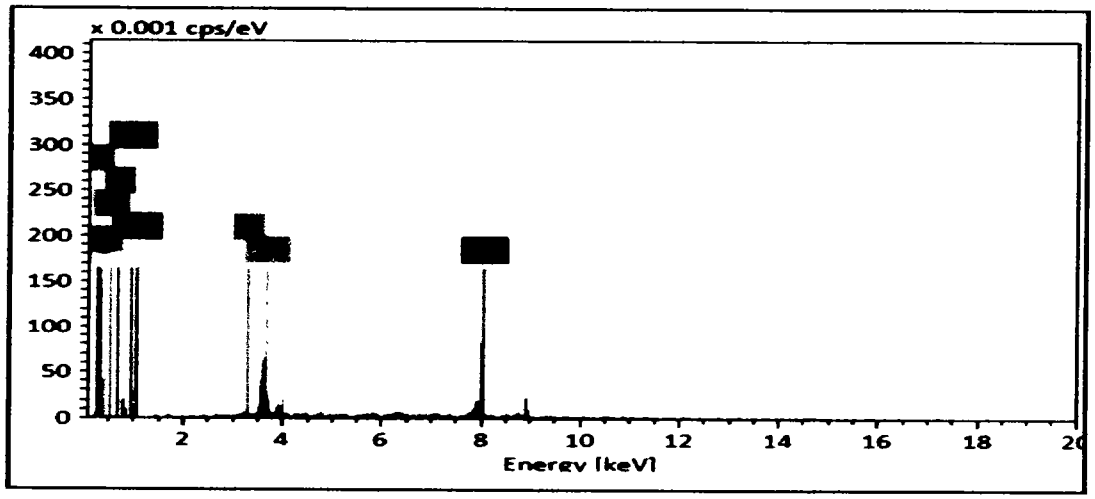

Figure 9: EDS Spectra of Unused BC250

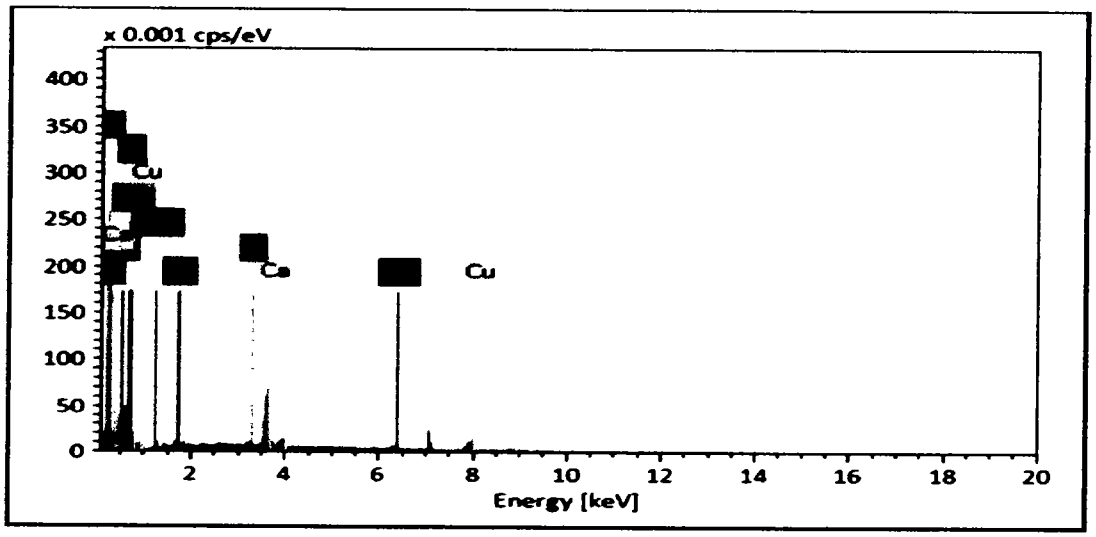

Figure 10: EDS Spectra of Used BC250

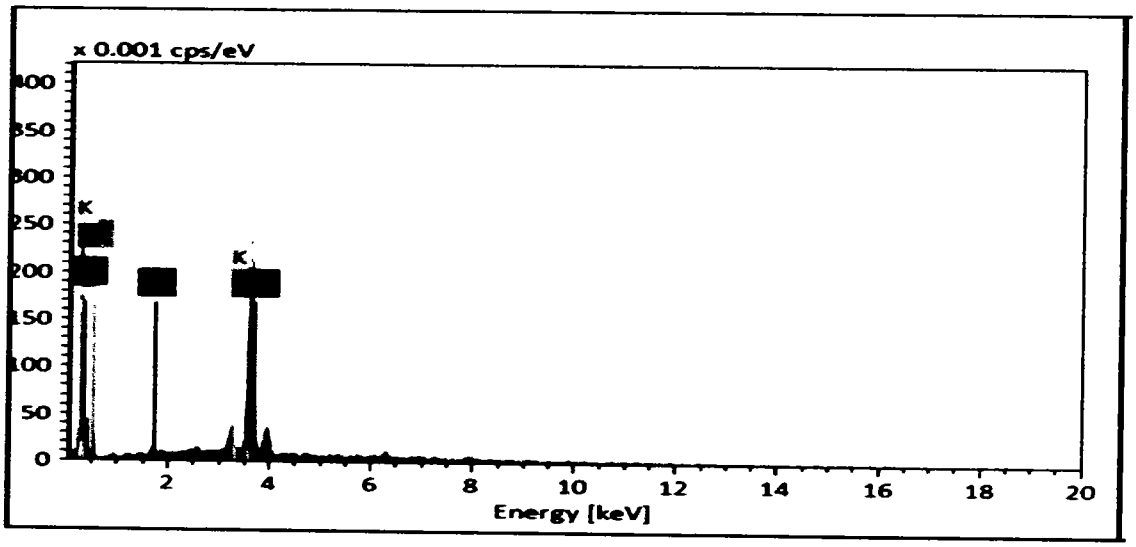

Figure 11: EDS Spectra of Unused BC500

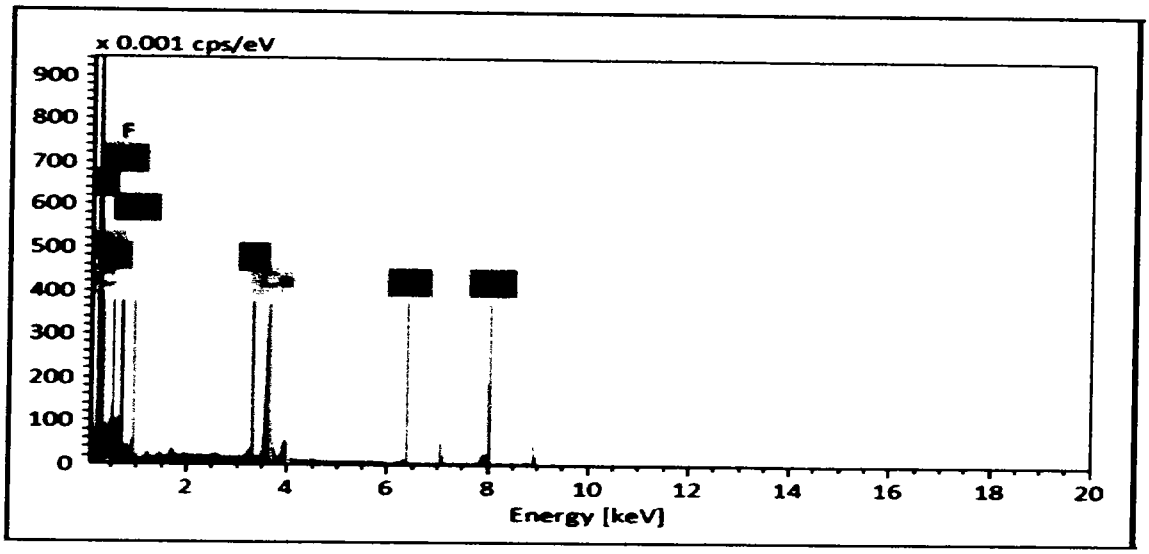

Figure 12: EDS Spectra of Used BC500

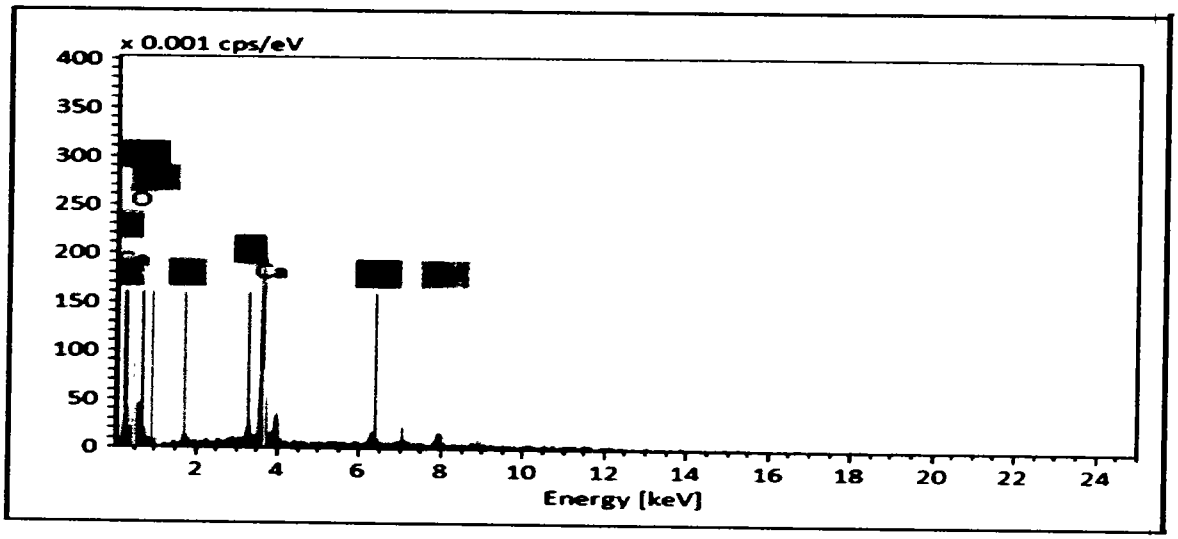

Figure 13: EDS Spectra of Unused BC750

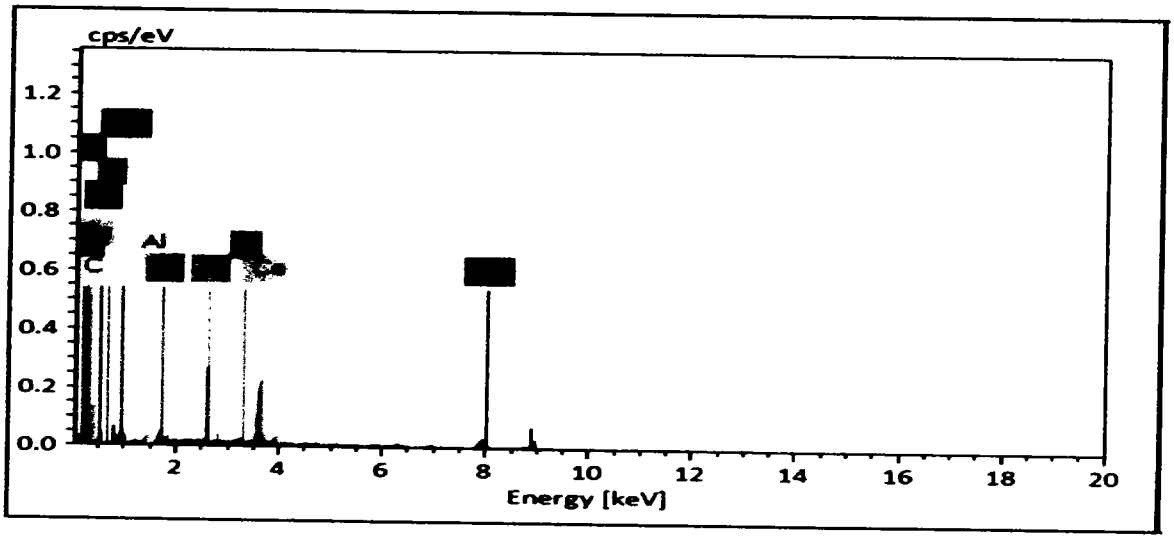

Figure 14: EDS Spectra of Used BC750

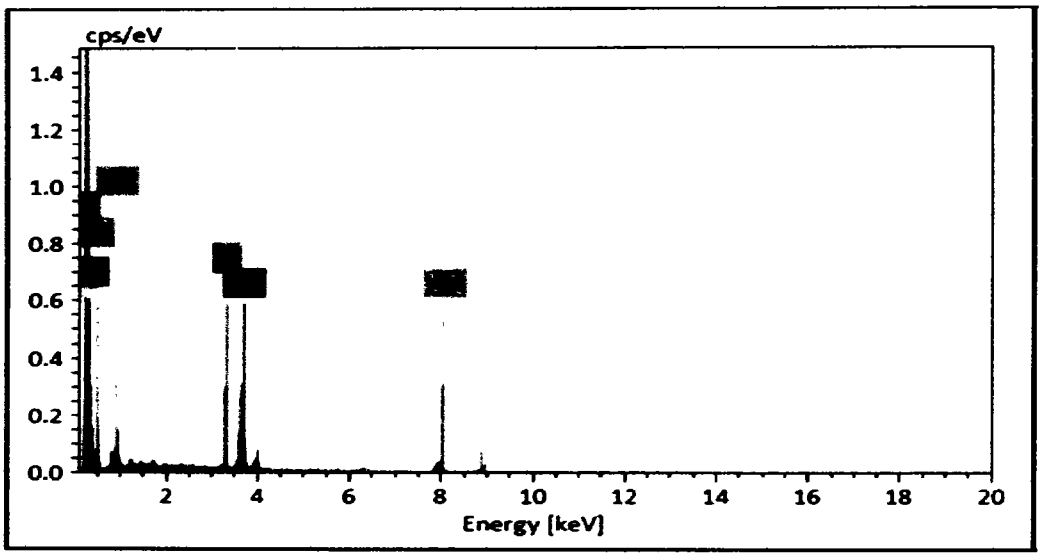

Figure 15: EDS Spectra of Unused BC1000

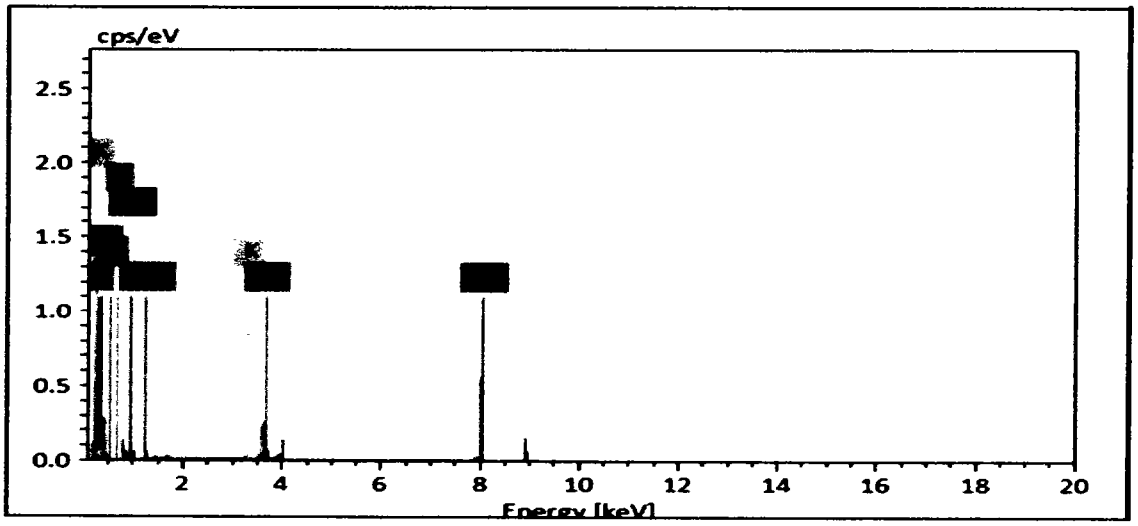

Figure 16: EDS Spectra of Used BC1000

e) FTIR

The FTIR spectrum of the prepared biochar samples, before and after F^- adsorption represents many vibration bands which indicate different functional groups (Figure 17). The occurrence of these functional groups is important for the removal of F^- through biochar. From

the available literature the functional groups in the studied biochar samples were identified and it was observed that the band 3446 cm^{-1} represents stretching vibration for –OH group, while symmetric and asymmetric aliphatic C–H stretching was indicated by 2884 cm^{-1} and 2900 cm^{-1} bands, respectively (Choudhary et al., 2017; Hu et al., 2020; Mohan et al., 2014). 2370 cm^{-1} depicts CO_2 adsorption in micro-pores (Herbert et al., 2012; Mohan et al., 2014), Near 1735 cm^{-1} the C=O mode was noticed and is made by breakdown of bark hemicellulose (Reyes-Escobar et al., 2015). Aromatic C=C ring stretching (Dong et al., 2011; Yuan et al., 2011), and –COO– anionic-bond-vibration (Luo et al., 2011; Yuan et al., 2011) was confirmed from 1412 cm^{-1}. 1363 cm^{-1} represent the phenolic–OH bending or aliphatic-deformation of CH_2 and CH_3 classes (Wu et al., 2012). 817 and 780 cm^{-1} peaks specifies the aromatic C–H bending vibration or aromatic out of plane deformation (Domingues et al., 2017; Uchimiya et al., 2011).

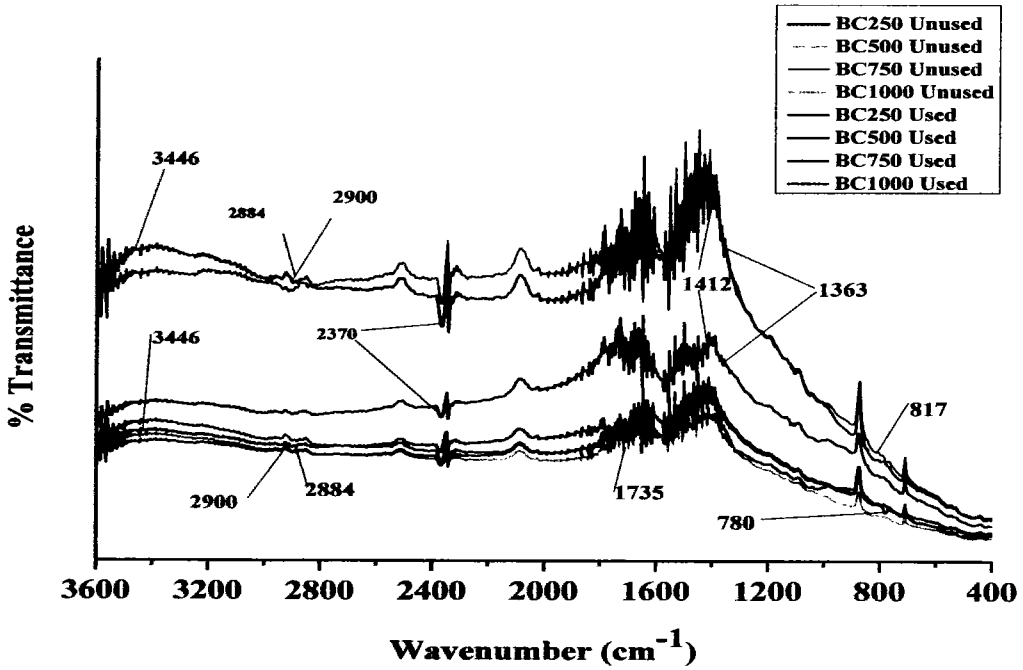

Figure 17: FTIR Range of Biochar Prepared at Different Temperatures

4.9. BATCH ADSORPTION STUDIES

The factors viz. amount of dosage, pH, contact time, and initial F^- level effect is discussed as below.

4.9.1. Effect of pH on Fluoride Removal

pH greatly affect the removal of pollutants from aqueous media (Moubarik & Grimi, 2015). The percent (%) F^- removal by using all the selected adsorbents decreased as pH increases, except for clay particles which shows a gradual increase in F^- removal with pH increment (Figure 18). For DLP, Clay, GAC, BC250, BC500, BC750 and BC1000, the % F^- removal efficiency was 45%, 5%, 40%, 85%, 80%, 90% and 75%, respectively, at pH 2. The better F^- adsorption at pH 2, may be because of plenty H^+ ions existing at lowest pH, which in turns neutralizes the hydroxyl (OH^-) ions on the surface thus minimizing difficulty to the flow of F^- ions. As stated in the literature, where supreme F^- was noted at acidic pH (Naghizadeh et al., 2017; Tomar et al., 2014; Zazouli et al., 2015). The biochar samples were efficient in F^- removal at pH 7, which shows its practical applicability for treating F^- containing groundwater (Figure 18).

Sufficient F^- removal with biochar samples was mostly observed from 2 to 8.6 pH range, because of pHpzc values of the biochar samples (Figure 19 & Table 5). The pH at which adsorbent surface have equivalent amount of positive and negative charges is known as point of zero charge (Amin et al., 2015). At pH values > pHpzc values, the surface of adsorbent get negative charge, where F^- repulsion occurs and causes little F^- removal. While biochar surface develop positive charge at pH values < pHpzc, which results in maximum F^- adsorption via electrostatic attraction. The results were supported by the previous literature (Wang et al., 2018; Zhou et al., 2019).

Table 5: Characterization of prepared biochar types

Biochar type	pH	pH_{PZC}	EC µS/cm	% yield	% moisture content	Bulk density/cm^3
BC250	5.4	5.7	680	63.6	9.305	0.4
BC500	8	7.2	386	35.7	8.92	0.4
BC750	10.7	8.6	312	33.5	6.37	0.5
BC1000	9	7.6	205	31.3	4.78	0.5

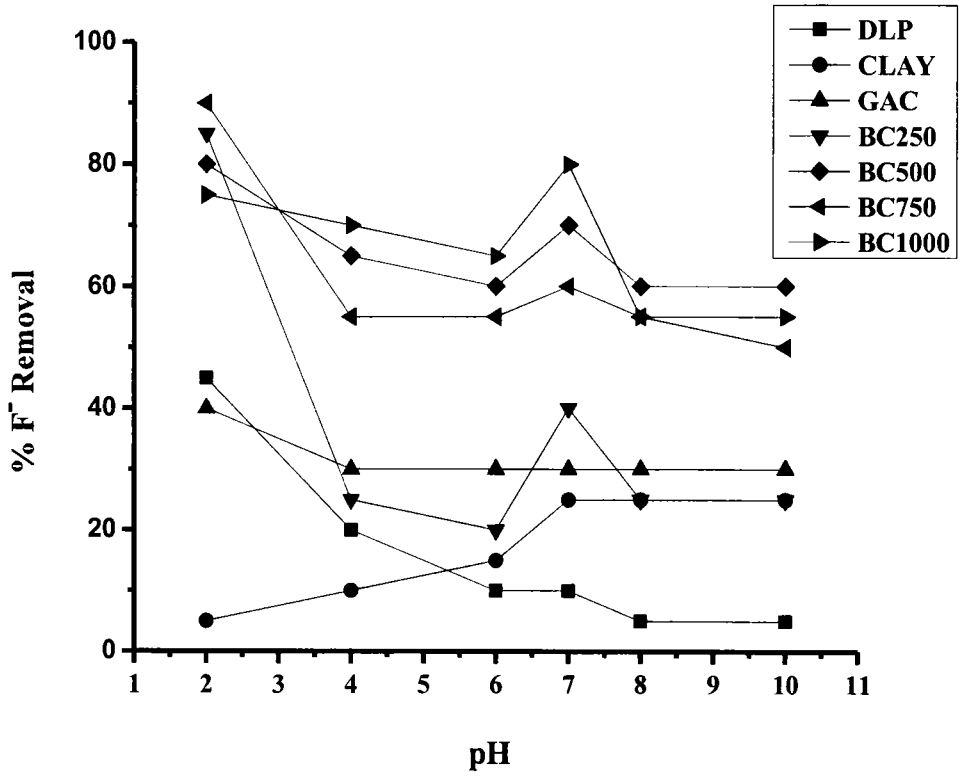

Figure 18: Influence of pH on F^- Removal at 2 mg/L, at Dose (5g Biochar), (1 g GAC & Clay) 10g (DLP), 145 minutes

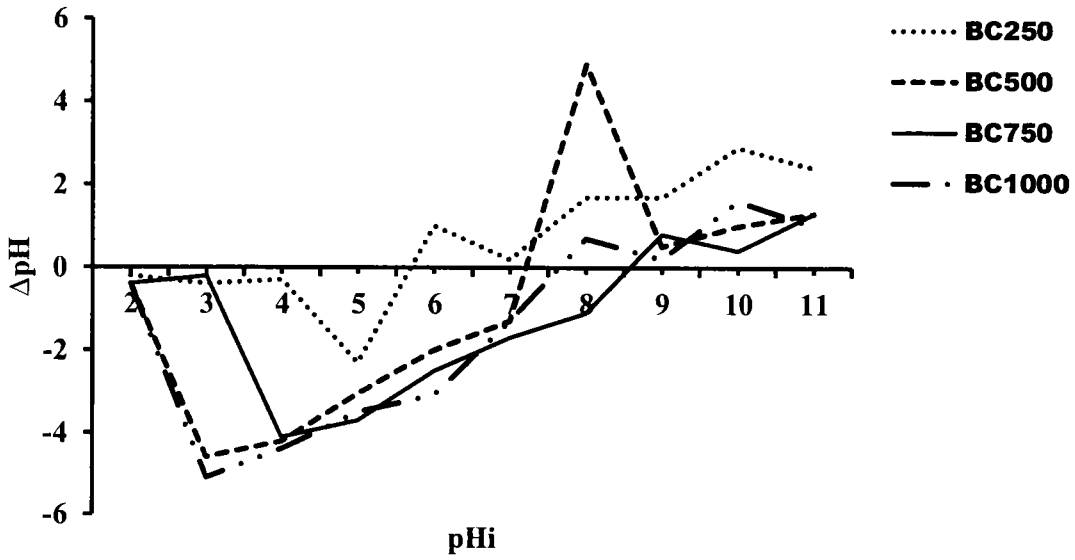

Figure 19: pH_{PZC} of Biochar

4.9.2. Effect of Dosage

Adsorbent doses were used in different amounts i.e. 1 to 7 g/50 mL at pH 7, 2 mg/L of F^- solution, rpm 200, temperature 30 °C and time 145 minutes except DLP adsorbent whose dose range was from 1 to 10 g/50 ml at pH 2 while keeping other conditions similar to other adsorbents. The influence of adsorbent quantity on F^- adsorption using the selected materials is shown in Figure 20, which indicate that F^- removal was increased from 30 to 40 %, from 40 to 70%, 40 to 60% and 50 to 80% as the dose amount increased from 1 to 5g for BC250, BC500, BC750 and BC1000, respectively. The F^- removal for GAC remains at 30 % as the GAC amount was maximized from 1 to 7 g/50 ml. The F^- percent removal was also raised from 10 to 45 % as the dosage of the DLP was augmented from 1 to 10 g/50 ml. The F^- adsorption using clay particles was decreased from 25 to 20 % for 1 to 7 g/50ml.

The results show that as the amount of dose increases, the number of active sites for F^- removal also increases, which accelerate F^- adsorption (Figure 20 & 21). It was noticed that further increment in dose amount of BC250, BC500, BC750 and BC1000 from 5 to 7 does not show satisfactory results and almost gained equilibrium, which may be ascribed to the saturation of active spaces at high dosages, hence minimizing the effective surface-area for adsorbate adsorption (Asgari et al., 2012). Therefore, 5 g of biochar was chosen as the final dose for further study. Similarly 1g was selected as the optimum dose for further study of F^- removal from water using GAC and clay particles. Further increase of DLP dose from 10 g showed no significant F^- removal, thus 10 g was noted as optimum dose for further study using DLP. The results were in agreement with previous researches (Dobaradaran et al., 2015; Mahvi et al., 2018; Papari et al., 2017; Wang et al., 2018).

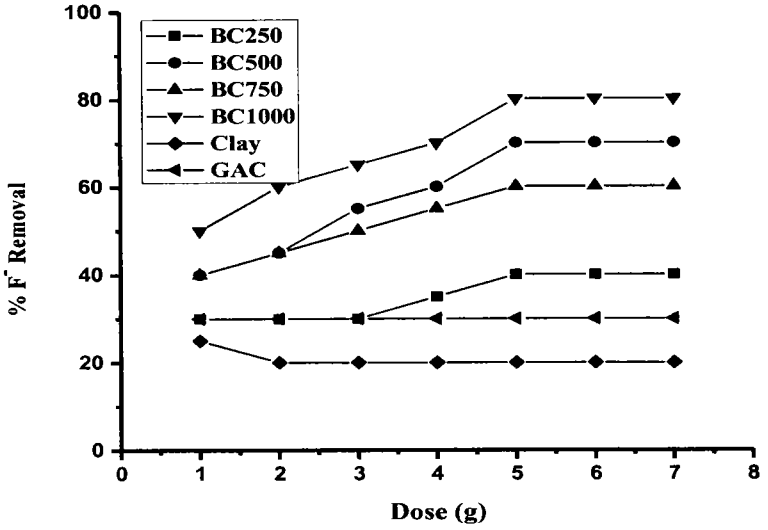

Figure 20: Dosage effect on the adsorption of F^- (2mg/L, pH 7 and 145 minutes

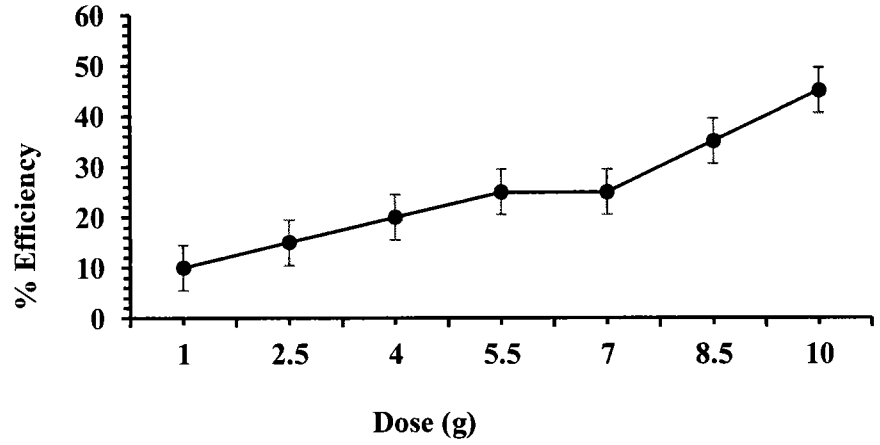

Figure 21: DLP Dose Effect on the F^- Removal (2 mg/L, pH 2 and 145 minutes

4.9.3. Initial Concentration Effect on Fluoride Adsorption

The Clay, GAC, BC250, BC500, BC750, BC1000, and DLP, removal capacity for F^- was detected at different F^- concentration (2-10 mg/L), while keeping the remaining factors constant at temperature 30 °C, contact time 145 minutes, rpm 200 and pH at 7 except for DLP where pH was maintained at 2. The results stated that F^- adsorption reduced with rise in the initial F^- level in the solution. The figures (22, 23) showed that 40%, 70%, 60%, 80%, 30%, 25%, and 45% of F^- was removed by BC250, BC500, BC750, BC1000, GAC, clay and DLP from 2 mg/l F^- solution, respectively. It was observed that the defluoridation capability of the adsorbents decreases as the F^- level increases and the possible cause may be the more F^- ions occurrence than the adsorbents adsorption ability (Papari et al., 2017; Tirkey et al., 2018; Tomar et al., 2014; Wu et al., 2016).

Although, percent F^- removal reduced with increase in the initial concentration of F^- but the qe (mg/g) value increased with the increase in F^- concentration (Figure 24). The possible reason may be that when the F^- concentration increases, the chances for F^- transferring from solution to the surface of adsorbent also increases, thus causing maximum F^- adsorption per unit mass of the adsorbing material. The results concluded that qe (mg/g) and percent F^- removal both are greatly reliant on the F^- initial concentration in the solution (George & Tembhurkar, 2018; Tirkey et al., 2018).

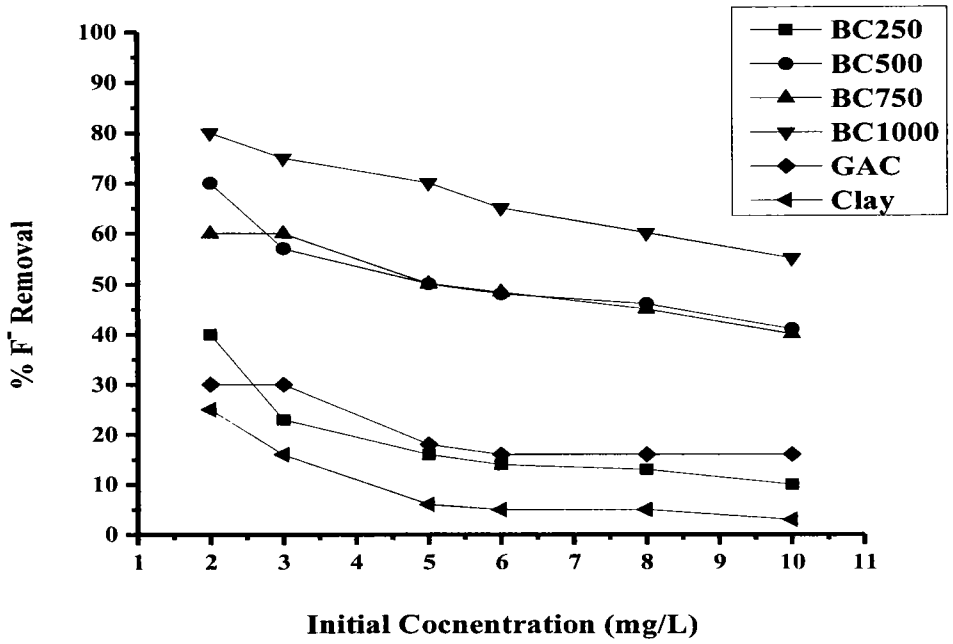

Figure 22: Initial F⁻ Concentration Effect on the Removal of F⁻ Ion (5 g of Biochar and 1 g of GAC & 1 g Clay, at Temp of 30 °C, pH 2 and 145 minutes

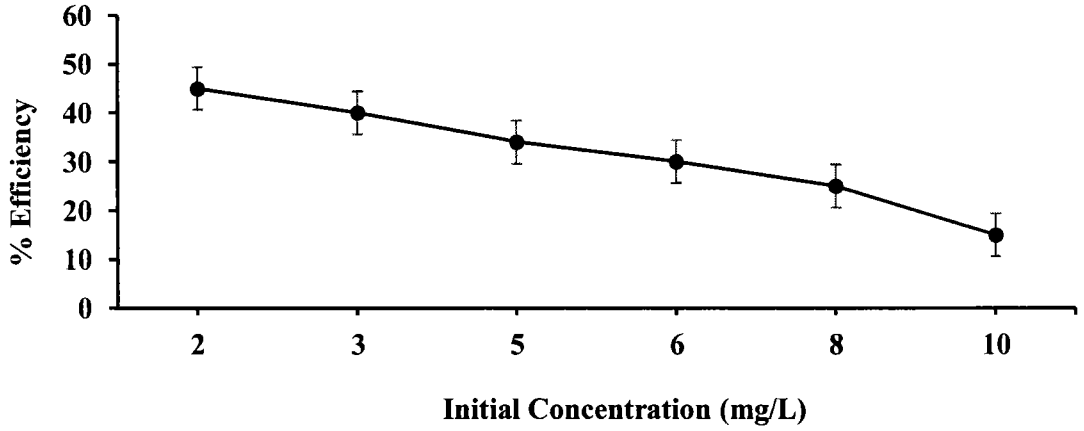

Figure 23: Influence of Initial concentration on F⁻ Removal, 10 g DLP, 30 °C, pH 2 and 145 minutes

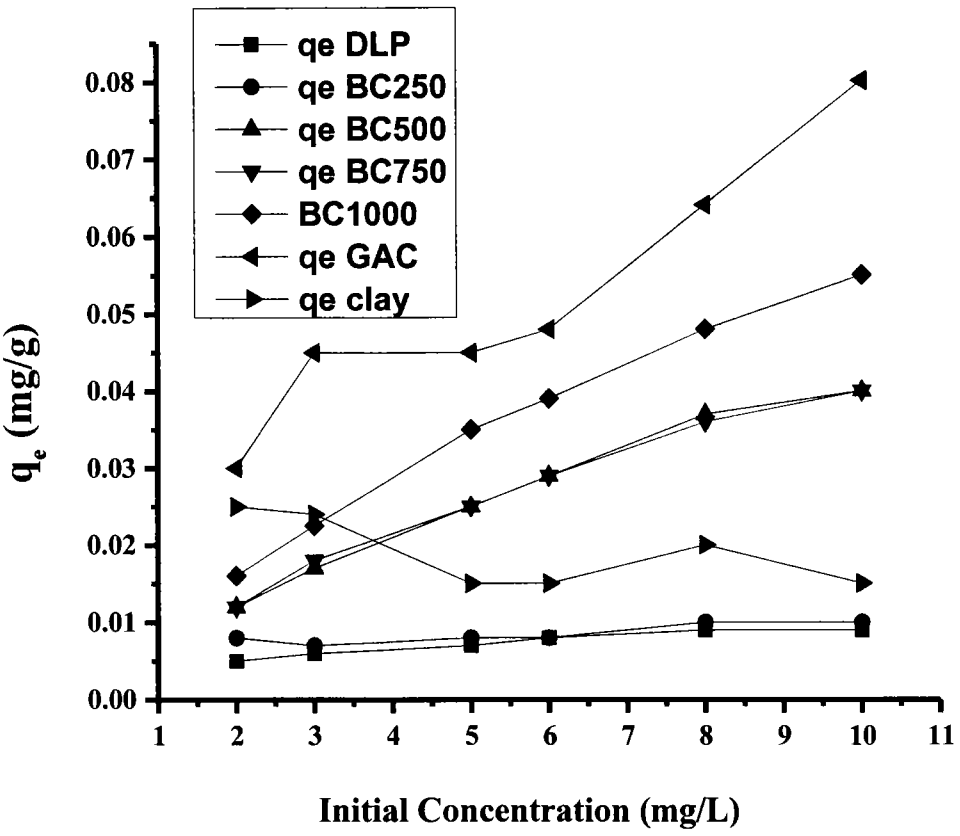

Figure 24: Effect of F− Concentration on the qe Values

4.9.4. Influence of Contact Time

The time effect of various adsorbents for F^- removal was studied in the range from 5 to 145 minutes (Figure 25) and was indicated that high adsorption was observed as the time increases. The results mentioned that at initial stages the removal percentage was maximum due to the presence of more vacant spaces at the surface and the adsorption rate was speedy, but as the time passes, these sites were occupied, hence leading to adsorption reduction.

The optimum contact time for BC250, BC500, BC750, BC1000, GAC, DLP and clay were 95 minutes, 145 minutes, 125 minutes, 145 minutes, 15 minutes, 145 minutes and 75 minutes,

respectively. The possible reason for high removal with increase in contact time is that F^- in solution find much time to catch free areas on the adsorbent (Khosravi et al., 2014). Above 145 min, no increase was noticed in the F^- removal rate (not shown in Figure) because of minimum vacant spaces availability on the surface. Results were supported by past findings (Papari et al., 2017; Wu et al., 2016).

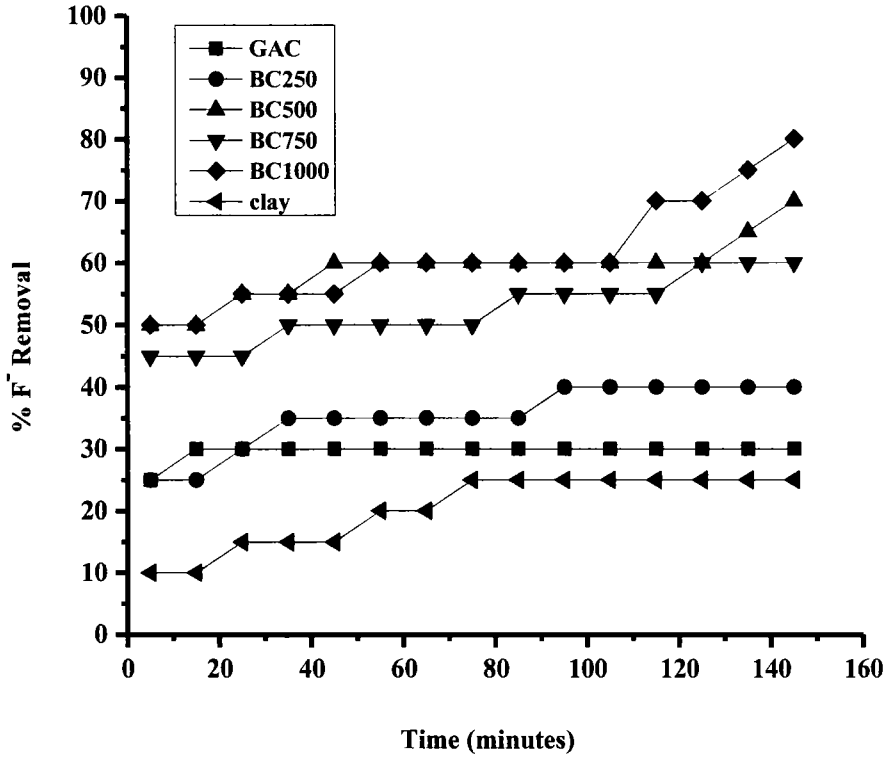

Figure 25: Contact Time Effect on F^- adsorption

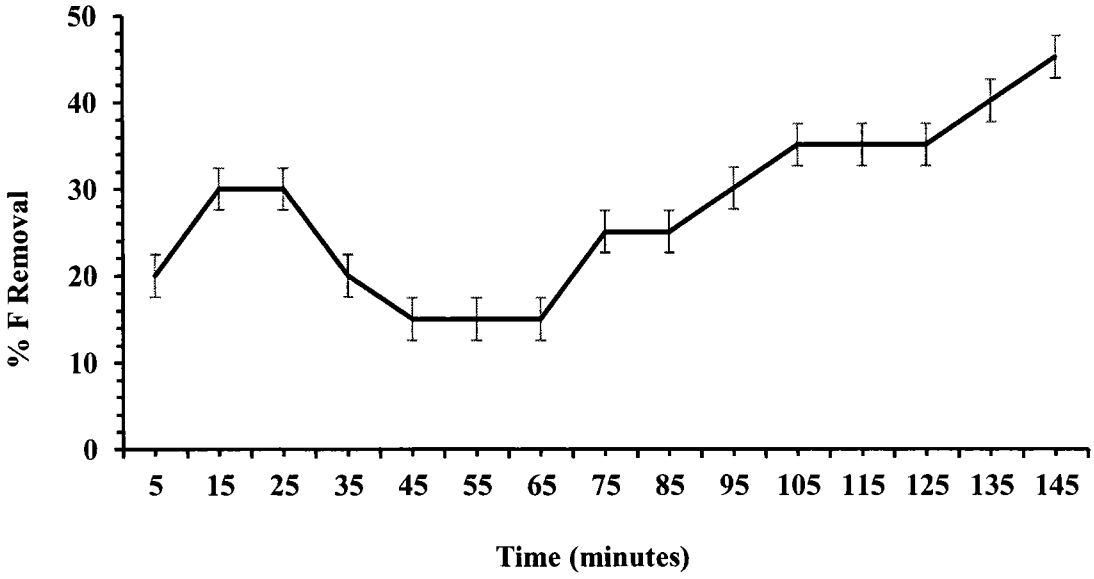

Figure 26: Effect of Contact Time on F^- Removal using DLP

4.10. ADSORPTION ISOTHERMS STUDY

The obtained data were applied over the two frequently using batch adsorption models described in below sections.

4.10.1. Freundlich

The model linear form was calculated between Log q_e and Log C_e for all the adsorbents used in this study (Figure 27, 28, 29, 30, 31, 32 and 33). K_f and 1/n represent the intercept (K_f) and slope (1/n), which were obtained from the graph line (Table 6). The R^2 (Coefficient of regression) values (Table 6) showed strong fitting to explain the adsorption process of F^- by BC500, BC750, BC1000 and GAC as compared to BC250, clay and DLP, R^2 values. This means that F^- adsorption on BC500, BC750, BC1000 and GAC surface occurs heterogeneously.

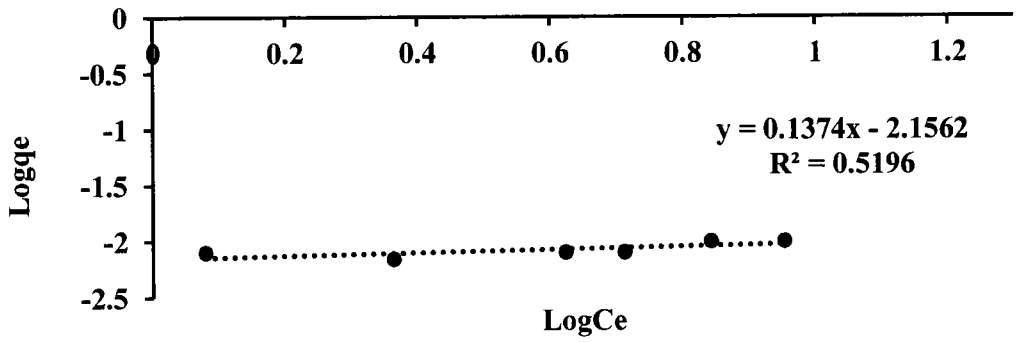

Figure 27: Freundlich Model of BC250

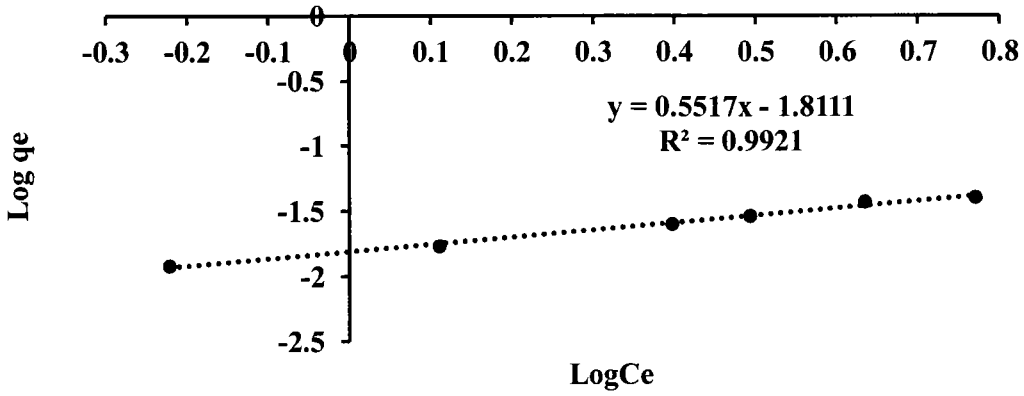

Figure 28: Freundlich Model of BC500

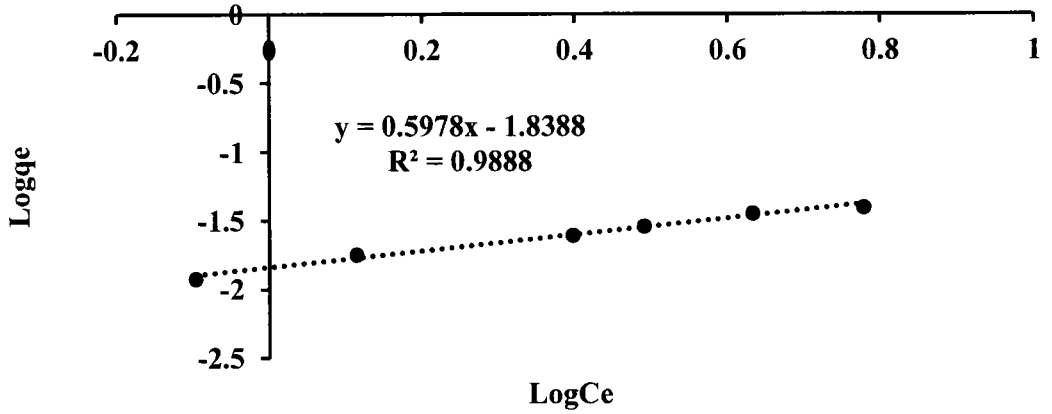

Figure 29: Freundlich Model of BC750

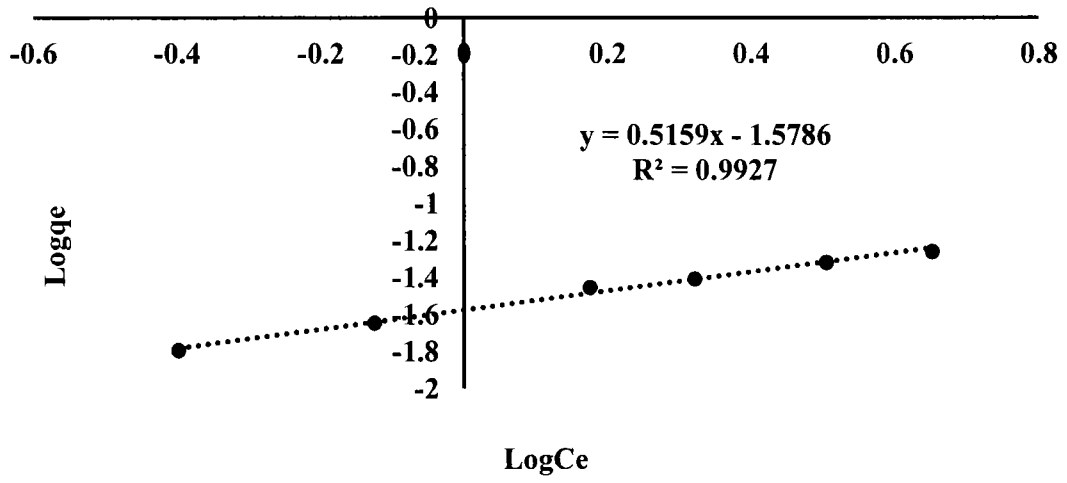

Figure 30: Freundlich model of BC1000

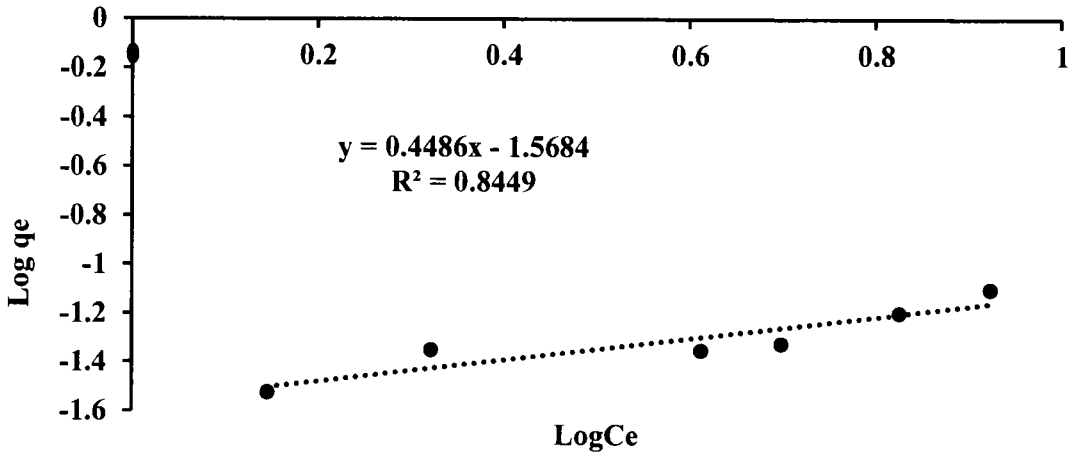

Figure 31: Freundlich Model of GAC

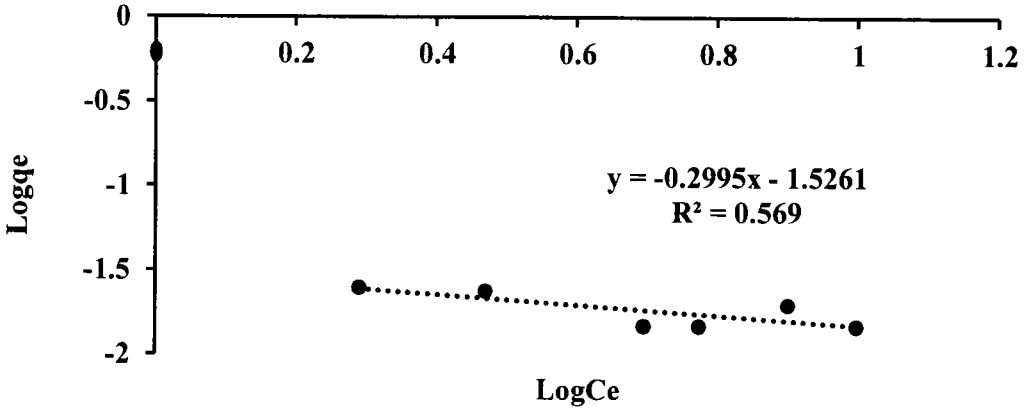

Figure 32: Freundlich Model of Clay

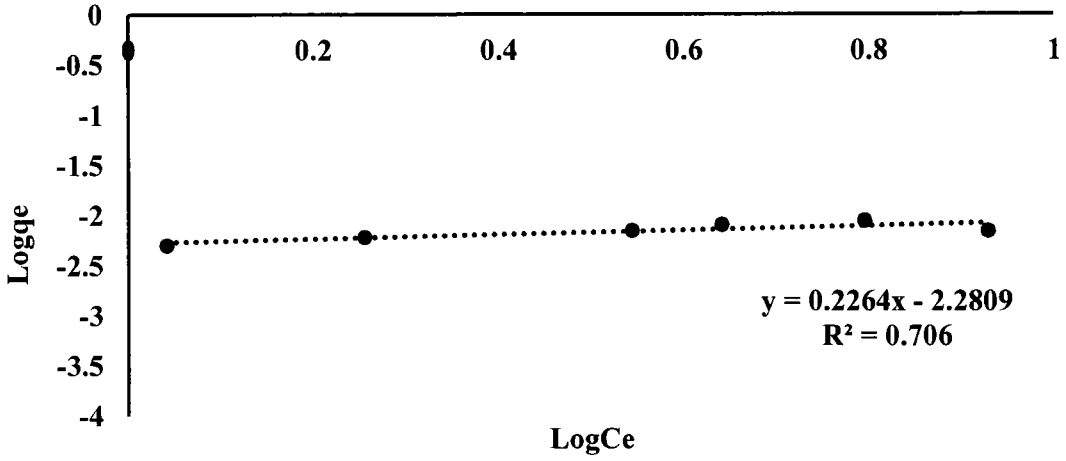

Figure 33: Freundlich Model of DLP

Table 6: Values of Freundlich model constants

Adsorbents	Equations	R^2	$\frac{1}{n}$ (slope)	n	(Intercept)	K_f
BC250	y = (Slope) 0.1374x (intercept) -2.1562	0.5196	0.1374	7.278	-2.1562	0.00697
BC500	y = (Slope) 0.5517x (intercept) -1.8111	0.9921	0.5517	1.813	- 1.8111	0.0154
BC750	y = (Slope) 0.5978x (intercept)-1.8388	0.9888	0.5978	1.673	- 1.8388	0.0145
BC1000	y = (Slope) 0.5159x (intercept)-1.5786	0.9927	0.5159	1.938	-1.5786	0.0264
DLP	y = (Slope) 0.2264x (intercept)-2.2809	0.706	0.2264	4.425	- 2.2809	0.00524
GAC	y = (Slope)0.4486x (intercept) -1.5684	0.8449	0.4486	2.229	- 1.5684	0.027
Clay	y = (Slope)-0.2995x(intercept)-1.5261	0.569	-0.2995	-3.339	- 1.5261	0.0298

Note: K_f can be calculated by taking antilog of the intercept value in the equation

4.10.2. Langmuir

In this model, the graph was drawn between $1/Q_e$ and $1/C_e$ values. The slope and intercepts were equal to $1/b.Q_0$ and $1/Q_0$, respectively, from which the (b and Q_0) were calculated. (Table 7). The values of R^2 for all the adsorbents showed that this model was best followed by the F^- removal data, Figure (34, 35, 36, 37, 38, 39 and 40). The model is suitable for homogeneous adsorption and presume that all the adsorption sites have the same affinity for adsorbate and adsorbate molecules resist the transmigration. The R^2 values of F^- adsorption data shows, that BC500, BC750, BC1000, GAC and DLP adsorbents were well fitted to Langmuir model.

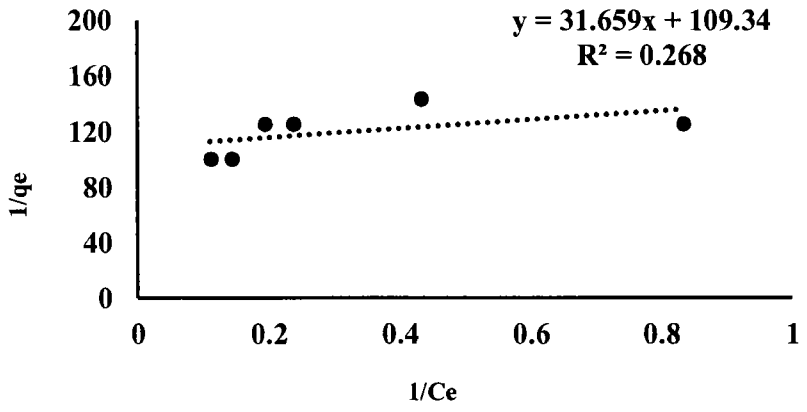

Figure 34: Langmuir Model BC250

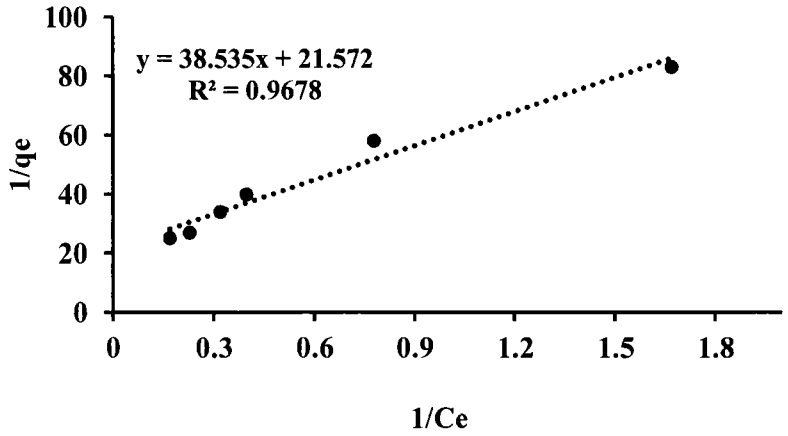

Figure 35: Langmuir Model BC500

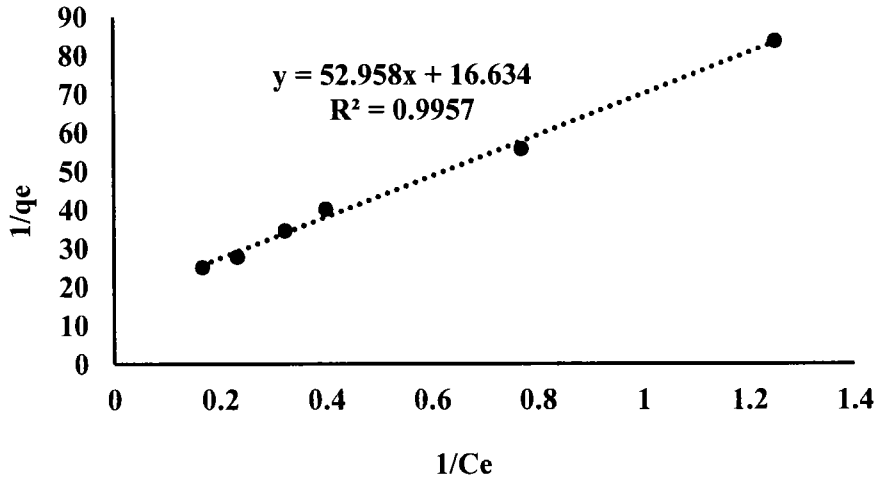

Figure 36: Langmuir Model BC750

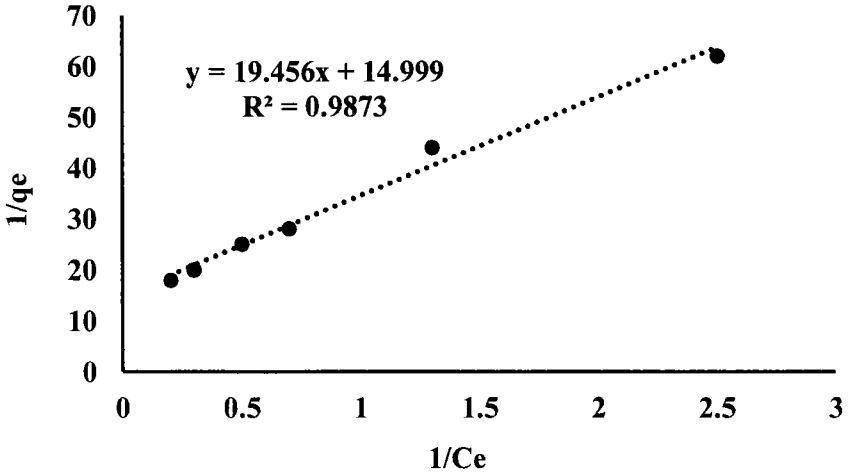

Figure 37: Langmuir Model BC1000

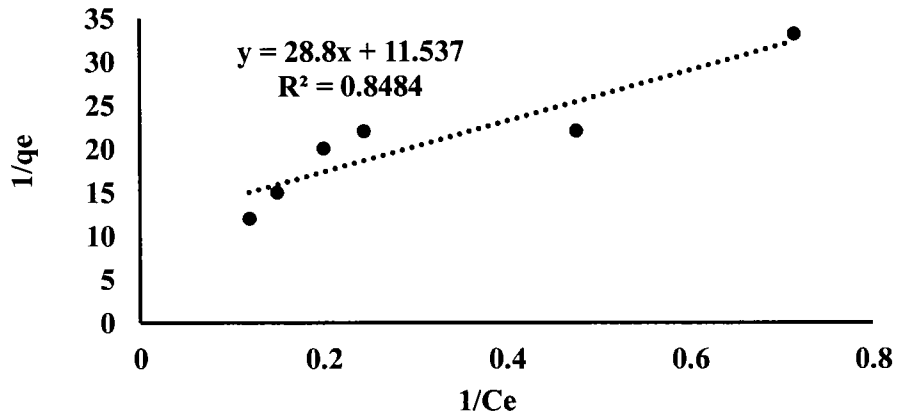

Figure 38: Langmuir Model of GAC

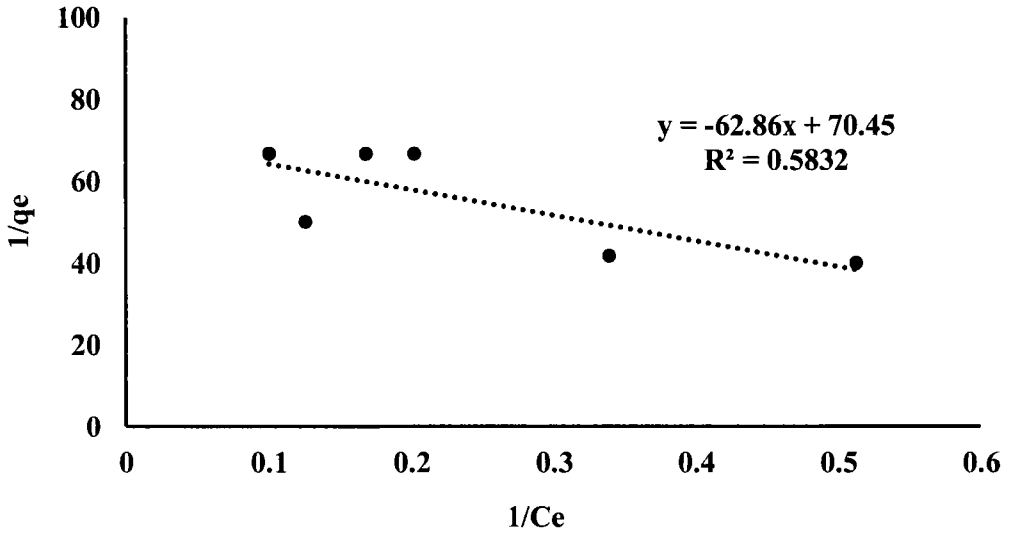

Figure 39: Langmuir Model Clay

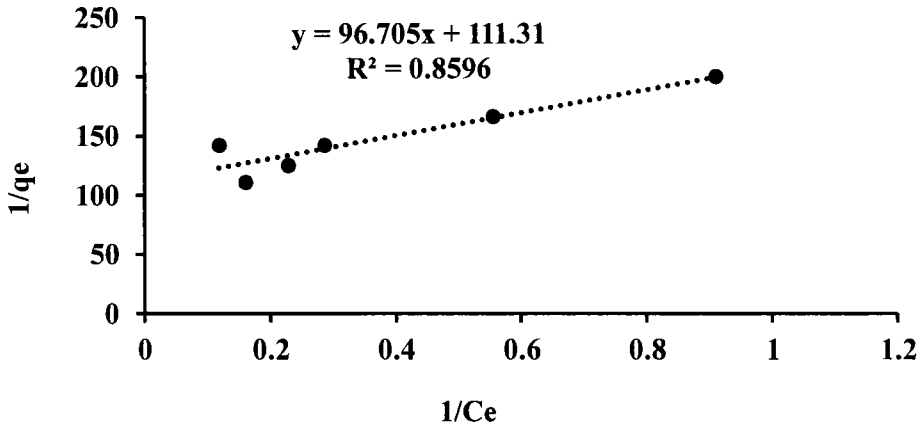

Figure 40: Langmuir Model DLP

Table 7: Values of constant for Langmuir model calculated for the selected adsorbents

Adsorbent	Equations	R^2	$\frac{1}{Q0}$ (Intercept)	Q_0	$\frac{1}{b.Q0}$ (Slope)	$\frac{1}{b}$	b= intercept/slope
BC250	y =(slope)31.659x+(intercept)109.34	0.268	109.34	0.009	31.659	0.289	3.460
BC500	y =(slope)38.535x+(intercept)21.572	0.967	21.572	0.046	38.535	1.786	0.559
BC750	y =(slope)52.958x+(intercept)16.634	0.995	16.634	0.0601	52.958	3.184	0.314
BC1000	y =(slope)19.456x+(intercept)14.999	0.987	14.999	0.0667	19.456	1.297	0.771
DLP	y =(slope)96.705x+(intercept)111.31	0.859	111.31	0.008	96.705	0.868	1.151
GAC	y =(slope)28.8x+(intercept)11.537	0.848	11.537	0.087	28.8	2.496	0.401
Clay	y =(slope)-62.86x+(intercept)70.45	0.583	70.45	0.014	-62.86	-0.892	-1.121

4.11. KINETICS STUDY

The kinetics studies are helpful in the selection of residence time of the adsorbents for F^- removal. The method for assessment of kinetic parameters is similar to that of batch equilibrium experiments. It describe the F^- adsorption rate, which helps to measure the residence time of F^- at the adsorbent solution Interface. The samples were taken at a known time and residual F^- was calculated via respective meter.

Adsorption kinetics gives important information for planning the kinetics adsorption on to the active site of the adsorbent (Munagapati et al., 2018). Likewise, the kinetic study is an significant study through which many factors such as structural pattern of adsorbent, nature of adsorbate and medium and interaction pattern between adsorbate and adsorbent can be understood (Zhang et al., 2017).

The kinetics models of the F^- removal by using BC250, BC500, BC750, BC1000, GAC, DLP and clay are presented as below.

4.11.1. Pseudo-First-Order

The model was applied for all selected adsorbents to know the rate of adsorption on the basis of their efficiency. The calculated plots for BC250, BC500, BC750, BC1000, GAC, DLP and Clay for 2 mg/L concentration of F^- at pH 7 (at pH 2 only for DLP) are given in Figure (41,42, 43, 44, 45, 46 and 47). The calculated parameters of this model are shown in Table 8.

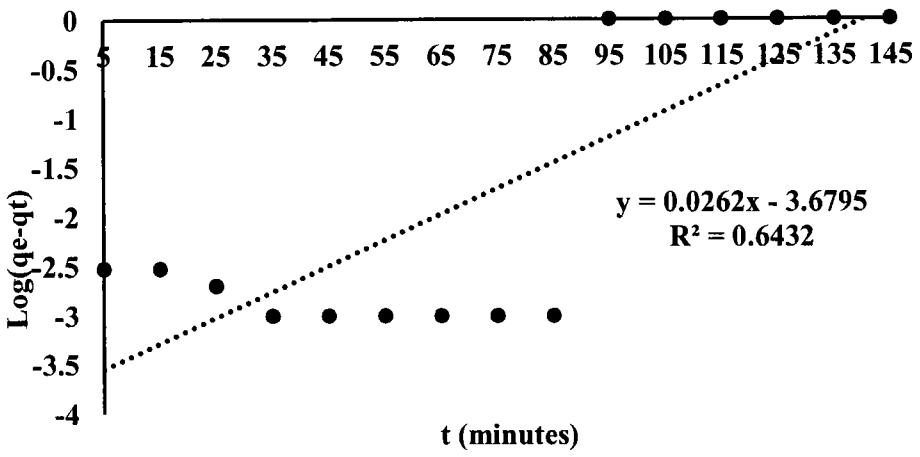

Figure 41: Pseudo-First-Order of BC250

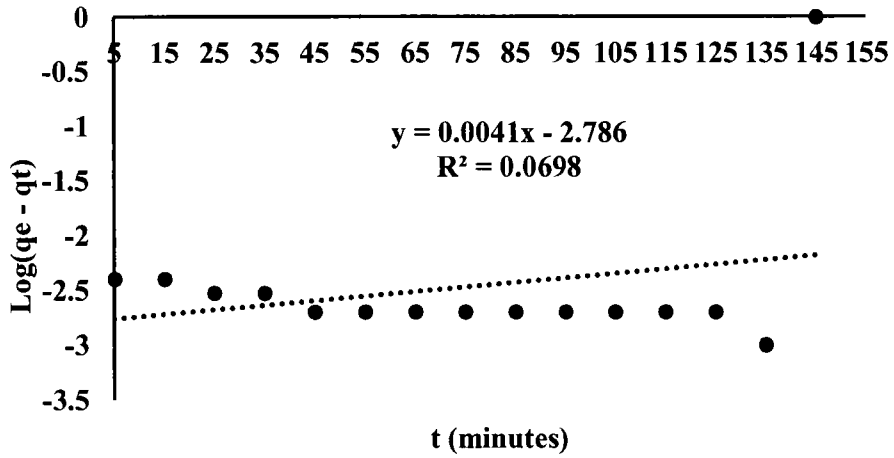

Figure 42: Pseudo First Order of BC500

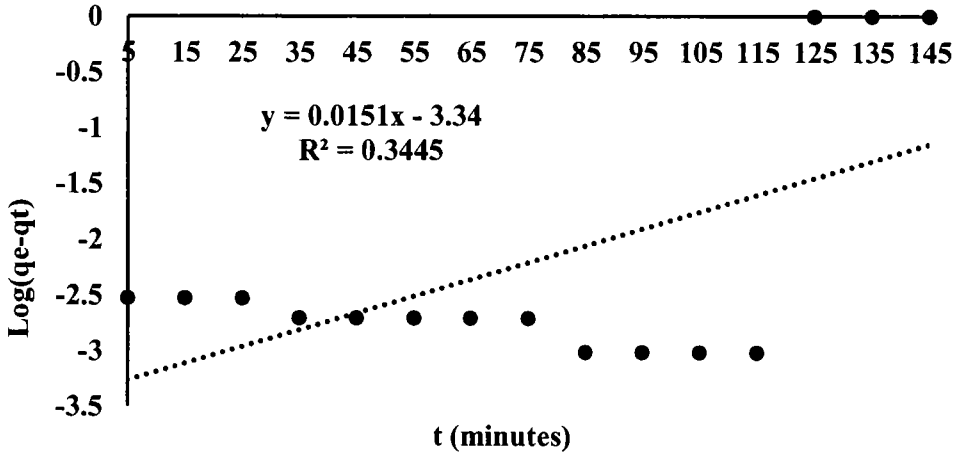

Figure 43: Pseudo First-Order of BC750

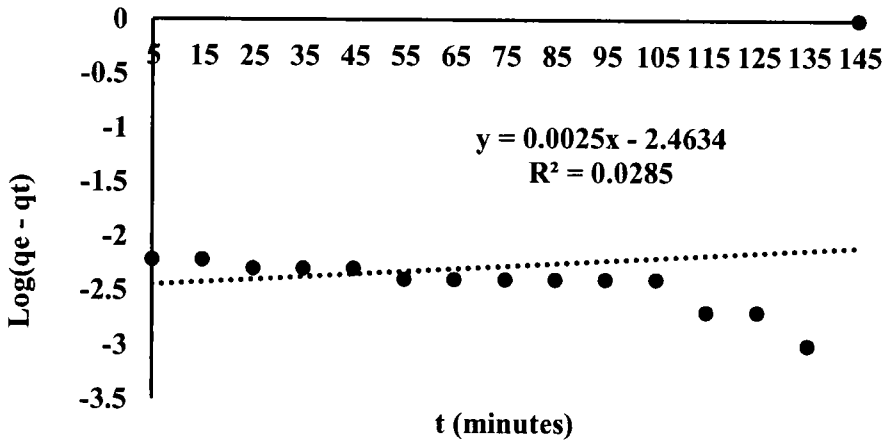

Figure 44: Pseudo First Order of BC1000

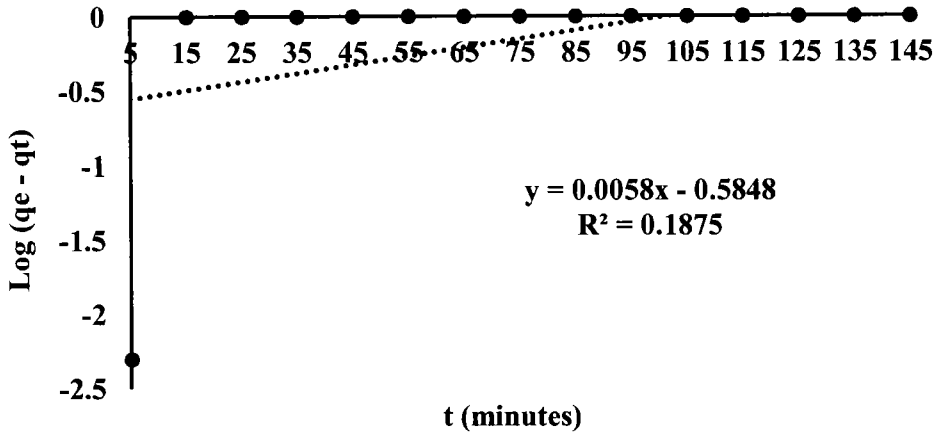

Figure 45: Pseudo First-Order Kinetics Model of GAC

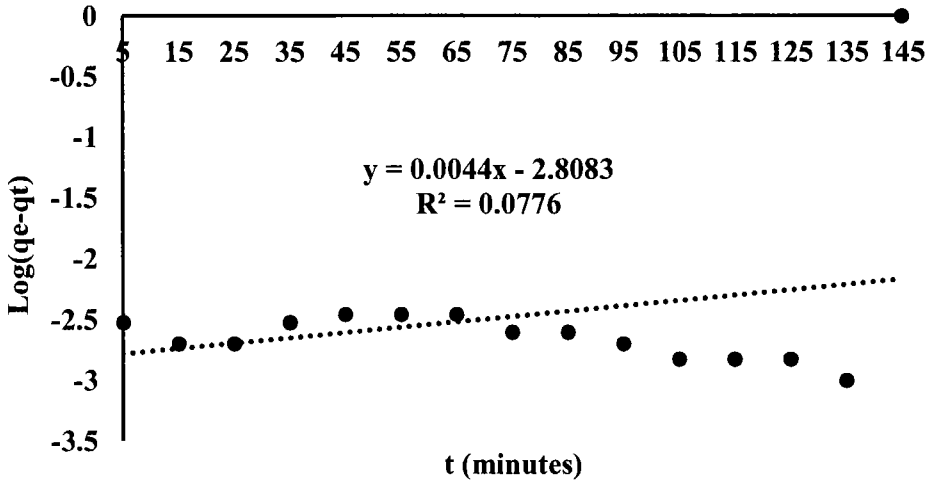

Figure 46: Pseudo First Order of DLP

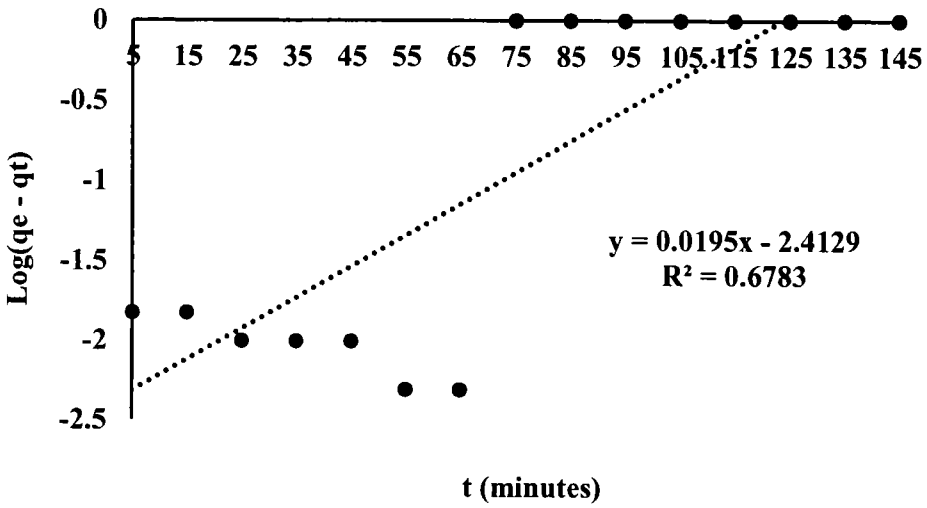

Figure 47: Pseudo First Order Kinetics for Clay

Table 8: Pseudo First-order parameters determined for the studied adsorbents

Adsorbents	Equations	R^2	q_e (calculated) = antilog of intercept	q_e (Experimental)	K_1 = Slope×2.303
BC250	y = 0.0262x - 3.6795	0.6432	2.09	0.008	0.06
BC500	y = 0.0041x - 2.786	0.0698	0.002	.014	0.009
BC750	y = 0.0151x - 3.34	0.3445	4.57	0.012	0.035
BC1000	y = 0.0025x - 2.4634	0.0285	0.003	0.016	0.006
GAC	y = 0.0058x - 0.5848	0.1875	0.26	0.03	0.013
DLP	y = 0.0044x - 2.8083	0.0776	0.002	0.005	0.01
CLAY	y = 0.0195x - 2.4129	0.6783	0.0039	0.025	0.045

The small R^2 values explain that the F^- adsorption is not happening completely on single site (Nuhoglu & Malkoc, 2009) and the qe calculated value should be identical to the experimental qe values. The model stated that the values of qe (cal) and qe (exp) for the adsorbents (used in the study) are different from one another, which means that this model is not properly appropriate with the selected time for the target adsorbents (Annadurai et al., 2019; Choong et al., 2020; George & Tembhurkar, 2018; Nabbou et al., 2019; Naghizadeh et al., 2017).

4.11.2. Pseudo-Second Order

The F^- adsorption efficiency of BC250, BC500, BC750, BC1000, GAC, DLP and clay was studied for 2 mg/L F^- solution at 30 ^{0}C, 200 rpm, 145 minutes and pH 7. The data obtained was applied over the model and is presented in figures (48, 49, 50, 51, 52, 53 and 54). In this model, the removal rate and number of active areas are directly proportional to each other. Values of K_2 (rate constant), qe (adsorption at equilibrium) and h (initial adsorption rate) were determined from the fitting curves of the figures and are displayed in the Table 9.

The R^2 (Coefficient of correlation) values obtained from the equation of linear form of the model were quite greater due to the presence of variable 't' at both X and Y axes (Tseng et al., 2010). It is obvious from the figures that the values of qe calculated and qe experimental were almost same.

If the materials used for the F^- removal follows the model, it means that the process is chemical in nature, where the rate limiting step is related to the attraction forces via electrons transferring or sharing (Yuan et al., 2014). The study obey the past works (Annadurai et al., 2019; Choong et al., 2020; George & Tembhurkar, 2018; Nabbou et al., 2019; Naghizadeh et al., 2017).

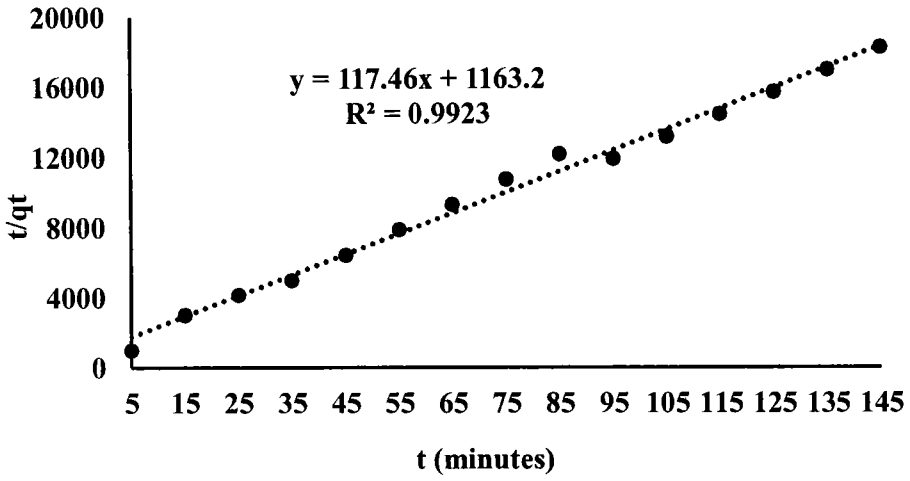

Figure 48: Pseudo Second Order of BC250

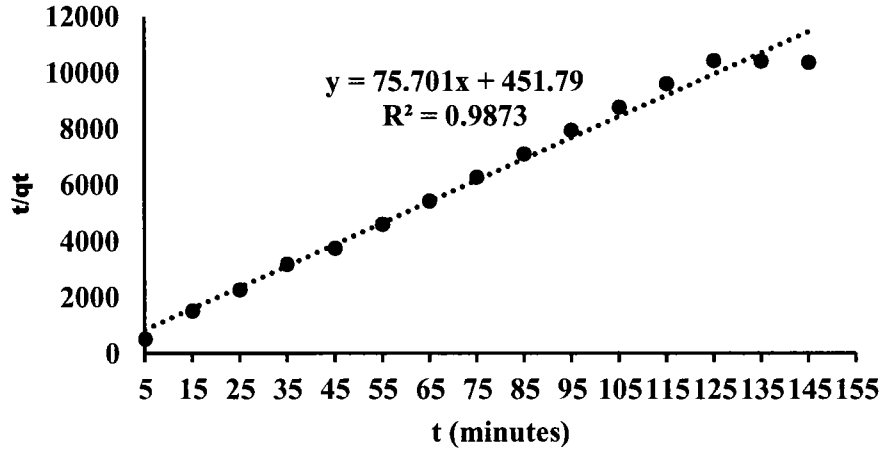

Figure 49: Pseudo Second-Order (BC500)

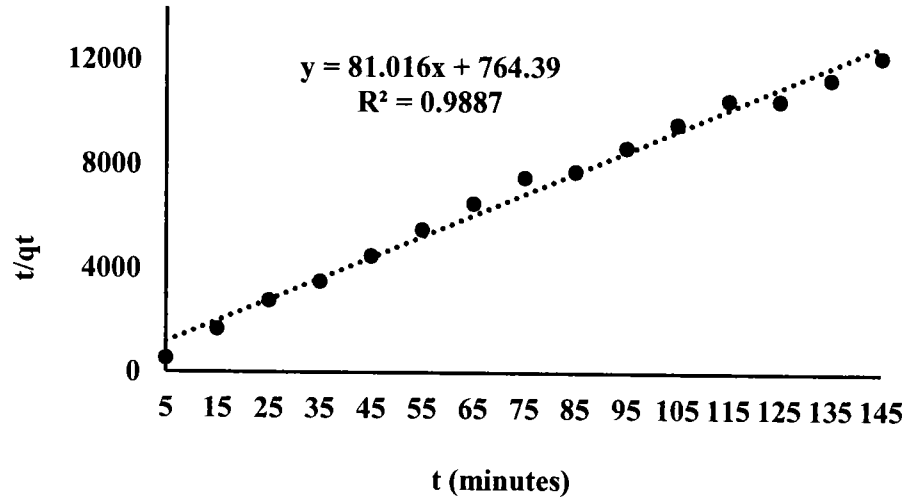

Figure 50: Pseudo Second Order Model of BC750

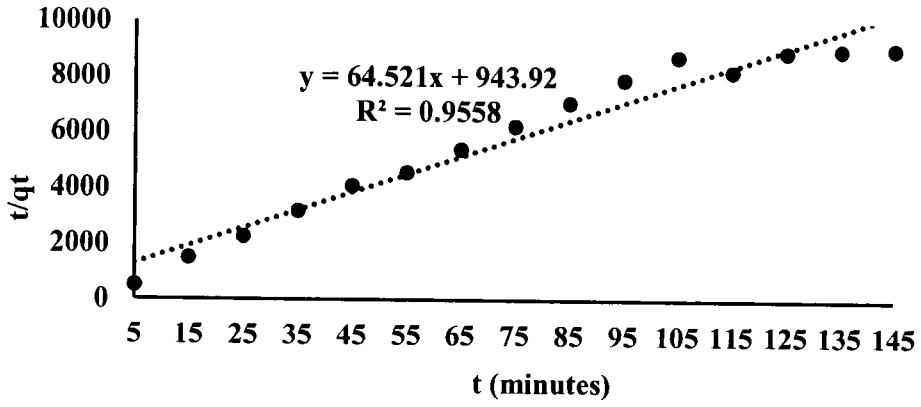

Figure 51: Pseudo Second Order of BC1000

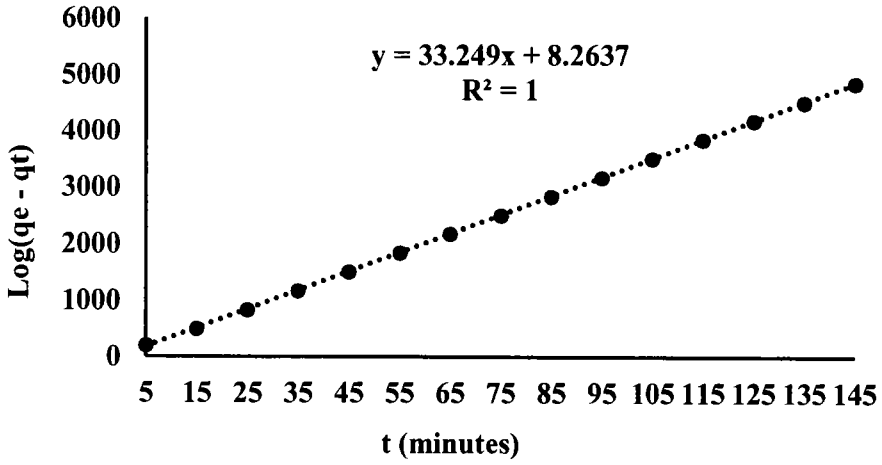

Figure 52: Pseudo Second-Order of GAC

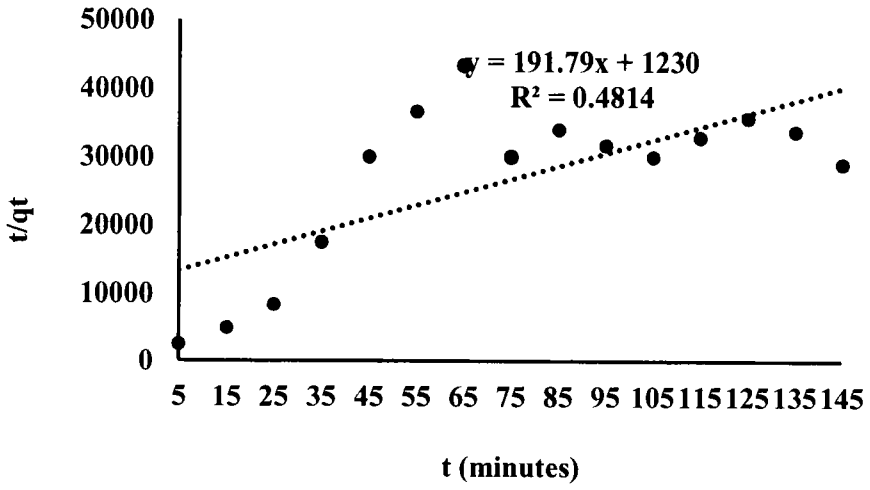

Figure 53: Pseudo Second-Order of DLP

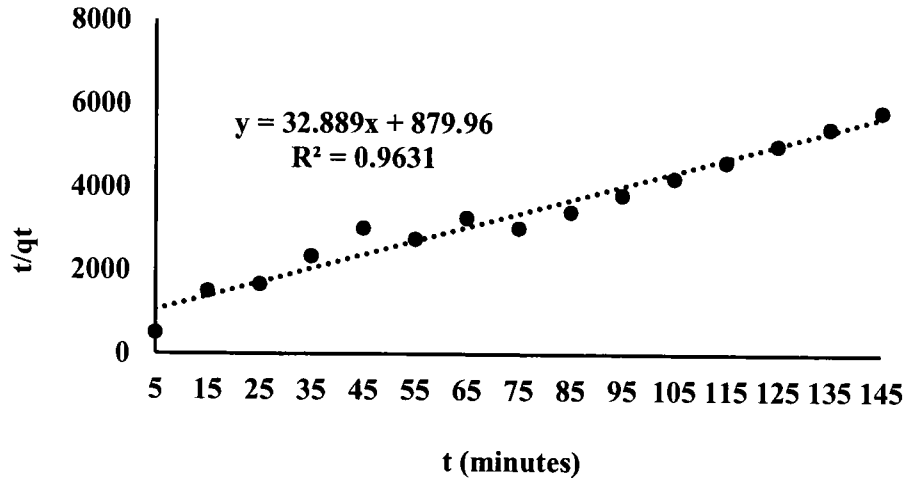

Figure 54: Pseudo Second Order of Clay

Table 9: Pseudo second order calculated parameters

Adsorbents	Equations	R^2	q_e (Cal) $= \frac{1}{Slope}$	qe (Exp)	$K_2 = \frac{h}{qe2}$	$h = k_2qe^2$ or $h = \frac{1}{intercept}$
BC250	y = 117.46x + 1163.2	0.9923	0.008	0.008	14.06	0.0009
BC500	y = 75.701x + 451.79	0.9873	0.013	0.014	10.204	0.002
BC750	y = 84.897x + 604.58	0.9925	0.012	0.012	13.888	0.002
BC1000	y = 64.521x + 943.92	0.9558	0.015	0.016	3.9	0.001
GAC	y = 33.249x + 8.2637	1	0.03	0.03	134.444	0.121
DLP	y = 191.79x + 1230	0.4814	0.005	0.005	32	0.0008
CLAY	y = 32.889x + 879.96	0.9631	0.03	0.025	1.11	0.001

CHAPTER 5
CONCLUSIONS AND RECOMMENDATIONS

5.1. CONCLUSIONS

The collected water samples were analyzed for the F^- as well as for different physio-chemical parameters. The results obtained showed that F^- in almost samples were beyond WHO limit, hence was concluded that water in the region is unfit for human consumption. The study further validated that F^- comes from the dissolution of minerals present in the parent rocks. Gibbs diagram showed that water-rock contact is the major chemical mechanism in the area. Piper plot represented that mixed CA-Mg-Cl water class, is the result of water interaction with minerals (rocks) and reverse ion-exchange mechanisms. The survey concluded that the risk of percent fluorosis was maximum in that area, where the F^- grade was higher in the water.

Batch adsorption experiments were performed by using various materials i.e. Biochar, commercial granular activated carbon (GAC), local clay particles and *Dodonaea* leaf powder for the removal of F^- from water. Biochar type BC750 shows maximum F^- removal capacity of 90%, followed by BC250 (85%), > BC500 (80%) > BC1000 (80%) > DLP (45%) > GAC (40%) from 2 mg/L F^- solution at their optimum removal conditions, which indicated that F^- could be brought down to its permissible level by applying these materials. The experimental work proved that the adsorbent removal capacity increases as the dosage and time quantity improves. Likewise, the adsorption efficiency was declining with increase in the F^- and pH level. The optimum contact time for BC250, BC500, BC750, BC1000, GAC, DLP and clay was 95 minutes, 145 minutes, 125 minutes, 145 minutes, 15 minutes, 145 minutes and 75 minutes, respectively. From SEM images, it is evident that biochar surface was porous and coarse which makes the F^- adsorption easy.

The removal capacity of biochar was compared with GAC, DLP and clay particles and the findings indicated that the biochar has more affinity for de-fluoridation than GAC, DLP and clay particles and is economical as it is prepared from the local abundantly available plant bark.

The FTIR spectra of biochar samples shows that the surface of biochar contains several functional groups and are greatly accountable for F^- extraction from the liquids. The functional group study indicated that carbon bonding with oxygen and hydrogen atom is significant for F^-

removal via lignocellulosic materials. Presence of adsorbed F^- could be easily confirmed from the SEM and EDS analysis of the biochar used as an adsorbent.

Maximum removal was noticed in the acidic range except BC1000, which removed 80% F^- at pH 7. The biochar removed a large amount of F^- at pH values below their pH_{PZC} values and this permits the ionic binding of F^- to the matching groups existing on the surface of adsorbing material. Biochar samples (BC250, BC500, BC750 and BC1000) shows 40%, 60%, 70% and 80% F^- adsorption at pH 7 from 2 mg/L F^- solution. The significant F^- adsorption at pH 7 by using these biochar samples shows its practical utilization as a suitable material for F^- remediation.

The attained adsorption data was in strong agreement with both models (Freundlich & Langmuir) and proposed both single and multilayer development on adsorbent surface. The kinetics study shows that Pseudo-Second-Order was more appropriate than the Pseudo First-Order model because the values of qe (cal) and qe (exp) were closely resembling for Pseudo-Second-Order.

Therefore, adsorption is a suitable technique for the elimination of F^- from water as compared to other available methods, because it is simple as well as easy to design and operate. Adsorption is an environment friendly and inexpensive method. This green technology would be applicable for treating F^- contaminated water at local level. The biochar used as an adsorbent for F^- removal can be disposed without costly regeneration because it is inexpensive and can be prepared from abundantly available plant materials.

The findings of this research work projected that the biochar prepared from the bark of *Dodonaea viscosa* plant is an efficient and eco-friendly adsorbent and can be applied for water de-fluoridation.

5.2. RECOMMENDATIONS

On the basis of results and findings of this study, the following are recommended

1. Provision of clean drinking water from the nearest safe water sources.
2. Installation of main water supply scheme with de-fluoridation facility
3. Installation of defluoridation facility at local levels and creating awareness in the community about the severe effects of fluorosis.

4. Provision of facilities at local BHUs (Basic Health Units) for initial examination of fluorosis.
5. Use of inexpensive defluoridation materials (biochar) for reducing the harmful effects of dental fluorosis.
6. Further studies on the preparation, regeneration, activation, and safe disposal of biochar.
7. Developing defluoridation kits at various levels.

REFERENCES

Abe, I., Iwasaki, S., Tokimoto, T., Kawasaki, N., Nakamura, T., Tanada, S. 2004. Adsorption of fluoride ions onto carbonaceous materials. *Journal Of Colloid And Interface Science*, **275**(1), 35-39.

Abouleish, M.Y.Z. 2016. Evaluation of fluoride levels in bottled water and their contribution to health and teeth problems in the United Arab Emirates. *The Saudi Dental Journal*, **28**(4), 194-202.

Adimalla, N., Li, P., Qian, H. 2019. Evaluation of groundwater contamination for fluoride and nitrate in semi-arid region of Nirmal Province, South India: a special emphasis on human health risk assessment (HHRA). *Human and Ecological Risk Assessment: An International Journal*, **25**(5), 1107-1124.

AHMAD, J., KHALIQ, A., SHAH, Z., IQBAL, S. 2003. Uranium occurrences in Maiakand granite and granitic gneisses, Maiakand Agency, NW Pakistan.

Alarcón-Herrera, M.T., Martin-Alarcon, D.A., Gutiérrez, M., Reynoso-Cuevas, L., Martín-Domínguez, A., Olmos-Márquez, M.A., Bundschuh, J. 2020. Co-occurrence, possible origin, and health-risk assessment of arsenic and fluoride in drinking water sources in Mexico: Geographical data visualization. *Science of the Total Environment*, **698**, 134168.

Amin, F., Talpur, F.N., Balouch, A., Surhio, M.A., Bhutto, M.A. 2015. Biosorption of fluoride from aqueous solution by white—rot fungus Pleurotus eryngii ATCC 90888. *Environmental Nanotechnology, Monitoring & Management*, **3**, 30-37.

Amor, T.B., Kassem, M., Hajjaji, W., Jamoussi, F., Amor, M.B., Hafiane, A. 2018. Study of Defluoridation of Water Using Natural Clay Minerals. *Clays and Clay Minerals*, **66**(6), 493-499.

Annadurai, S.T., Arivalagan, P., Sundaram, R., Mariappan, R., Munusamy, A.P. 2019. Batch and column approach on biosorption of fluoride from aqueous medium using live, dead and various pretreated Aspergillus niger (FS18) biomass. *Surfaces and Interfaces*, **15**, 60-69.

Antonijevic, E., Mandinic, Z., Curcic, M., Djukic-Cosic, D., Milicevic, N., Ivanovic, M., Carevic, M., Antonijevic, B. 2016. "Borderline" fluorotic region in Serbia: correlations among fluoride in drinking water, biomarkers of exposure and dental fluorosis in schoolchildren. *Environmental Geochemistry And Health*, **38**(3), 885-896.

APHA AWWA, W. 1998. Standard methods for the examination of water and wastewater 20th edition. American Public Health Association, American Water Work Association, Water Environment Federation, Washington, DC.

Asgari, G., Roshani, B., Ghanizadeh, G. 2012. The investigation of kinetic and isotherm of fluoride adsorption onto functionalize pumice stone. *Journal of Hazardous Materials*, **217**, 123-132.

Aslani, H., Zarei, M., Taghipour, H., Khashabi, E., Ghanbari, H., Ejlali, A. 2019. Monitoring, mapping and health risk assessment of fluoride in drinking water supplies in rural areas of Maku and Poldasht, Iran. *Environmental Geochemistry and Health*, **41**(5), 2281-2294.

Ayoob, S., Gupta, A.K. 2006. Fluoride in drinking water: a review on the status and stress effects. Critical *Reviews in Environmental Science and Technology*, **36**(6), 433-487.

Awasthi, P.K., Sankhla, S., Mathur, D. 2016. Natural biosorbents: A potential and economic alternative for water deflouridation. *Journal of Chemical, Biological and Physical Sciences (JCBPS)*, **6**(2), 402.

Balistrieri, L., Murray, J.W. 1981. The surface chemistry of goethite (alpha FeOOH) in major ion seawater. *American Journal of Science*, **281**(6), 788-806.

Bengharez, Z., Farch, S., Bendahmane, M., Merine, H., Benyahia, M. 2012. Evaluation of fluoride bottled water and its incidence in fluoride endemic and non endemic areas. *e-SPEN Journal,* 7(1), e41-e45.

Bharali, R.K., Bhattacharyya, K.G. 2015. Biosorption of fluoride on Neem (Azadirachta indica) leaf powder. *Journal of Environmental Chemical Engineering*, **3**(2), 662-669.

Budipramana, E., Hapsoro, A., Irmawati, E., Kuntari, S. 2002. Dental fluorosis and caries prevalence in the fluorosis endemic area of Asembagus, Indonesia. *International Journal of Paediatric Dentistry,* **12**(6), 415-422.

Çengeloğlu, Y., Kır, E., Ersöz, M. 2002. Removal of fluoride from aqueous solution by using red mud. *Separation and Purification Technology*, **28**(1), 81-86.

Chaudhry, M., Ashraf, M., Hussain, S., Iqbal, M. 1976. Geology and petrology of Malakand and a part of Dir: Toposheet 38 N/4. *Geol. Bull. Univ. Punjab*, **12**, 17-39.

Chaudhry, M.N., Jafferi, S., Saleemi, B.A. 1974. Geology and Petrology of the Malakand granite and its environs. *Geol. Bull. Punjab Univ*, **10**, 43-58.

Choong, C.E., Wong, K.T., Jang, S.B., Nah, I.W., Choi, J., Ibrahim, S., Yoon, Y., Jang, M. 2020. Fluoride removal by palm shell waste based powdered activated carbon vs. functionalized carbon with magnesium silicate: Implications for their application in water treatment. *Chemosphere*, **239**, 124765.

Choudhary, B., Paul, D., Singh, A., Gupta, T. 2017. Removal of hexavalent chromium upon interaction with biochar under acidic conditions: mechanistic insights and application. *Environmental Science and Pollution Research*, **24**(20), 16786-16797.

Currell, M., Cartwright, I., Raveggi, M., Han, D. 2011. Controls on elevated fluoride and arsenic concentrations in groundwater from the Yuncheng Basin, China. *Applied Geochemistry,* **26**(4), 540-552.

Daiwile, A.P., Tarale, P., Sivanesan, S., Naoghare, P.K., Bafana, A., Parmar, D., Kannan, K. 2019. Role of fluoride induced epigenetic alterations in the development of skeletal fluorosis. *Ecotoxicology and Environmental Safety*, **169**, 410-417.

Daifullah, A., Yakout, S., Elreefy, S. 2007. Adsorption of fluoride in aqueous solutions using KMnO4-modified activated carbon derived from steam pyrolysis of rice straw. *Journal of Hazardous Materials*, **147**(1-2), 633-643.

de Souza, C.F.M., Lima, J.F., Adriano, M.S.P.F., de Carvalho, F.G., Forte, F.D.S., de Farias Oliveira, R., Silva, A.P., Sampaio, F.C. 2013. Assessment of groundwater quality in a region of endemic fluorosis in the northeast of Brazil. *Environmental Monitoring and Assessment,* **185**(6), 4735-4743.

Dean, H.T. 1942. The investigation of physiological effects by the epidemiological method. *Fluorine and Dental Health*, 23-31.

Dean, H.T., Elvove, E. 1935. Studies on the minimal threshold of the dental sign of chronic endemic fluorosis (mottled enamel). *Public Health Reports* (1896-1970), 1719-1729.

Dobaradaran, S., Kakuee, M., Pazira, A., Keshtkar, M., Khorsand, M. 2015. Fluoride removal from aqueous solutions using Moringa oleifera seed ash as an environmental friendly and cheap biosorbent. *Fresenius Environmental Bulletin*, **24**(4), 1269-1274.

Doherty, A.L., Webster, J.D., Goldoff, B.A., Piccoli, P.M. 2014. Partitioning behavior of chlorine and fluorine in felsic melt–fluid (s)–apatite systems at 50 MPa and 850–950 C. *Chemical Geology*, **384**, 94-111.

Domingues, R.R., Trugilho, P.F., Silva, C.A., de Melo, I.C.N., Melo, L.C., Magriotis, Z.M., Sanchez-Monedero, M.A. 2017. Properties of biochar derived from wood and high-nutrient biomasses with the aim of agronomic and environmental benefits. PloS one, **12**(5).

Dong, X., Ma, L.Q., Li, Y. 2011. Characteristics and mechanisms of hexavalent chromium removal by biochar from sugar beet tailing. *Journal of Hazardous Materials*, **190**(1-3), 909-915.

Du, J., Zhang, L., Liu, T., Xiao, R., Li, R., Guo, D., Qiu, L., Yang, X., Zhang, Z. 2019. Thermal conversion of a promising phytoremediation plant (Symphytum officinale L.) into biochar: Dynamic of potentially toxic elements and environmental acceptability assessment of the biochar. *Bioresource Technology*, **274**, 73-82.

Dutta, M., Rajak, P., Khatun, S., Roy, S. 2017. Toxicity assessment of sodium fluoride in Drosophila melanogaster after chronic sub-lethal exposure. *Chemosphere*, **166**, 255-266.

Egor, M., Birungi, G. 2020. Fluoride contamination and its optimum upper limit in groundwater from Sukulu Hills, Tororo District, Uganda. *Scientific African*, **7**, e00241.

Fan, X., Parker, D.J., Smith, M.D. 2003. Adsorption kinetics of fluoride on low cost materials. *Water Research*, **37**(20), 4929-4937.

Fallahzadeh, R.A., Miri, M., Taghavi, M., Gholizadeh, A., Anbarani, R., Hosseini-Bandegharaei, A., Ferrante, M., Conti, G.O. 2018. Spatial variation and probabilistic risk assessment of exposure to fluoride in drinking water. *Food and Chemical Toxicology*, **113**, 314-321.

Fellet, G., Marmiroli, M., Marchiol, L. 2014. Elements uptake by metal accumulator species grown on mine tailings amended with three types of biochar. *Science of the Total Environment*, **468**, 598-608.

Freeze, R., Cherry, J. 1979. 1979, Groundwater. Prentice-Hall, Englewood Cliffs, NJ, 604 p.

Freundlich, H. 1906. Uber die adsorption in losungen, zeitschrift fur phtsikalische chemie. *American Chemical Society*, **62**(5), 121-125.

George, A.M., Tembhurkar, A. 2018. Biosorptive removal of fluoride from aqueous solution onto newly developed biosorbent from Ficus benghalensis leaf: Evaluation of equilibrium, kinetics, and thermodynamics. *Sustainable Chemistry and Pharmacy*, **10**, 125-133.

George, A.M., Tembhurkar, A.R. 2019. Analysis of equilibrium, kinetic, and thermodynamic parameters for biosorption of fluoride from water onto coconut (Cocos nucifera Linn.) root developed adsorbent. *Chinese Journal of Chemical Engineering*, **27**(1), 92-99.

Getachew, T., Hussen, A., Rao, V. 2015. Defluoridation of water by activated carbon prepared from banana (Musa paradisiaca) peel and coffee (Coffea arabica) husk. *International Journal of Environmental Science and Technology*, **12**(6), 1857-1866.

Ghosh, S.B., Mondal, N.K. 2019. Application of Taguchi method for optimizing the process parameters for the removal of fluoride by Al-impregnated Eucalyptus bark ash. *Environmental Nanotechnology, Monitoring & Management*, **11**, 100206.

Gibbs, R.J. 1970. Mechanisms controlling world water chemistry. Science, **170**(3962), 1088-1090.

Guissouma, W., Hakami, O., Al-Rajab, A.J., Tarhouni, J. 2017. Risk assessment of fluoride exposure in drinking water of Tunisia. *Chemosphere*, **177**, 102-108.

Guo, X., Zuo, R., Shan, D., Cao, Y., Wang, J., Teng, Y., Fu, Q., Zheng, B. 2017. Source apportionment of pollution in groundwater source area using factor analysis and positive matrix factorization methods. Human and Ecological Risk Assessment: *An International Journal*, **23**(6), 1417-1436.

Halder, G., Khan, A.A., Dhawane, S. 2016. Fluoride Sorption Onto a Steam-Activated Biochar Derived From Cocos nucifera Shell. *CLEAN–Soil, Air, Water*, **44**(2), 124-133.

Harikumar, P.S.P., Jaseela, C., Megha, T. 2012. Defluoridation of water using biosorbents.

Haritash, A., Aggarwal, A., Soni, J., Sharma, K., Sapra, M., Singh, B. 2018. Assessment of fluoride in groundwater and urine, and prevalence of fluorosis among school children in Haryana, India. *Applied Water Science*, **8**(2), 52.

He, J., An, Y., Zhang, F. 2013. Geochemical characteristics and fluoride distribution in the groundwater of the Zhangye Basin in Northwestern China. *Journal of Geochemical Exploration*, **135**, 22-30.

Herbert, L., Hosek, I., Kripalani, R. 2012. The characterization and comparison of biochar produced from a decentralized reactor using forced air and natural draft pyrolysis.

Hu, X., Zhang, X., Ngo, H.H., Guo, W., Wen, H., Li, C., Zhang, Y., Ma, C. 2020. Comparison study on the ammonium adsorption of the biochars derived from different kinds of fruit peel. *Science of the Total Environment*, **707**, 135544.

Hussain, S.S., Khan, T., Dawood, H., Khan, I. 1984. A note on Kot-Prang Ghar melange and associated mineral occurrences. *Geological Bulletin University of Peshawar*, **17**, 61-68.

IBI. 2012. Standardized product definition and product testing guidelines for biochar that is used in soil. IBI biochar standards.

Iriel, A., Bruneel, S.P., Schenone, N., Cirelli, A.F. 2018. The removal of fluoride from aqueous solution by a lateritic soil adsorption: kinetic and equilibrium studies. *Ecotoxicology and Environmental Safety*, **149**, 166-172.

Irigoyen-Camacho, M., Pérez, A.G., González, A.M., Alvarez, R.H. 2016. Nutritional status and dental fluorosis among schoolchildren in communities with different drinking water fluoride concentrations in a central region in Mexico. *Science of the Total Environment*, **541**, 512-519.

Kanouo, B.M.D., Allaire, S.E., Munson, A.D. 2018. Quality of biochars made from Eucalyptus tree bark and corncob using a pilot-scale retort kiln. *Waste and Biomass Valorization*, **9**(6), 899-909.

Khaliq, A., Ahmad, J., Shah, Z. 2003. New geological investigations regarding MCT along southwestern part of Malakand granite gneiss, Malakand agency, kpk Pakistan. *Geological Bulletin University of Peshawar*, **36**, 23-30.

Khosravi, R., Fazlzadehdavil, M., Barikbin, B., Taghizadeh, A.A. 2014. Removal of hexavalent chromium from aqueous solution by granular and powdered Peganum Harmala. *Applied Surface Science*, **292**, 670-677.

Kimambo, V., Bhattacharya, P., Mtalo, F., Mtamba, J., Ahmad, A. 2019. Fluoride occurrence in groundwater systems at global scale and status of defluoridation–state of the art. *Groundwater for Sustainable Development*, 100223.

Khound, N.J., Bharali, R.K. 2018. Biosorption of fluoride from aqueous medium by Indian sandalwood (Santalum album) leaf powder. *Journal of Environmental Chemical Engineering*, **6**(2), 1726-1735.

Kotha, A. 2017. Prevalence of dental fluorosis in school children of age ranged 8-15 years.

Kumar, S., Gupta, A., Yadav, J. 2008. Removal of fluoride by thermally activated carbon prepared from neem (Azadirachta indica) and kikar (Acacia arabica) leaves. *Journal of Environmental Biology*, **29**(2), 227.

Kumar, S.K., Rammohan, V., Sahayam, J.D., Jeevanandam, M. 2009. Assessment of groundwater quality and hydrogeochemistry of Manimuktha River basin, Tamil Nadu, India. *Environmental Monitoring and Assessment*, **159**(1-4), 341.

Kumari, U., Behera, S.K., Siddiqi, H., Meikap, B. 2020. Facile method to synthesize efficient adsorbent from alumina by nitric acid activation: Batch scale defluoridation, kinetics, isotherm studies and implementation on industrial wastewater treatment. *Journal of Hazardous Materials*, **381**, 120917.

Langmuir, I. 1916. The constitution and fundamental properties of solids and liquids. Part I. Solids. *Journal of the American Chemical Society*, **38**(11), 2221-2295.

Lee, J.-I., Hong, S.-H., Lee, C.-G., Park, S.-J. 2020. Experimental and model study for fluoride removal by thermally activated sepiolite. *Chemosphere*, **241**, 125094.

LeVan, M.D., Vermeulen, T. 1981. Binary Langmuir and Freundlich isotherms for ideal adsorbed solutions. *The Journal of Physical Chemistry*, **85**(22), 3247-3250.

Li, P., Wu, J., Qian, H., Zhang, Y., Yang, N., Jing, L., Yu, P. 2016. Hydrogeochemical characterization of groundwater in and around a wastewater irrigated forest in the

southeastern edge of the Tengger Desert, Northwest China. *Exposure and Health*, **8**(3), 331-348.

Lima-Arsati, Y.B.d.O., Gomes, A.R.L.F., Santos, H.K.A., Arsati, F., Oliveira, M.C., Freitas, V.S. 2018. Exposure to fluoride of children during the critical age for dental fluorosis, in the semiarid region of Brazil. *Ciencia & Saude Coletiva*, **23**(4), 1045-1054.

Luo, L., Wang, G., Shi, G., Zhang, M., Zhang, J., He, J., Xiao, Y., Tian, D., Zhang, Y., Deng, S. 2019. The characterization of biochars derived from rice straw and swine manure, and their potential and risk in N and P removal from water. *Journal of Environmental Management,* **245**, 1-7.

Luo, Y., Durenkamp, M., De Nobili, M., Lin, Q., Brookes, P. 2011. Short term soil priming effects and the mineralisation of biochar following its incorporation to soils of different pH. *Soil Biology and Biochemistry*, **43**(11), 2304-2314.

Maheshwari, R. 2006. Fluoride in drinking water and its removal. *Journal of Hazardous Materials*, **137**(1), 456-463.

Mahvi, A.H., Dobaradaran, S., Saeedi, R., Mohammadi, M.J., Keshtkar, M., Hosseini, A., Moradi, M., Ghasemi, F.F. 2018. Determination of fluoride biosorption from aqueous solutions using Ziziphus leaf as an environmentally friendly cost effective biosorbent. *Fluoride,* **51**(3), 220-229.

Mahvi, A.H., Mostafapour, F.K., Balarak, D. 2019. ADSORPTION OF FLUORIDE FROM AQUEOUS SOLUTION BY EUCALYPTUS BARK ACTIVATED CARBON: THERMODYNAMIC ANALYSIS. *Fluoride,* **52**(4).

Malago, J., Makoba, E., Muzuka, A.N. 2017. Fluoride levels in surface and groundwater in Africa: a review. *American Journal of Water Science and Engineering*, **3**(1), 1.

Ma, Y., Shi, F., Zheng, X., Ma, J., Gao, C. 2011. Removal of fluoride from aqueous solution using granular acid-treated bentonite (GHB): Batch and column studies. *Journal of Hazardous Materials*, **185**(2-3), 1073-1080.

Malde, M.K., Greiner-Simonsen, R., Julshamn, K., Bjorvatn, K. 2006. Tealeaves may release or absorb fluoride, depending on the fluoride content of water. *Science of the Total Environment*, **366**(2-3), 915-917.

Malinowska, E., Inkielewicz, I., Czarnowski, W., Szefer, P. 2008. Assessment of fluoride concentration and daily intake by human from tea and herbal infusions. *Food and Chemical Toxicology*, **46**(3), 1055-1061.

Mandinic, Z., Curcic, M., Antonijevic, B., Carevic, M., Mandic, J., Djukic-Cosic, D., Lekic, C.P. 2010. Fluoride in drinking water and dental fluorosis. *Science of the Total Environment*, **408**(17), 3507-3512.

Martinez-Mier, E. 2018. Guidelines for fluoride intake: First discussant. *Advances in Dental Research*, **29**(2), 177-178.

Meybeck, M. 1987. Global chemical weathering of surficial rocks estimated from river dissolved loads. *American Journal of Science*, **287**(5), 401-428.

Mobarak, M., Selim, A.Q., Mohamed, E.A., Seliem, M.K. 2018. Modification of organic matter-rich clay by a solution of cationic surfactant/H2O2: A new product for fluoride adsorption from solutions. *Journal of Cleaner Production*, **192**, 712-721.

Mohan, D., Kumar, S., Srivastava, A. 2014. Fluoride removal from ground water using magnetic and nonmagnetic corn stover biochars. *Ecological Engineering*, **73**, 798-808.

Mohan, D., Sharma, R., Singh, V.K., Steele, P., Pittman Jr, C.U. 2012. Fluoride removal from water using bio-char, a green waste, low-cost adsorbent: equilibrium uptake and sorption dynamics modeling. *Industrial & Engineering Chemistry Research*, **51**(2), 900-914.

Mohan, S., Singh, D.K., Kumar, V., Hasan, S.H. 2017. Effective removal of Fluoride ions by rGO/ZrO2 nanocomposite from aqueous solution: fixed bed column adsorption modelling and its adsorption mechanism. *Journal of Fluorine Chemistry*, **194**, 40-50.

Mondal, D., Dutta, G., Gupta, S. 2016. Inferring the fluoride hydrogeochemistry and effect of consuming fluoride-contaminated drinking water on human health in some endemic areas of Birbhum district, West Bengal. *Environmental Geochemistry and Health*, **38**(2), 557-576.

Moubarik, A., Grimi, N. 2015. Valorization of olive stone and sugar cane bagasse by-products as biosorbents for the removal of cadmium from aqueous solution. *Food Research International*, **73**, 169-175.

Muhammad, Z., Ali, H., Khan, W.M., Rehmanullah, G.J., Majeed, A. 2018. 1. Conservation status of plant resources of Hazar Nao hills, district Malakand, Pakistan. *Pure and Applied Biology (PAB)*, **7**(3), 931-945.

Mukherjee, S., Dutta, S., Ray, S., Halder, G. 2018. A comparative study on defluoridation capabilities of biosorbents: isotherm, kinetics, thermodynamics, cost estimation, and eco-toxicological study. *Environmental Science and Pollution Research*, **25**(18), 17473-17489.

Mukherjee, I., Singh, U.K. 2020. Fluoride abundance and their release mechanisms in groundwater along with associated human health risks in a geologically heterogeneous semi-arid region of east India. *Microchemical Journal*, **152**, 104304.

Munagapati, V. S., Yarramuthi, V., Kim, Y., Lee, K. M., & Kim, D. S. (2018). Removal of anionic dyes (Reactive Black 5 and Congo Red) from aqueous solutions using Banana Peel Powder as an adsorbent. *Ecotoxicology and Environmental Safety*, 148, 601-607.

Mwakabona, H.T., Machunda, R.L., Njau, K.N. 2014. The influence of stereochemistry of the active compounds on fluoride adsorption efficiency of the plant biomass.

Nabbou, N., Belhachemi, M., Boumelik, M., Merzougui, T., Lahcene, D., Harek, Y., Zorpas, A.A., Jeguirim, M. 2019. Removal of fluoride from groundwater using natural clay (kaolinite): optimization of adsorption conditions. *Comptes Rendus Chimie,* **22**(2-3), 105-112.

Nagarajan, R., Rajmohan, N., Mahendran, U., Senthamilkumar, S. 2010. Evaluation of groundwater quality and its suitability for drinking and agricultural use in Thanjavur city, Tamil Nadu, India. *Environmental Monitoring and Assessment*, **171**(1-4), 289-308.

Naghizadeh, A., Shahabi, H., Derakhshani, E., Ghasemi, F., Mahvi, A.H. 2017. SYNTHESIS OF NANOCHITOSAN FOR THE REMOVAL OF FLUORIDE FROM AQUEOUS SOLUTIONS: A STUDY OF ISOTHERMS, KINETICS, AND THERMODYNAMICS. *Fluoride*, **50**(2).

Narsimha, A., Sudarshan, V. 2017. Contamination of fluoride in groundwater and its effect on human health: a case study in hard rock aquifers of Siddipet, Telangana State, India. *Applied Water Science*, **7**(5), 2501-2512.

Neisi, A., Mirzabeygi, M., Zeyduni, G., Hamzezadeh, A., Jalili, D., Abbasnia, A., Yousefi, M., Khodadadi, R. 2018. Data on fluoride concentration levels in cold and warm season in City area of Sistan and Baluchistan Province, Iran. *Data in Brief*, **18**, 713.

Nuhoglu, Y., Malkoc, E. 2009. Thermodynamic and kinetic studies for environmentaly friendly Ni (II) biosorption using waste pomace of olive oil factory. *Bioresource Technology*, **100**(8), 2375-2380.

Olaka, L.A., Wilke, F.D., Olago, D.O., Odada, E.O., Mulch, A., Musolff, A. 2016. Groundwater fluoride enrichment in an active rift setting: Central Kenya Rift case study. *Science of The Total Environment*, **545**, 641-653.

Papari, F., Najafabadi, P.R., Ramavandi, B. 2017. Fluoride ion removal from aqueous solution, groundwater, and seawater by granular and powdered Conocarpus erectus biochar. *Desal Water Treat*, **65**, 375-386.

Patel, P., Raju, N.J., Reddy, B.S.R., Suresh, U., Gossel, W., Wycisk, P. 2016. Geochemical processes and multivariate statistical analysis for the assessment of groundwater quality in the Swarnamukhi River basin, Andhra Pradesh, India. *Environmental Earth Sciences*, **75**(7), 611.

Piper, A.M. 1944. A graphic procedure in the geochemical interpretation of water-analyses. Eos, Transactions American Geophysical Union, **25**(6), 914-928.

Piyush, K.P., Madhurima, P., Rekha, S. 2012. Defluoridation of water by a biomass: Tinospora cordifolia. *Journal of Environmental Protection*, **2012**.

Poudyal, M., Babel, S. 2015. Removal of fluoride using granular activated carbon and domestic sewage sludge. Proceedings of the 4th International Conference on Informatics, Environment, Energy and Applications, Pattaya. pp. 139-143.

Pramanik, S., Saha, D. 2017. The genetic influence in fluorosis. *Environmental Toxicology and Pharmacology*, **56**, 157-162.

Purushotham, D., Prakash, M., Rao, A.N. 2011. Groundwater depletion and quality deterioration due to environmental impacts in Maheshwaram watershed of RR district, AP (India). *Environmental Earth Sciences*, **62**(8), 1707-1721.

Qureshi, S., Khan, M., Ahmad, M. 2008. A survey of useful medicinal plants of Abbottabad in northern Pakistan. *Trakia Journal of Sciences*, **6**(4), 39-51.

Radfarda, M., Gholizadehc, A., Azhdarpoorb, A., Badeenezhada, A., Mohammadid, A.A., Yousefie, M. 2019. Health risk assessment to fluoride and nitrate in drinking water of rural residents living in the Bardaskan city, arid region, southeastern Iran. *Water Treat*, **145**, 249-256.

Rafique, T., Naseem, S., Ozsvath, D., Hussain, R., Bhanger, M.I., Usmani, T.H. 2015. Geochemical controls of high fluoride groundwater in Umarkot sub-district, Thar Desert, Pakistan. *Science of the Total Environment*, **530**, 271-278.

Rajapaksha, A.U., Ok, Y.S., El-Naggar, A., Kim, H., Song, F., Kang, S., Tsang, Y.F. 2019. Dissolved organic matter characterization of biochars produced from different feedstock materials. *Journal of Environmental Management*, **233**, 393-399.

Ramanjaneyulu, V., Jaipal, M., Yasovardhan, N., Sharada, S. 2013. Kinetic studies on removal of fluoride from drinking water by using tamarind shell and pipal leaf powder. *International Journal of Emerging Trends in Engineering and Development*, **5**(3), 146-155.

Rango, T., Bianchini, G., Beccaluva, L., Tassinari, R. 2010. Geochemistry and water quality assessment of central Main Ethiopian Rift natural waters with emphasis on source and occurrence of fluoride and arsenic. *Journal of African Earth Sciences*, **57**(5), 479-491.

Ranjan, R., Ranjan, A. 2015. Sources of fluoride toxicity. in: Fluoride Toxicity in Animals, Springer, pp. 11-20.

Rashid, A., Guan, D.-X., Farooqi, A., Khan, S., Zahir, S., Jehan, S., Khattak, S.A., Khan, M.S., Khan, R. 2018. Fluoride prevalence in groundwater around a fluorite mining area in the flood plain of the River Swat, Pakistan. *Science of the Total Environment*, **635**, 203-215.

Rasool, A., Farooqi, A., Xiao, T., Ali, W., Noor, S., Abiola, O., Ali, S., Nasim, W. 2018. A review of global outlook on fluoride contamination in groundwater with prominence on the Pakistan current situation. *Environmental Geochemistry and Health*, **40**(4), 1265-1281.

Razdan, P., Patthi, B., Kumar, J.K., Agnihotri, N., Chaudhari, P., Prasad, M. 2017. Effect of fluoride concentration in drinking water on intelligence quotient of 12–14-year-old children

in Mathura district: A cross-sectional study. *Journal of International Society of Preventive & Community Dentistry*, **7**(5), 252.

Regassa, M., Melak, F., Birke, W., Alemayehu, E. 2016. Defluoridation of water using natural and activated coal. *Int. Adv. Res. J. Sci. Eng. Technol*, **3**, 1-7.

Reyes-Escobar, J., Zagal, E., Sandoval, M., Navia, R., Muñoz, C. 2015. Development of a biochar-plant-extract-based nitrification inhibitor and its application in field conditions. *Sustainability*, **7**(10), 13585-13596.

Roy, S., Sengupta, S., Manna, S., Das, P. 2018. Chemically reduced tea waste biochar and its application in treatment of fluoride containing wastewater: Batch and optimization using response surface methodology. *Process Safety and Environmental Protection*, **116**, 553-563.

Roy, S., Das, P. 2017. Assessment of De-fluoridation in Waste Water Using Activated Biochar: Thermodynamic and Kinetic Study. *J Chem Appl Chem Eng* 1, **1**, 2.

Ruan, X., Sun, Y., Du, W., Tang, Y., Liu, Q., Zhang, Z., Doherty, W., Frost, R.L., Qian, G., Tsang, D.C. 2019. Formation, characteristics, and applications of environmentally persistent free radicals in biochars: a review. *Bioresource Technology*.

Ruiz-Pico, Á., Cuenca, Á.P., Agila, R.S., Criollo, D.M., Leiva-Piedra, J., Salazar-Campos, J. 2019. Hydrochemical characterization of groundwater in the Loja Basin (Ecuador). *Applied Geochemistry*.

Saby, M., Larocque, M., Pinti, D.L., Barbecot, F., Sano, Y., Castro, M.C. 2016. Linking groundwater quality to residence times and regional geology in the St. Lawrence Lowlands, southern Quebec, Canada. *Applied Geochemistry*, **65**, 1-13.

Sah, O., Maguire, A., Zohoori, F. 2020. Effect of altitude on urinary, plasma and nail fluoride levels in children and adults in Nepal. *Journal of Trace Elements in Medicine and Biology*, **57**, 1-8.

Sajjad, M., Khan, S., Ali Baig, S., Munir, S., Naz, A., Ahmad, S.S., Khan, A. 2017. Removal of potentially toxic elements from aqueous solutions and industrial wastewater using activated carbon. *Water Science and Technology*, **75**(11), 2571-2579.

Samanta, P., Mukherjee, A.K., Pal, S., Senapati, T., Mondal, S., Ghosh, A.R. 2013. Major ion chemistry and water quality assessment of waterbodies at Golapbag area under Barddhaman Municipality of Burdwan District, West Bengal, India. *International Journal of Environmental Sciences*, **3**(6), 1938-1956.

Sezgin, B.I., Onur, Ş.G., Menteş, A., Okutan, A.E., Haznedaroğlu, E., Vieira, A.R. 2018. Two-fold excess of fluoride in the drinking water has no obvious health effects other than dental fluorosis. *Journal of Trace Elements in Medicine and Biology*, **50**, 216-222.

Shahid, M.K., Kim, J.Y., Choi, Y.-G. 2019. Synthesis of bone char from cattle bones and its application for fluoride removal from the contaminated water. *Groundwater for Sustainable Development*, **8**, 324-331.

Shyam, R., Kalwania, G. 2014. Removal of fluorides in drinking water by aloe vera and calcium chloride. *Chemical Science Transactions*, **3**(1), 29-36.

Singh, K., Lataye, D.H., Wasewar, K.L. 2017. Removal of fluoride from aqueous solution by using bael (Aegle marmelos) shell activated carbon: kinetic, equilibrium and thermodynamic study. *Journal of Fluorine Chemistry*, **194**, 23-32.

Sofuoglu, S.C., Kavcar, P. 2008. An exposure and risk assessment for fluoride and trace metals in black tea. *Journal of Hazardous Materials*, **158**(2-3), 392-400.

Song, Q., Zhao, H.-y., Xing, W.-l., Song, L.-h., Yang, L., Yang, D., Shu, X. 2018a. Effects of various additives on the pyrolysis characteristics of municipal solid waste. *Waste Management*, **78**, 621-629.

Sracek, O., Wanke, H., Ndakunda, N., Mihaljevič, M., Buzek, F. 2015. Geochemistry and fluoride levels of geothermal springs in Namibia. *Journal of Geochemical Exploration*, **148**, 96-104.

Srimurali, M., Pragathi, A., Karthikeyan, J. 1998. A study on removal of fluorides from drinking water by adsorption onto low-cost materials. *Environmental pollution*, **99**(2), 285-289.

Sun, L., Gao, Y., Liu, H., Zhang, W., Ding, Y., Li, B., Li, M., Sun, D. 2013. An assessment of the relationship between excess fluoride intake from drinking water and essential hypertension in adults residing in fluoride endemic areas. *Science of the Total Environment*, **443**, 864-869.

Sun, X., Atiyeh, H.K., Kumar, A., Zhang, H., Tanner, R.S. 2018. Biochar enhanced ethanol and butanol production by Clostridium carboxidivorans from syngas. *Bioresource Technology*, **265**, 128-138.

Suneetha, M., Sundar, B.S., Ravindhranath, K. 2015. Removal of fluoride from polluted waters using active carbon derived from barks of Vitex negundo plant. *Journal of Analytical Science and Technology*, **6**(1), 15.

Suthar, S. 2011. Contaminated drinking water and rural health perspectives in Rajasthan, India: an overview of recent case studies. *Environmental Monitoring and Assessment*, **173**(1-4), 837-849.

Tang, Y., Alam, M.S., Konhauser, K.O., Alessi, D.S., Xu, S., Tian, W., Liu, Y. 2019. Influence of pyrolysis temperature on production of digested sludge biochar and its application for ammonium removal from municipal wastewater. *Journal of Cleaner Production*, **209**, 927-936.

Thivya, C., Chidambaram, S., Rao, M., Thilagavathi, R., Prasanna, M., Manikandan, S. 2017. Assessment of fluoride contaminations in groundwater of hard rock aquifers in Madurai district, Tamil Nadu (India). *Applied Water Science*, **7**(2), 1011-1023.

Tirkey, P., Bhattacharya, T., Chakraborty, S. 2018. Optimization of fluoride removal from aqueous solution using Jamun (Syzygium cumini) leaf ash. *Process Safety and Environmental Protection*, **115**, 125-138.

Tomar, V., Prasad, S., Kumar, D. 2014. Adsorptive removal of fluoride from aqueous media using Citrus limonum (lemon) leaf. *Microchemical Journal*, **112**, 97-103.

Tripathy, S.S., Bersillon, J.-L., Gopal, K. 2006. Removal of fluoride from drinking water by adsorption onto alum-impregnated activated alumina. *Separation and Purification Technology*, **50**(3), 310-317.

Tseng, R.-L., Wu, F.-C., Juang, R.-S. 2010. Characteristics and applications of the Lagergren's first-order equation for adsorption kinetics. *Journal of the Taiwan Institute of Chemical Engineers*, **41**(6), 661-669.

Uchimiya, M., Wartelle, L.H., Klasson, K.T., Fortier, C.A., Lima, I.M. 2011. Influence of pyrolysis temperature on biochar property and function as a heavy metal sorbent in soil. *Journal of Agricultural and Food Chemistry*, **59**(6), 2501-2510.

Verma, A., Shetty, B.K., Guddattu, V., Chourasia, M.K., Pundir, P. 2017. High prevalence of dental fluorosis among adolescents is a growing concern: A school based cross-sectional study from Southern India. *Environmental Health and Preventive Medicine*, **22**(1), 17.

Vikas, C., Kushwaha, R., Ahmad, W., Prasannakumar, V., Reghunath, R. 2013. Genesis and geochemistry of high fluoride bearing groundwater from a semi-arid terrain of NW India. *Environmental Earth Sciences*, **68**(1), 289-305.

Vinati, A., Mahanty, B., Behera, S. 2015. Clay and clay minerals for fluoride removal from water: a state-oFthe-art review. *Applied Clay Science*, **114**, 340-348.

Viswanathan, G., Jaswanth, A., Gopalakrishnan, S. 2009. Mapping of fluoride endemic areas and assessment of fluoride exposure. *Science of the Total Environment*, **407**(5), 1579-1587.

Wang, J., Chen, N., Li, M., Feng, C. 2018. Efficient removal of fluoride using polypyrrole-modified biochar derived from slow pyrolysis of pomelo peel: sorption capacity and mechanism. *Journal of Polymers and the Environment,* **26**(4), 1559-1572.

Wu, J., Li, P., Qian, H., Duan, Z., Zhang, X. 2014. Using correlation and multivariate statistical analysis to identify hydrogeochemical processes affecting the major ion chemistry of waters: a case study in Laoheba phosphorite mine in Sichuan, China. *Arabian Journal of Geosciences*, **7**(10), 3973-3982.

Wu, S., Zhang, K., He, J., Cai, X., Chen, K., Li, Y., Sun, B., Kong, L., Liu, J. 2016. High efficient removal of fluoride from aqueous solution by a novel hydroxyl aluminum oxalate adsorbent. *Journal of Colloid and Interface Science,* **464**, 238-245.

Wu, W., Yang, M., Feng, Q., McGrouther, K., Wang, H., Lu, H., Chen, Y. 2012. Chemical characterization of rice straw-derived biochar for soil amendment. *Biomass and Bioenergy*, **47**, 268-276.

Xiao, J., Jin, Z., Zhang, F. 2015. Geochemical controls on fluoride concentrations in natural waters from the middle Loess Plateau, China. *Journal of Geochemical Exploration*, **159**, 252-261.

Yadav, A.K., Abbassi, R., Gupta, A., Dadashzadeh, M. 2013. Removal of fluoride from aqueous solution and groundwater by wheat straw, sawdust and activated bagasse carbon of sugarcane. *Ecological Engineering*, **52**, 211-218.

Yadav, K.K., Gupta, N., Kumar, V., Khan, S.A., Kumar, A. 2018. A review of emerging adsorbents and current demand for defluoridation of water: bright future in water sustainability. *Environment International*, **111**, 80-108.

Yao, Y., Gao, B., Inyang, M., Zimmerman, A.R., Cao, X., Pullammanappallil, P., Yang, L. 2011. Biochar derived from anaerobically digested sugar beet tailings: characterization and phosphate removal potential. *Bioresource Technology*, **102**(10), 6273-6278.

Young, S.M., Pitawala, A., Ishiga, H. 2011. Factors controlling fluoride contents of groundwater in north-central and northwestern Sri Lanka. *Environmental Earth Sciences*, **63**(6), 1333-1342.

Yousefi, M., Ghoochani, M., Mahvi, A.H. 2018. Health risk assessment to fluoride in drinking water of rural residents living in the Poldasht city, Northwest of Iran. *Ecotoxicology and Environmental safety*, **148**, 426-430.

Yuan, J.-H., Xu, R.-K., Zhang, H. 2011. The forms of alkalis in the biochar produced from crop residues at different temperatures. *Bioresource Technology*, **102**(3), 3488-3497.

Yuan, L., Fei, W., Jia, F., Jun-ping, L., Qi, L., Fang-ru, N., Xu-dong, L., Shu-lian, X. 2020. Health risk in children to fluoride exposure in a typical endemic fluorosis area on Loess Plateau, north China, in the last decade. *Chemosphere*, **243**, 125451.

Yuan, Q., Chi, Y., Yu, N., Zhao, Y., Yan, W., Li, X., Dong, B. 2014. Amino-functionalized magnetic mesoporous microspheres with good adsorption properties. *Materials Research Bulletin,* **49**, 279-284.

Zabihullah, Q., Rashid, A., Akhtar, N. 2006. Ethnobotanical survey in kot Manzaray Baba valley Malakand agency, Pakistan. *Pak J Plant Sci*, **12**(2), 115-121.

Zazouli, M.A., Mahvi, A.H., Mahdavi, Y., Balarak, D. 2015. Isothermic and kinetic modeling of fluoride removal from water by means of the natural biosorbents sorghum and canola. *Fluoride*, **48**(1), 37.

Zhang, L., Zhao, L., Zeng, Q., Fu, G., Feng, B., Lin, X., Liu, Z., Wang, Y., Hou, C. 2020. Spatial distribution of fluoride in drinking water and health risk assessment of children in typical fluorosis areas in north China. *Chemosphere*, **239**, 124811.

Zhang, S., Niu, Q., Gao, H., Ma, R., Lei, R., Zhang, C., Xia, T., Li, P., Xu, C., Wang, C. 2016. Excessive apoptosis and defective autophagy contribute to developmental testicular toxicity induced by fluoride. *Environmental Pollution*, **212**, 97-104.

Zhang, Y., Huang, H., Gong, B., Duan, L., Sun, L., He, T., Cheng, X., Li, Z., Cui, L., Ba, Y. 2017. Do Environmental Fluoride Exposure and ESRα Genetic Variation Modulate Methylation Modification on Bone Changes in Chinese Farmers? *Chemical Research in Toxicology*, **30**(6), 1302-1308.

Zhang, C., Li, Y., Jiang, Y., & Wang, T. J. (2017). Size-dependent fluoride removal performance of a magnetic Fe3O4@ Fe–Ti adsorbent and its defluoridation in a fluidized bed. *Industrial & Engineering Chemistry Research*, 56(9), 2425-2432.

Zhou, J., Liu, Y., Han, Y., Jing, F., Chen, J. 2019. Bone-derived biochar and magnetic biochar for effective removal of fluoride in groundwater: Effects of synthesis method and coexisting chromium. *Water Environment Research*.

Zohoori, F.V., Duckworth, R.M. 2017. Fluoride: Intake and Metabolism, Therapeutic and Toxicological Consequences. in: Molecular, Genetic, and Nutritional Aspects of Major and Trace Minerals, Elsevier, pp. 539-550.

Annexures

ANNEXURE A

ARTICLES PUBLISHED/ACCEPTED/SUBMITTED FROM THIS STUDY

1. https://www.fluorideresearch.online/531Pt1/files/FJ2020_v53_n1Pt1_p090-096_sfs.pdf

DEFLUORIDATION OF WATER USING *DODONAEA VISCOSA* LEAFPOWDER: A STUDY OF ADSORPTION ISOTHERMS

Fazli Aziz,[a,b,*] Islamud Din,[a,†] Sardar Khan,[c] Ghulam Mustafa,d,[‡] Mumtaz Khan,[a] Juma Muhammad,[b] Abdullah Jalal[e], Islamabad, Pakistan

ABSTRACT: This study was carried out to remove excessive fluoride from drinking water through adsorption phenomenon by using *Dodonaea viscosa* leaf powder as an adsorbent. Various parameters like pH (2–8), contact time (5–145 min), adsorbent dose (1–10 g), and initial fluoride concentrations (2–10 mg/L) have been optimized. The maximum defluoridation (45%) was achieved in an acidic environment and the Langmuir isotherm model fitted well in this study. The *Dodonaea viscosa* leaf powder was foundto be a very cost-effective adsorbent for fluoride ions and may be an effective and environment friendly method for the defluoridation of drinking water.

Key words: Adsorbent; Adsorption; Defluoridation; *Dodonaea viscosa* leaf powder (DLP); Water.

[a]Department of Environmental Science, Faculty of Basic and Applied Sciences, International Islamic University Islamabad, P.O. 44000, Pakistan; [b]Department of Environmental Sciences,Shaheed Benazir Bhutto University, Sheringal Dir Upper 18050, Pakistan; [c]Department ofEnvironmental Sciences, University of Peshawar, Pakistan; [d]Sulaiman Bin Abdullah Aba Al-

KhailCenter for Interdisciplinary Research in Basic Sciences (SA-CIRBS), International Islamic University Islamabad, P.O. 44000, Pakistan; [e]Institute of Biotechnology and Genetical Engineering, University of Agriculture, Peshawar, Pakistan.

For correspondence: *Fazli Aziz, Department of Environmental Science, Faculty of Basic and Applied Sciences, International Islamic University Islamabad, P.O. 44000, Pakistan. E-mail: aziziiui@yahoo.com; †Islamud Din, Department of Environmental Science, Faculty of Basic and Applied Sciences, International Islamic University Islamabad, P.O. 44000, Pakistan. E-mail: idd_nwa2000@yahoo.com; ‡Ghulam Mustafa, Sulaiman Bin Abdullah Aba Al-Khail Center for Interdisciplinary Research in Basic Sciences (SA-CIRBS),International Islamic University Islamabad, P.O. 44000, Pakistan. E-mail: gmustafa@iiu.edu.pk

2. Accepted in Polish Journal of Environmental Studies (PJOES)

Fluorides in Drinking Water and its Health Risk Assessment in District Malakand, Khyber-Pakhtunkhwa, Pakistan

Fazli Aziz[1,2*], Islamud Din[1*], Sardar Khan[3], Mumtaz Khan[1], Ghulam Mustafa[4], Imran Khan[1].

[1]Department of Environmental Science, FBAS, International Islamic University, H/10, P.O. 44000, Islamabad, Pakistan.

[2]Department of Environmental Sciences, Shaheed-Benazir- Bhutto University, Sheringal, Dir (U) 18050, Pakistan.

[3]Department of Environmental Sciences, University of Peshawar, 25120, Pakistan.

[4]Center for Interdisciplinary Research in Basic Sciences (CIRBS), International Islamic University, H/10; Islamabad; Pakistan.

***E-mails:** aziziiui@yahoo.com, idd_nwa2000@yahoo.com

ABSTRACT

The study was about the assessment of fluorides (F^-) in drinking water, its possible sources and threats to human health in Malakand District, Khyber Pakhtunkhwa. Fluoride (F^-) concentration in drinking water samples was measured by F^- meter and was found substantially

high in most of the samples than the WHO limits. The cationic and anionic concentrations were found in the order of; Na > Ca > Mg > K, and SO_4 > HCO^-_3 > Cl^- > F, respectively. Among the anions, sulfates (SO_4) were found as dominant specie in all water samples while among cations, sodium (Na^+) was the element found in excess in all water samples except in Batoo locality, where Ca^{+2} exceeds the Na^+. As given by the Gibbs diagram, water and rock contact is the main reason for ions distribution in groundwater of the study area. Piper trilinear depicts that the mixed Ca-Mg-Cl and $CaCl_2$ are the main water forms found in the study area. Health risk assessment i.e., community fluorosis index, was assessed via Dean's classification, which showed that the drinking water samples were not suitable for use owing to the higher concentration of F^- than recommended by WHO.

Keywords: CFI, contaminated water, fluoride, fluorosis, gibbs diagram

ANNEXURE B

***Dodoneae Viscosa* Plant**

DLP preparation

Dry *Dodoneae Viscosa* Plant Bark

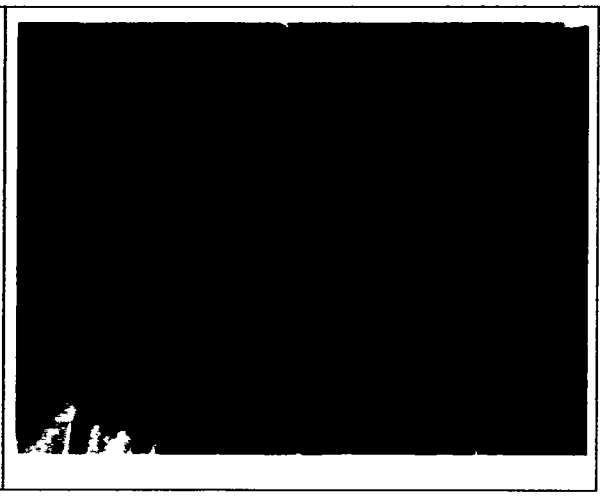

Washing of Plant Bark

Plant Bark Washing

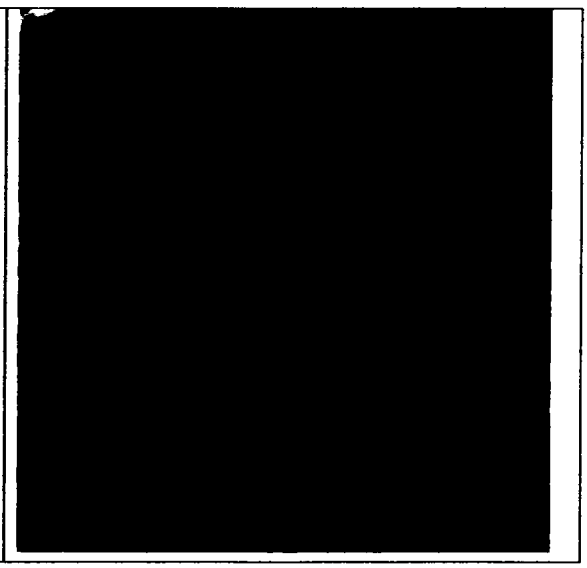

Ground Bark After Washing

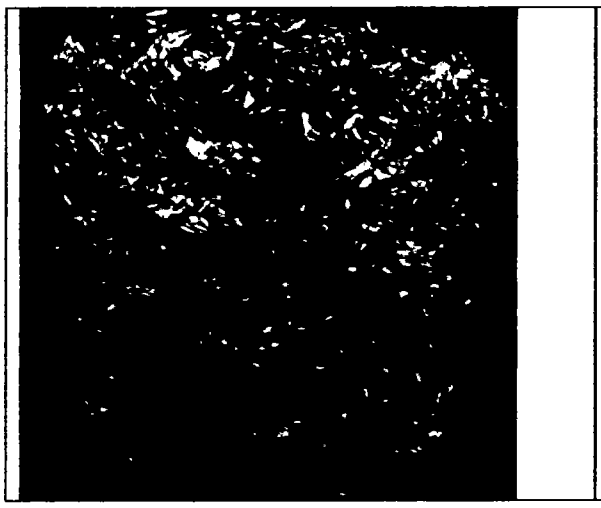

Before Heating in Furnace (Covered with Al-Foil)

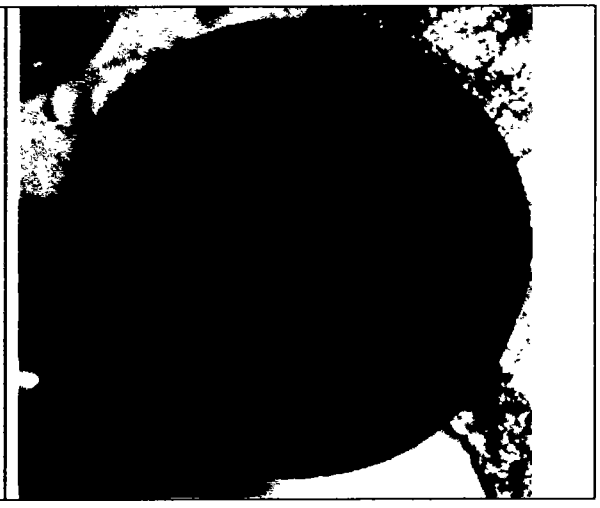

Prepared Biochar

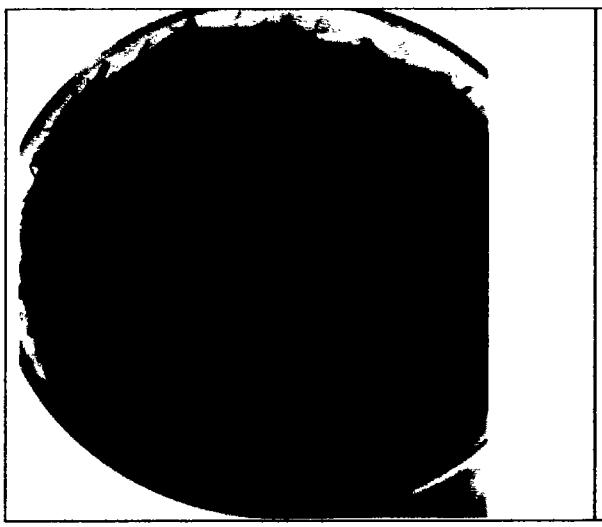

Biochar for Grinding

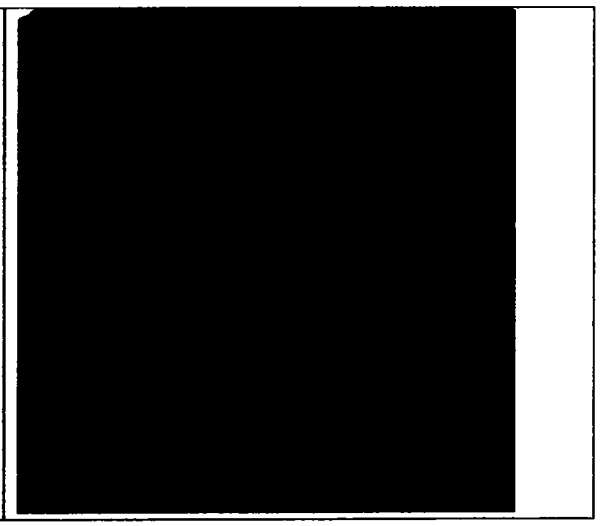

Biochar Ready For Use